FUNCTIONAL CHARACTERIZATION OF THE MITOTIC-SPINDLE AND KINETOCHORE ASSOCIATED PROTEIN ASTRIN

Dissertation
zur Erlangung des Doktorgrades der Naturwissenschaften
der Fakultät für Biologie der Ludwig-Maximilians-Universität
München

vorgelegt von
Diplom Biotechnologin
Kerstin Thein
München, 2007

Dissertation eingereicht am: 20.11.2007

Tag der Disputation: 23.01.2008

Erstgutachter: Prof. Erich A. Nigg

Zweitgutachter: PD Dr. Angelika Boettger

Hiermit erkläre ich, dass ich die vorliegende Dissertation selbstständig und ohne unerlaubte Hilfe angefertigt habe. Sämtliche Experimente wurden von mir selbst durchgeführt, soweit nicht explizit auf Dritte verwiesen wird. Ich habe weder an anderer Stelle versucht, eine Dissertation oder Teile einer solchen einzureichen bzw. einer Prüfungskommission vorzulegen, noch eine Doktorprüfung zu absolvieren.

München, den 20.11.2007

SUMMARY

Chromosome segregation in mitosis requires the formation of a bipolar mitotic spindle with stably attached chromosomes. Key structural components involved in this process are microtubules (MTs), kinetochores (KTs) and centrosomes. KTs, proteinaceous structures associated with centromere DNA, form the attachment sites for the spindle MTs on the chromosomes. Centrosomes direct the formation of the bipolar spindle. Once all the chromosomes are attached to the bipolar spindle, the connection between the sister chromatids is severed by the cysteine protease separase and the sister chromatids segregate to opposite poles. Separase also promotes centriole disengagement during exit from mitosis, a mechanism that limits centriole duplication to once in every cell cycle (Tsou and Stearns, 2006a; Tsou and Stearns, 2006c; Wong and Stearns, 2003).

Here we analyse the function of the spindle- and KT associated protein astrin, which is required for progression through mitosis (Chang et al., 2001; Gruber et al., 2002; Mack and Compton, 2001). The first part of the work concerns initial characterization of astrin's localization, regulation and interaction partners. Immunofluorescence analysis revealed that astrin localizes preferentially to KTs of aligned chromosomes and that this localization depends on stable KT-MT interactions. Nocodazole release experiments showed that astrin is highly phosphorylated during mitosis, suggesting that astrin's function is regulated by phosphorylation. By two approaches, bi-dependency analysis and immuno-precipitation, the mitotic motor protein CENP-E, the phosphatase hCdc14A and the mitotic kinase Plk1 were identified as three interesting candidates for being interactors of astrin. The second part of the work concerns the functional analysis of astrin during mitosis. We demonstrate that in the absence of astrin KT-MT attachments are impaired resulting in a spindle checkpoint arrest. Moreover, depletion of astrin results in cells with multipolar spindles and separated sister chromatids, consistent with untimely separase activation. Supporting this idea, astrin depleted cells contain active separase, and double depletion of astrin and separase suppresses the premature sister chromatid separation and centriole disengagement in these cells. We suggest that astrin contributes to the regulatory network that controls separase activity.

INTRODUCTION

1. The cell cycle and M phase

The cell is the basic metabolically functional unit of life. Cells multiply via the cell cycle, a sequence of events resulting in the replication of the genome and segregation of the replicated chromosomes into the two nascent daughter cells.

1.1. General overview of the cell cycle

The cell cycle consists of two major stages, interphase and M phase (M stands for mitotic) (Mitchison, 1971). Interphase is the period between two successive cell divisions consisting of three distinct stages: S phase (S stands for synthesis) and the so called gap phases, G1 and G2. In S phase, the DNA is replicated and centrosomes are duplicated. During the gap phases cells grow and progression to the next cell cycle stage is controlled by a variety of intracellular and extracellular signals. G1 takes place before S phase and G2 before M phase. Cells that have temporarily or reversibly stopped dividing enter a state of quiescence called G0 (G zero). M phase is composed of two tightly coupled processes: nuclear division (mitosis) in which the cell's chromosomes are segregated, and cell division (cytokinesis), in which the cell's cytoplasm divides forming two distinct daughter cells.

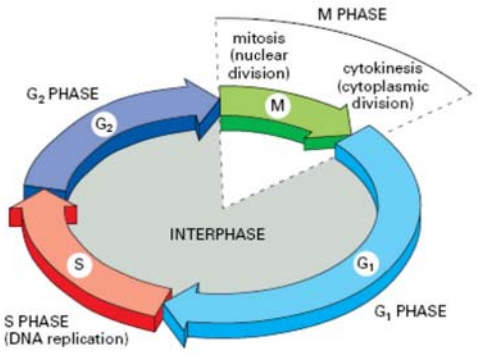

Figure 1. The cell cycle of eukaryotic cells. Interphase consists of S phase, G1 and G2. M phase is composed of nuclear division (mitosis) and cell division (cytokinesis). Illustration adapted from (Alberts, 2002).

1.2. The different stages of M phase

Mitosis has been studied since the early 1880s. Walther Flemming (1843-1905) originally coined the term mitosis from the Greek word for thread, reflecting the shape of mitotic chromosomes. He developed new methods for staining a fibrous scaffold in the nucleus, which was therefore named Chromatin ('stainable material'). Flemming's studies (Flemming, 1882) became the foundation for all further research into mitosis (Figure 2).

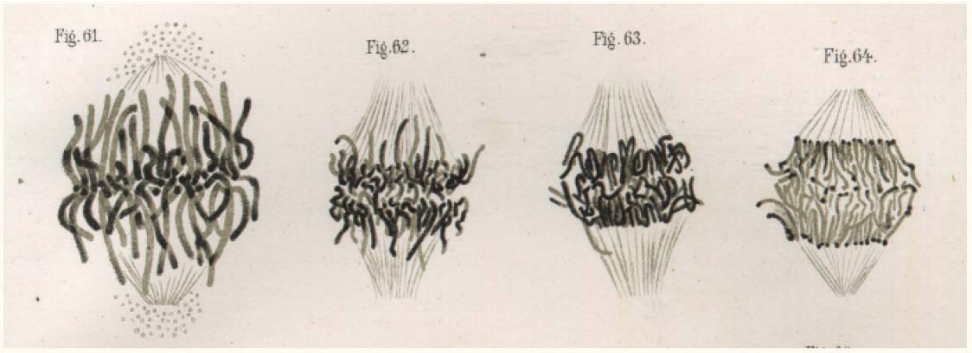

Figure 2. Illustration from Zellsubstanz, Kern und Zelltheilung by Walter Flemming (Flemming, 1882). Drawing of salamander cells, stained with hämatoxylin. Illustration adapted from (Paweletz, 2001)

Today mitosis is divided up into five discrete stages according to the morphology of the cell, prophase, prometaphase, metaphase, anaphase and telophase (Figure 3). In prophase the chromatin condenses and the chromosomes with the two sister chromatids and the central centromere, a heterochromatic DNA region at which the sister chromatids are held together, are apparent through a microscope. The two centrosomes, consisting of one centriole pair each, separate and migrate to opposite sides of the nucleus. Each centrosome starts to nucleate a radial MT array (aster); the bipolar mitotic spindle will form between them. The next stage, prometaphase, begins with nuclear envelope breakdown and is defined by the search-and-capture behaviour of MTs as the KTs are attached to the mitotic spindle (Figure 3). KTs are protein complexes at the centromere of a chromosome. The attached chromosomes are moved to the central region of the cell in a process called congression. Once all KTs are completely attached to the bipolar spindle and have migrated to its central region (metaphase plate), the cell is defined as being in metaphase. The bipolar mitotic spindle consists of different kinds of MTs, the KT MTs, which are attached to the KT, the astral MTs, which link the spindle poles to the cell cortex and the interpolar MTs that overlap in an anti-parallel fashion at the cell equator.

Metaphase ends with the rapid and almost synchronous separation of the cohesion links between sister chromatids, which then begin to segregate to opposite poles of the spindle by shortening of the KT MTs in anaphase A, followed by elongation of the spindle in anaphase B. Mitosis is completed in telophase, when each set of sister chromatids has reached opposite spindle poles, the chromatids begin to decondense and the nuclear envelope reforms. The mitotic spindle is disassembled. During anaphase and telophase an actomyosin-based contractile ring is formed and the cell itself begins to divide (cytokinesis). Finally, abscission takes place resulting in two genetically identical daughter cells with one set of chromosomes and a single centrosome.

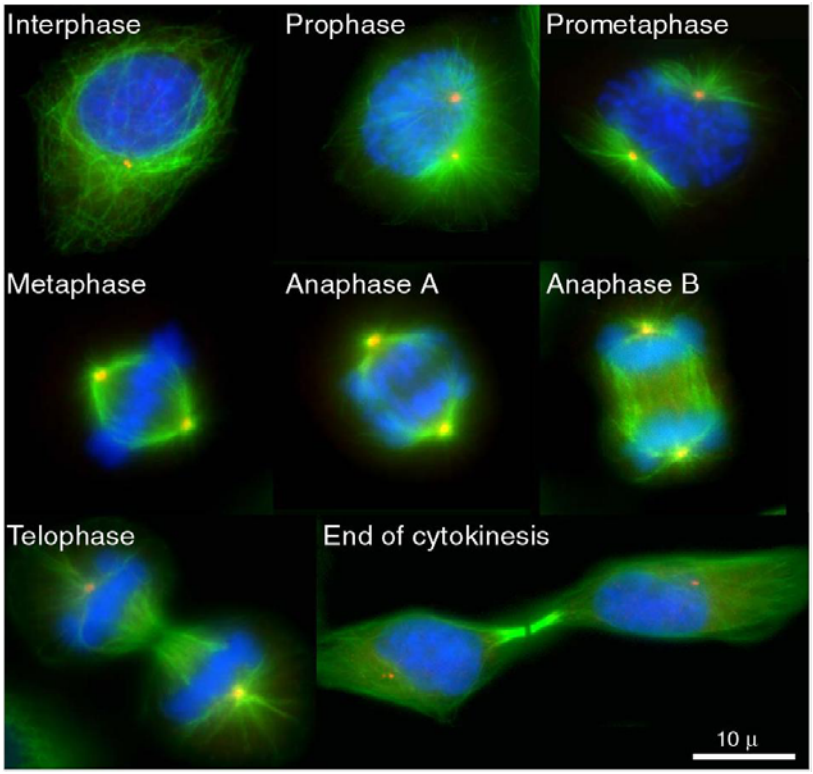

Figure 3. The different stages of M phase. The figure summarizes the stages of M phase. The immunofluorescence pictures illustrate HeLa cells in different cell cycle stages. The mitotic spindle is shown in green (α-tubulin), the spindle poles (γ-tubulin) in orange and DNA in blue (DAPI staining). The picture was kindly provided by P. Meraldi.

2. Principles of mitotic regulation

The major regulatory mechanisms controlling mitotic progression are protein phosphorylation and proteolysis. Phosphorylation is a reversible protein modification,

which is ideal for the control of reversible mitotic processes such as spindle assembly. Proteolysis is an irreversible mechanism which gives the cell cycle directionality. Both mechanisms are linked since the proteolytic machinery is controlled by phosphorylation, whereas several mitotic kinases are downregulated by degradation (Nigg, 2001; Pines, 2006). The serine/threonine kinase Cdk1 is the key mitotic kinase working in concert with additional protein kinases such as members of the Polo, the Aurora and NIMA (never in mitosis A) families (Nigg, 2001).

2.1. Cell cycle regulation

To ensure that each newly formed daughter cell receives a complete genome progression through the cell cycle is controlled by a series of biochemical switches that trigger the events of the cell cycle in the correct sequence. The central components of the cell cycle control system are the cyclin-dependent protein kinases (Cdks), which are controlled by transient associations with cyclin regulatory subunits, phosphorylation and inhibitory proteins. Concentrations of Cdks are constant throughout the cell cycle and their activities depend primarily on the changing levels of the associated cyclins. Based on the timing of expression and their function, the cyclins can be divided into four classes, G1 cyclins, G1/S cyclins, S cyclins and M cyclins. G1 cyclins (D-type cyclins in vertebrates) bind and activate Cdk4 and Cdk6, which stimulate the entry into a new cell cycle in response to external factors. G1/S cyclins (cyclin E in vertebrates) activate Cdk2 and trigger G1/S transition; their concentrations peak in late G1. S cyclins (cyclin A in vertebrates) bind Cdk2 and Cdk1 and are necessary for DNA synthesis; their concentrations rise and remain high during S phase, G2 and early mitosis. Cdk1 in association with the M cyclin, cyclin B1, is the key regulator of both mitotic entry and progression through mitosis (Murray, 2004).

2.2. The key mitotic kinase Cdk1

Genetic studies in budding yeast and fission yeast provided the first indication that a network of genes regulates the onset of mitosis; core to this network was the *Saccharomyces cerevisiae* Cdc28p/ *Shizosaccharomyces pombe* Cdc2p (renamed Cdk1) protein kinase activated by the Cdc25p phosphatase and inhibited by the Wee1p protein kinase (Hartwell and Smith, 1985; Nurse, 1990). Since then further studies made the

regulation of Cdk1 and its function in mitosis fairly well understood (Doree and Hunt, 2002; Ferrari, 2006). The activation of Cdk1 at the G2/M transition depends on the dephosphorylation of two neighbouring residues in the ATP-binding site (threonine 14 and tyrosine 15) by the dual-specificity phosphatase Cdc25C (Izumi and Maller, 1993; Krek and Nigg, 1991). At G2/M transition the activity of Cdc25C towards Cdk1 exceeds that one of the opposing kinases Wee1 and Myt1 (Nigg, 2001). Wee1 and Myt1 are part of the machinery that detects completion of DNA synthesis and successful repair of damaged DNA (Ferrari, 2006). Cdk1 enhances its own activity by a variety of positive feedback loops. Cdk1 phosphorylates and thus stimulates its activator Cdc25C (Hoffmann et al., 1993) and inactivates Wee1 by phosphorylation (Watanabe et al., 2004). Cdk1 may also promote its own activation by stimulating Polo-like kinase 1 (Plk1) activity, which further stimulates Cdc25C by phosphorylation (Kumagai and Dunphy, 1996; Strausfeld et al., 1994). Activated Cdk1/cyclin B1 fulfils different functions during mitosis (Figure 4) by phosphorylating various substrates. For instance Cdk1 is involved in chromosome condensation by phosphorylating condensins (Kimura et al., 1998), in nuclear envelope break down by phosphorylation of lamins (Peter et al., 1991). It contributes to centrosome separation and assembly of the mitotic spindle by phosphorylating MT associated proteins and the kinesin-related motor protein Eg5 (Blangy et al., 1995). Furthermore, Cdk1/cylin B1 contributes to the regulation of the anaphase-promoting complex/cyclosome (APC/C) (Sudakin et al., 1995; Zachariae et al., 1998), a multisubunit E3 ubiquitin ligase that catalyzes the attachment of multiubiquitin chains to mitotic regulators such as the inhibitors of anaphase onset and cyclins, thus promoting their degradation by the 26S proteasome and mitotic exit (Peters, 2002). Upon APC/C mediated cyclin B1 destruction, Cdk1 is inactivated and cells exit mitosis.

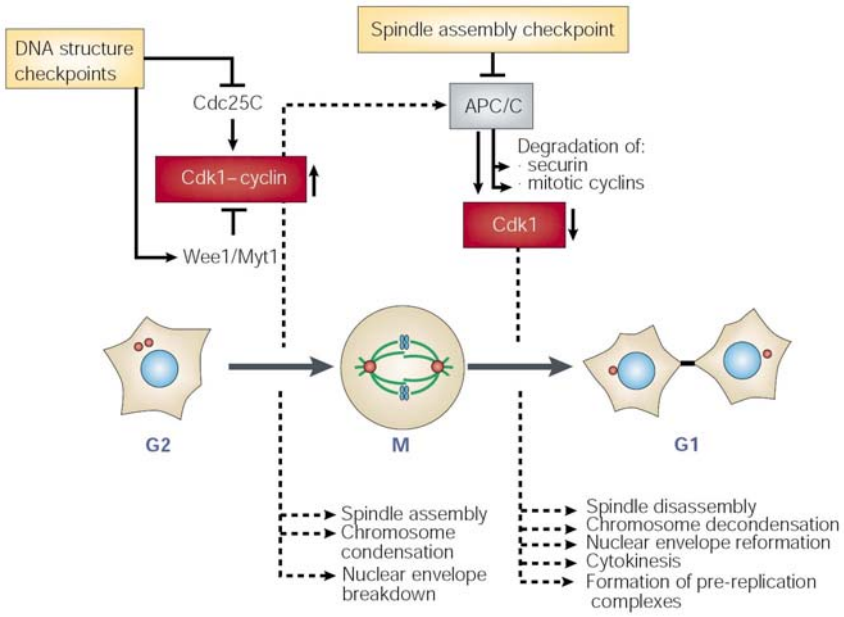

Figure 4. Overview of Cdk1 functions and its regulation. Mitotic entry results from the activation of Cdk1/cyclin complexes. Factors that activate and inhibit Cdk1 function are illustrated. Cdk1/cyclin functions in various processes during mitosis. Upon cyclin destruction Cdk1 gets inactivated and cells exit mitosis. Checkpoints that can delay entry into mitosis (DNA structure checkpoints) or anaphase onset (spindle assembly checkpoint) are shown. Illustration adapted from (Nigg, 2001).

2.3. The mitotic kinase Plk1

The first member of the Polo family, a conserved subfamily of serine/threonine protein kinases, was identified in *Drosophila* (Sunkel and Glover, 1988). Subsequently, four Plk family members have been identified in humans, Plk1, Plk2, Plk3 and Plk4 (Sak) (Barr et al., 2004; Glover et al., 1998), with Plk1 being the best studied member. Plk1 is characterized by an N-terminal kinase domain and two structurally homologous polo-boxes, named Polo-box domain (PBD), at the C-terminus (Elia et al., 2003b; Leung et al., 2002) (Figure 5A). The PBD has different established functions, it acts as an autoinhibitory domain (Mundt et al., 1997), whose inhibitory role is relieved through phosphorylation at the T-loop site T210 (Jang et al., 2002), it is required for Plk1's subcellular localization (Figure 5B) and its targeting to substrates (Hanisch et al., 2006; Lee et al., 1998; Reynolds and Ohkura, 2003). The latter two functions are mediated by the phosphopeptide-binding domain of the PBD, which binds with maximal affinity to phosphorylated residues containing the consensus sequence S-pS/pTP/X (Elia et al.,

2003a). Binding of the PBD to the docking proteins results in a relief of autoinhibition by the PBD and an increased activity of Plk1, which phosphorylates either the docking protein or other downstream targets (Elia et al., 2003a; Elia et al., 2003b; Lowery et al., 2005). The docking sites are generated by serine/threonine kinases (priming-kinases). In the early stages of mitosis, Cdk1 creates theses docking sites (Elia et al., 2003a; Elia et al., 2003b), whereas in anaphase Plk1 self-primes its docking sites on proteins required for cytokinesis (Neef et al., 2007; Neef et al., 2003). Plk1 localizes to different mitotic structures, the centrosomes, spindle poles, and KTs in prophase and metaphase, the central spindle in anaphase and the midbody during cytokinesis (Figure 5B).

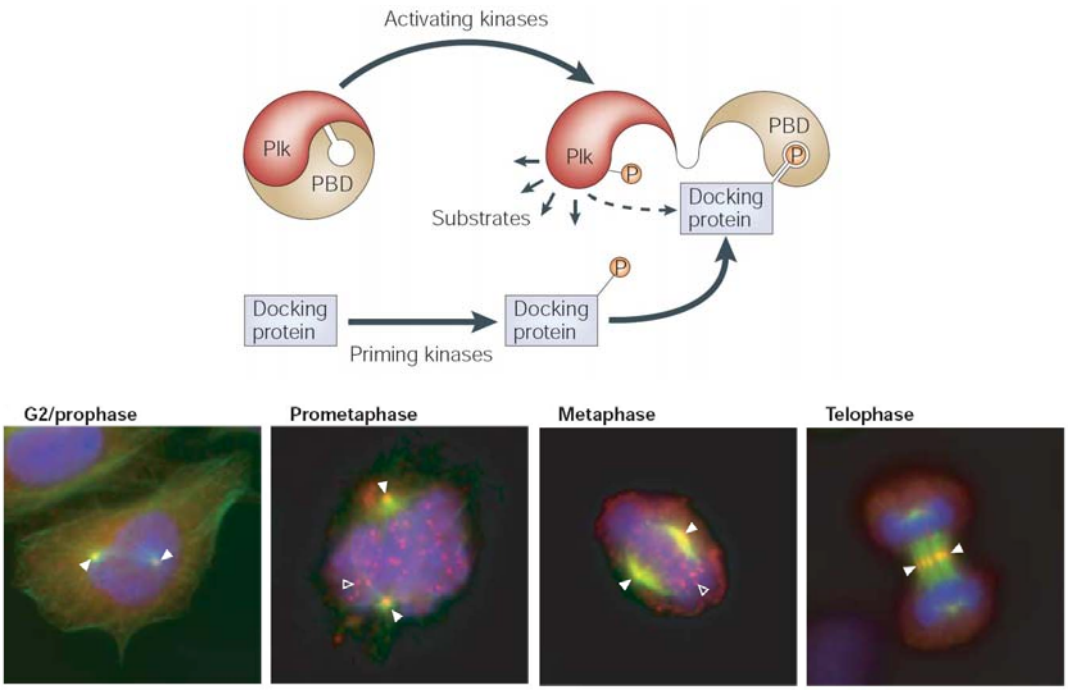

Figure 5. Targeting to docking proteins and localization of Plk1. (A) Model of polo-box domain mediated targeting of Plk1 to prephosphorylated docking proteins resulting in an increase of Plk1 activity. Moreover, Plk1 activity is stimulated upon phosphorylation by an upstream kinase. (B) Immuno-fluorescence images illustrating the localization of Plk1 during the cell cycle. Plk1 (in red, arrows) localizes to the centrosomes, spindle poles, and KTs in prophase and metaphase, the central spindle and the midbody upon anaphase. Illustrations adapted from (Barr et al., 2004).

Consistent with the dynamic localization of Plk1 in mitosis, it has been shown that Plk1 has various functions during mitotic progression (Figure 6). As mentioned previously Plk1 has been implicated in the activation of Cdk1/cyclin B1 at mitotic entry (Toyoshima-Morimoto et al., 2002; Toyoshima-Morimoto et al., 2001; Watanabe et al.,

2004), centrosome maturation and bipolar spindle formation (Lane and Nigg, 1996; Sumara et al., 2004; van Vugt and Medema, 2004). Plk1 also assists sister chromatid resolution by removing cohesion from chromosome arms in early prophase and prometaphase (Hauf et al., 2005; Sumara et al., 2002). However it seems not to be essential for sister chromatid separation, since even in Plk1-depleted cells chromosomes are still able to separate by cleavage when forced to enter anaphase (Gimenez-Abian et al., 2004). Moreover, Plk1 is involved in the recruitment of spindle assembly checkpoint (SAC) proteins at the KT (Ahonen et al., 2005; Kang et al., 2006; Wong and Fang, 2006). A recent study revealed that tension sensitive Plk1 phosphorylation on BubR1 regulates the stability of KT-MT interactions (Elowe et al., 2007). Besides, Plk1 is involved in late mitotic events and cytokinesis (Lindon and Pines, 2004; Neef et al., 2003; Petronczki et al., 2007; Santamaria et al., 2007; Seong et al., 2002; Zhou et al., 2003). Recently it has been proposed that late mitotic Plk1 activity promotes recruitment of Ect2 to the central spindle, triggering the initiation of cytokinesis and contributing to cleavage plane specification (Brennan et al., 2007; Burkard et al., 2007; Petronczki et al., 2007). Ect2, a Rho guanine nucleotide exchange factor (GEF), plays a role in the processes which specify the cleavage plane (Chalamalasetty et al., 2006; Yuce et al., 2005). Taken together, Plk1 is involved in multiple steps during mitosis, but still there are numerous open questions concerning Plk1's function in the orchestration of cell division.

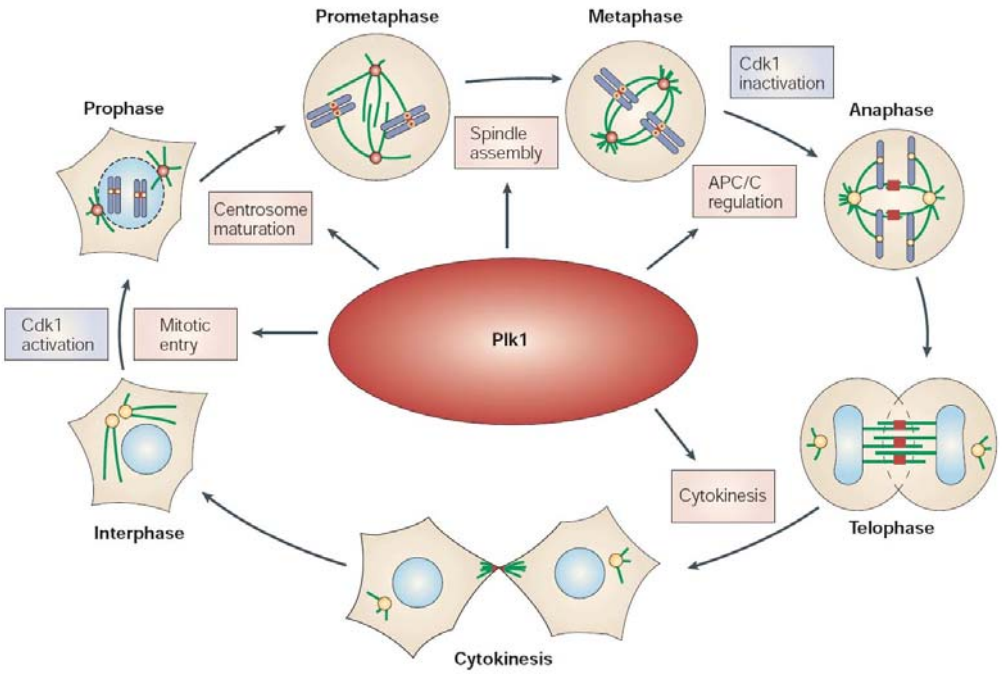

Figure 6. Overview of the various functions of Plk1 in the cell cycle. Illustration adapted from (Barr et al., 2004).

2.4. Mitotic phosphatases

Besides kinases also phosphatases play an important role in the regulation of mitosis, by reversing protein phosphorylations. Recent studies revealed how the dual specificity protein phosphatases Cdc14 and Cdc25 and the protein serine/threonine phosphatases PP2A and PP1 contribute to mitotic regulation. PP2A is involved in the control of sister chromatid cohesion. It protects centromeric cohesin by dephosphorylation of the cohesin complex subunit SA2, and thus counteracts Plk1-dependent phosphorylation of cohesin (for further details see introduction, chapter 3.2) (Kitajima et al., 2006; McGuinness et al., 2005; Riedel et al., 2006; Tang et al., 2006; Watanabe and Kitajima, 2005). Moreover, budding yeast PP2A has been implicated to play a role in the regulation of mitotic exit (Wang and Ng, 2006). PP1 has been suggested to play a role in chromosome segregation in budding yeast (Pinsky et al., 2006) and to contribute to centrosome structure in mammalian cells (Meraldi and Nigg, 2001).

As mentioned in chapter 2.2, Cdc25 is involved in the regulation of early mitotic events (Hoffmann et al., 1993; Hofmann et al., 1998). In contrast to that, Cdc14 is

involved in the regulation of late mitotic events. Budding yeast Cdc14p plays a key role in mitotic exit by dephosphorylating Cdk targets (Bardin and Amon, 2001; Jaspersen et al., 1998; Visintin et al., 1998). Mammalian cells express two homologs of Cdc14, termed hCdc14A and hCdc14B, which are both functional homologs of yeast Cdc14 (Vazquez-Novelle et al., 2005). The functions of the human paralogs hCdc14A and B are not well understood. HCdc14A has been implicated in the centrosome duplication cycle, the regulation of chromosome segregation, anaphase and cytokinesis (Kaiser et al., 2002; Mailand et al., 2002).

3. Mitotic structures and spindle assembly

Mitosis involves a complex self organization process that drives the transient assembly of dynamic MTs into a bipolar spindle around the chromosomes to segregate them to the daughter cells. Centrosomes and KTs are key structural components involved in this process.

3.1. The centrosome

Centrosomes are MT organizing centres (MTOC) of animal cells (Bornens, 2002; Doxsey, 2001; Lange, 2002). They influence all MT dependent processes, including organelle transport, cell shape, polarity and motility (Meraldi and Nigg, 2002). In mitosis, centrosomes contribute to the formation of the bipolar spindle and might also be involved in cytokinesis (Gromley et al., 2003; Piel et al., 2001). The mammalian centrosome comprises a pair of orthogonally arranged barrel shaped centrioles surrounded by the fibrous pericentriolar matrix (PCM), an electron dense structure (Doxsey, 2001) (Figure 7). The PCM is the site of MT nucleation and it provides docking sites for numerous proteins involved in this process, chiefly members of the γ-tubulin ring complex (γTuRC) (Moritz et al., 1995; Zheng et al., 1995). The PCM acts primarily as the MTOC, which nucleates the interphase microtubular array and essentially all the spindle MTs during mitosis (Euteneuer and McIntosh, 1981).

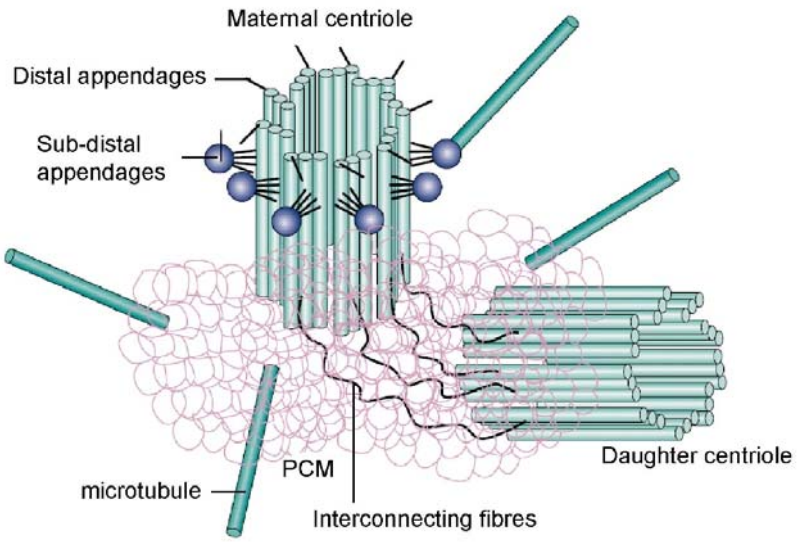

Figure 7. Structure of the centrosome. Illustration of the centrosome, showing that one centrosome consists of two centrioles (maternal and daughter centriole). The centrosome is surrounded by the pericentriolar matrix (PCM). Illustration adapted from (Doxsey, 2001).

Like chromosomes, centrosomes duplicate precisely once every cell cycle (Figure 8) (Nigg, 2002). The fidelity and correct timing of centrosome duplication is essential for ensuring that this process is effectively coupled to cell cycle progression and DNA replication (Hinchcliffe and Sluder, 2001). G1 cells contain a single centrosome, which acts as the sole MTOC by nucleating MTs. The centrosome duplicates during S phase, when new centrioles form adjoining to each of the two pre-existing ones. Hence in G2 the cell contains two centrosomes, each consisting of two closely associated (engaged) centrioles. The two centrosomes remain tightly associated until entry into mitosis, when centriole separation takes place, which involves the activation of several kinases, including Nek2, Cdk1, Aurora A and Plk1 (Berdnik and Knoblich, 2002; Blangy et al., 1995; Fry et al., 1998; Glover et al., 1995; Golsteyn et al., 1995; Hannak et al., 2001; Lane and Nigg, 1996; Sawin and Mitchison, 1995). In addition to these proteins, also the phosphatase Cdc14A may be involved in centrosome separation (Mailand et al., 2002). Upon entry into mitosis each centrosome nucleates MTs and acts as a MTOC so that two prominent mitotic asters are generated forming the bipolar MT array. During exit from M phase the two centrioles present within each centrosome disengage, in response to the activation of the protease separase (Tsou and Stearns, 2006a). This has led to an appealing model according to which centriole disengagement constitutes a licensing mechanism for

ensuring that centrioles duplicate only once in every cell cycle (Tsou and Stearns, 2006a; Tsou and Stearns, 2006c; Wong and Stearns, 2003).

Deregulation of centrosome duplication results in cells with multiple centrosomes and the assembly of multipolar spindles leading to chromosome instability (Brinkley, 2001; Nigg, 2002). In fact, cells from many tumors are known to exhibit extra copies of centrosomes (Carroll et al., 1999; Lingle et al., 1998; Pihan et al., 1998), indicating an underlying deregulation of centrosome structure, segregation, disengagement or duplication.

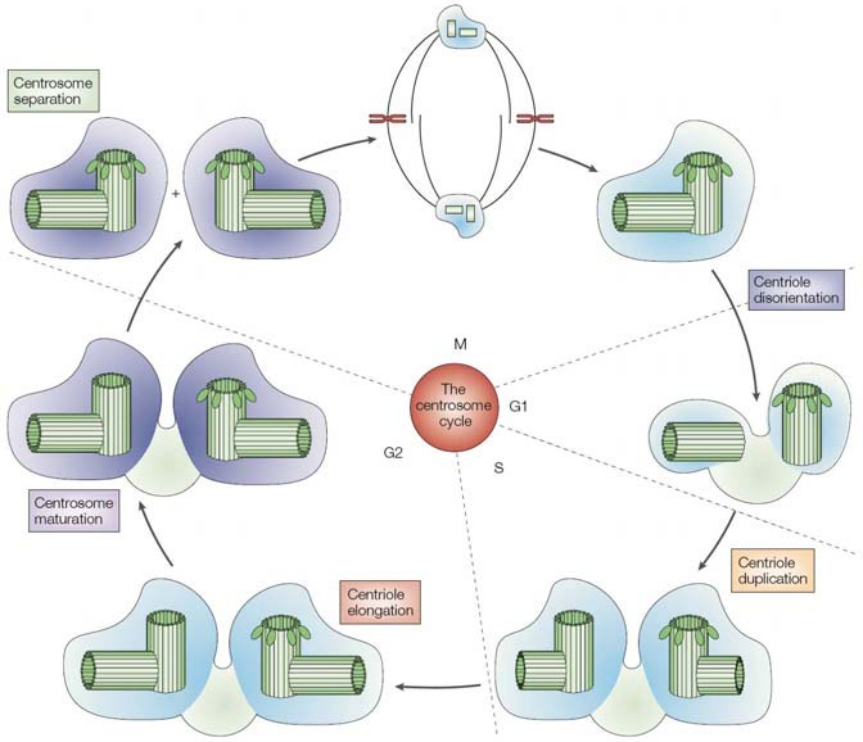

Figure 8. The centrosome cycle. Illustration showing the different stages during the centrosome cycle. Note centriole disorientation is also named centriole disengagement. Illustration adapted from (Nigg, 2002).

At least four mechanisms exist that allow cells to acquire additional centrosomes: deregulation of centrosome duplication, *de novo* formation of centrioles, cell fusion or cytokinesis failure (Goepfert, 2004).

Centriole duplication may be deregulated by defects in the mechanism that ensures duplication is restricted to once per cell cycle (Tsou and Stearns, 2006a; Wong and Stearns, 2003). This has been observed in some transformed cell lines, such as

Chinese Hamster Ovary (CHO) cells, when centrosome duplication was dissociated from cycles of DNA synthesis and mitotic division by arresting cells at the G1/S boundary of the cell cycle using either hydroxyurea or aphidicolin. These cells underwent multiple rounds of centrosome replication during a prolonged S phase (Balczon et al., 1995). Centriole overduplication can also be induced by overexpression of human Sas-6 or Plk4, the key regulator of centriole duplication (Habedanck et al., 2005; Leidel et al., 2005). Additional MTOCs may be obtained by *de novo* formation of centrioles, a mechanism normally suppressed by pre-existing centrioles (Khodjakov et al., 2000), splitting of existing centriole pairs, thereby generating two centrosomes consisting of one single centriole and PCM (Hut et al., 2003; Keryer et al., 1984; Sluder and Rieder, 1985) or by overexpressing PCM components that lead to the formation of acentriolar centrosome fragments with MT nucleating abilities. All these mechanisms result in the formation of diploid cells with supernumerary centrosomes.

Moreover failure of cytokinesis results in excess centrosome numbers, which will lead to centrosome amplification and polyploidy and has been shown to result in tumorigenesis (Fujiwara et al., 2005). Apart from numerical aberrations structural changes of the centrosome through deregulated gene expression of centrosomal proteins or altered posttranslational modifications, such as aberrant phosphorylation may stimulate or suppress MT nucleation (Casenghi et al., 2003; Lingle and Salisbury, 2001). Loss of MT anchoring proteins, such as TOGp, which functions primarily to maintain the integrity of centrosomes and the spindle poles during mitosis, results in fragmentation of the centrosome and multipolarity (Cassimeris and Morabito, 2004; Holmfeldt et al., 2004). Taken together, these data indicate that centrosome duplication and centrosome structure have to be tightly regulated for ensuring correct function of this organelle during the cell cycle.

3.2. The kinetochore and sister chromatid cohesion

KTs are specialized protein complexes, which are located on opposite sides of the centromere region and function as major sites of MT chromosome attachment (Brinkley and Stubblefield, 1966; Jokelainen, 1967). Electron microscopy analysis reveals that the vertebrate KT is composed of several distinct layers (McEwen et al., 1998), the inner

plate, the interzone, the outer plate and the fibrous corona (Figure 9) (Rieder and Salmon, 1998). The inner plate exists as a discrete heterochromatin domain throughout the cell cycle and is essential for KT assembly. It is formed on highly repetitive α-satellite sequences and characterized by the incorporation of the centromere specific histone H3 variant centromeric protein A (CENP-A) (Palmer et al., 1991; Sullivan et al., 1994). CENP-A is the earliest protein during KT assembly and required for the recruitment of most known KT components (Howman et al., 2000). It has been shown that, together with CENP-A, six inner plate KT proteins assemble hierarchically and co-dependently, CENP-A, Mis12, CENP-C, CENP-H and CENP-I (Figure 9) (Amor et al., 2004). Recent studies revealed that there are additional inner plate KT proteins involved in this assembly pathway, e.g. CENP-M, CENP-N, CENP-T (Foltz et al., 2006). The protein composition of the interzone is not known (Chan et al., 2005). The outer plate and its associated fibrous corona assembles and functions only during mitosis. It is a proteinaceous structure with very dynamic components, which regulates MT attachments and dynamics and is involved in checkpoint signalling. It comprises structural components, such as the Hec1/Ndc80 complex (Ciferri et al., 2005; DeLuca et al., 2005), checkpoint proteins (e.g. Mad1, Mad2, BubR1) (Musacchio and Hardwick, 2002) that monitor the integrity of KT-MT attachments (see 4.1, introduction), non-motor MT associated proteins (MAPs), such as CLASPs, CLIP-170, EB1 (Dujardin et al., 1998; Maiato et al., 2003; Pereira et al., 2006; Tirnauer et al., 2002) and MT dependent motor proteins as CENP-E and dynein (Steuer et al., 1990; Yao et al., 1997; Yen et al., 1992). The centromeric heterochromatin, the region between two sister KTs, contains the proteins of the chromosomal passenger complex (CPC) (Vagnarelli and Earnshaw, 2004) and the depolymerase MCAK (Kline-Smith et al., 2004), which are involved in the correction of improper MT attachments (Andrews et al., 2004).

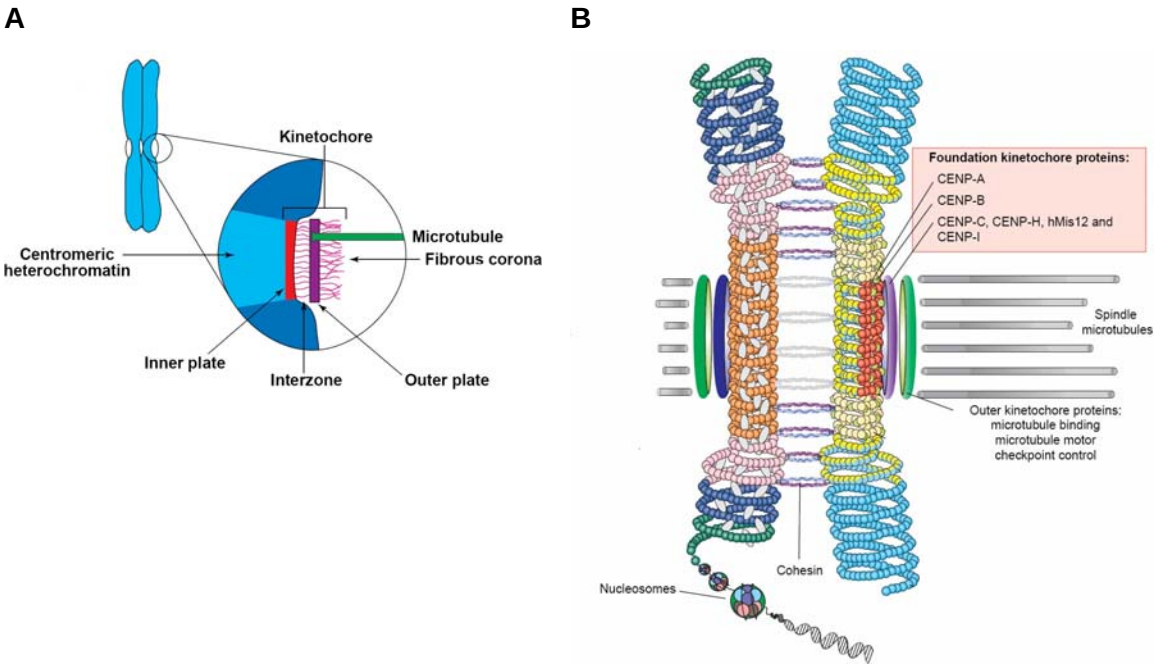

Figure 9. **Illustrations showing the structure of the vertebrate KT.** (A) Illustration adapted from (Rieder and Salmon, 1998). (B) Simplified model of the 3D organization of the human centromere. Illustration adapted from (Amor et al., 2004).

Sister chromatids are tightly interlinked by the evolutionary conserved cohesin complex (Figure 9) of four core subunits: the kleisin family protein SCC1; two subunits of the structural maintenance of chromosomes (SMC) family Smc1 and Smc3; and an accessory subunit Scc3, which has two orthologs in mammals called SA1 and SA2. The cohesin complex has been proposed to form a ring structure that encircles sister chromatids (Hirano, 2005; Nasmyth and Haering, 2005). Sister chromatid cohesion is established during S phase, maintained through metaphase (Guacci et al., 1994; Uhlmann and Nasmyth, 1998), when it allows each sister pair to be attached to the spindle with a bipolar orientation, and then dissolved at anaphase onset to enable sister chromatids to segregate. The dissolution of cohesin during mitosis happens in two steps, most of the cohesin dissociates from the chromosome arms before metaphase, in a process called "prophase pathway". Plk1 phosphorylation of the SA2 subunit triggers the dissociation of cohesin from chromosome arms (Hauf et al., 2005; Sumara et al., 2002). Aurora B kinase may contribute to this process (Hauf et al., 2005). Moreover, the protein Wapl was recently identified as an essential component of the cohesion removal pathway that operates during prophase (Gandhi et al., 2006; Kueng et al., 2006).

The dissociated cohesin is not cleaved, but instead relocates to chromatin in telophase to function in the next cell cycle.

A small fraction of cohesin is maintained at the centromeric region until anaphase onset. This centromeric cohesin is protected from the prophase pathway by the centromeric protein Shugoshin (Sgo) and a specific subtype of serine/threonine phosphatase 2A (PP2A) associating with Shugoshin. PP2A protects centromeric cohesin by dephosphorylation of SA2, and thus counteracts Plk1-dependent phosphorylation of cohesin. This prevents dissociation of cohesin from the centromeres (Kitajima et al., 2006; McGuinness et al., 2005; Riedel et al., 2006; Tang et al., 2006; Watanabe and Kitajima, 2005). However Shugoshin may have another unidentified activity that protects cohesin at the centromere independently of PP2A (Kitajima et al., 2006). Upon anaphase onset the Scc1 subunit of the residual centromeric cohesin is cleaved by the cysteine protease separase, leading to sister chromatid separation (Hauf et al., 2001)

3.3. Mitotic spindle assembly

The basic structural components of the mitotic spindle are MTs, polar dynamic fibres that polymerize from tubulin subunits (Desai and Mitchison, 1997), as well as hundreds of other proteins that function together to orchestrate chromosome segregation. The mitotic spindle starts forming during prophase when the two radial MT arrays nucleated at the centrosome migrate apart to form the bipolar spindle, a movement which involves the motor protein Eg5 (Blangy et al., 1995). These MT arrays will finally form an antiparallel array of MTs with their minus ends anchored at the spindle poles and their plus ends projecting towards the chromosomes (Figure 10). This polar lattice serves as a track for MT based motor proteins of the dynein and kinesin superfamily, which use ATP hydrolysis to generate movement, alter MT dynamics and function in spindle organization (Hirokawa et al., 1998; Kim and Endow, 2000; Sharp et al., 2000).

Spindle MTs are highly dynamic structures with a half-life of 60-90 seconds, this characteristic known as dynamic instability is fundamental to mitotic spindle structure and regulation (Joshi, 1998; Mitchison and Kirschner, 1984; Saxton et al., 1984). The dynamic instability of MTs was the prerequisite for the “search and capture” model of how KTs acquire MTs during mitosis (Mitchison and Kirschner, 1984). This model

describes the *in vitro* and *in vivo* behaviour of MTs wherein MT plus ends undergo dynamic instability, with stochastic switching from growth to shortening ('catastrophe'), and from shortening to growth ('rescue'). Thus the plus ends of MTs nucleated at the centrosomes grow, shrink and regrow, randomly (Figure 10). Contact of these 'searching' MTs with a KT results in 'capture' of a chromosome and stabilization of MTs, whereas those that fail to capture KTs depolymerize (Hayden et al., 1990). Once this association is established, the KT is rapidly transported poleward along the MT lattice (Rieder and Alexander, 1990), by a mechanism that is not dependent on MT depolymerization, but most likely accomplished by the minus-end directed motor activity of dynein (Sharp et al., 2000). The attached KT can now capture the sides or plus-ends of additional MTs. As a result, the KT establishes a relatively stable connection to the pole. This monooriented chromosome is pushed away form the spindle pole to the cell equator by MT dependent polar ejection forces (PEFs). PEFs are postulated to be caused by plus-end-directed MT based motor proteins on the chromosome arms, named chromokinesins, and the elongation of spindle MTs (Brouhard and Hunt, 2005; Mazumdar and Misteli, 2005). Moreover, the protein kinase Aurora B is involved in the destabilization of mono-attached MTs, which results in a stabilization of only bipolar attachments (Andrews et al., 2004; Hauf et al., 2003; Tanaka et al., 2002).

Once both sister KTs of a chromosome are attached to MTs from opposite poles (bipolar attachment), the newly bioriented chromosome will congress, i.e. progressively move, to the spindle equator (Figure 10A). Thus it is assumed that chromosome congression requires the prior connection to the opposite poles of the bipolar spindle. However, recently it has been shown that chromosomes near the poles can congress to the metaphase plate before becoming bioriented, by attaching to and sliding along the MT fibre of another already aligned chromosome [Figure 9C (4)]. This congression mechanism is dependent on the KT-associated, plus end–directed MT motor CENP-E (kinesin-7) (Kapoor et al., 2006).

However, the 'search and capture' model does not coincide with mathematical modelling of KT capture, which predicted that several hours would elapse before each of 92 KTs in a human cell had captured MTs (Wollman et al., 2005). Furthermore, mitotic spindles assemble independently of centrosomes, when centrosomes are removed from

mitotic cells by laser ablation or from interphase cells with a microneedle (Hinchcliffe et al., 2001; Khodjakov et al., 2000). These observations indicated that beyond the search and capture model based on the intrinsic behaviour of centrosome-nucleated MTs alternative and/or supplementary spindle assembly mechanisms exist. Spindle assembly experiments with *Xenopus* egg extract revealed that spindles can form in the absence of KTs, or even chromosomes, by addition of DNA coated beads to *Xenopus* egg extract (Heald et al., 1996). It was shown that this is caused by the presence of Ran-GTP, which promotes MT nucleation and stabilization (Carazo-Salas et al., 1999; Wilde et al., 2001) and is present in a concentration gradient around mitotic chromosomes (Kalab et al., 2002). The gradient is established by the chromatin-bound Ran-GTP exchange factor RCC1 (Carazo-Salas et al., 1999) and has been proposed to contribute to spindle formation through two mechanisms. The first involves direct stimulation of MT nucleation by chromatin (Heald et al., 1996; Karsenti and Vernos, 2001); the second acts by creating a local concentration of MT stabilizing factors around the chromosomes to promote the capture of astral MTs (Bastiaens et al., 2006). Ran-GTP-dependent spindle assembly has so far been demonstrated primarily in extracts of *Xenopus* eggs, and it remains unclear whether it is the predominant mechanism by which chromosomes stimulate spindle assembly in all cells. Other mechanisms clearly exist. As mentioned earlier, the action of MT based motor proteins of the dynein and kinesin families promote spindle assembly and bipolarity. For instance the plus-end directed motor CENP-E, the minus-end directed motor protein dynein and the chromokinesin KIF4A contribute to spindle assembly (Kapoor et al., 2006; Mazumdar et al., 2004; Merdes et al., 2000). Thus many factors important for mitotic spindle assembly and function exist and still some basic principles will be uncovered by future research.

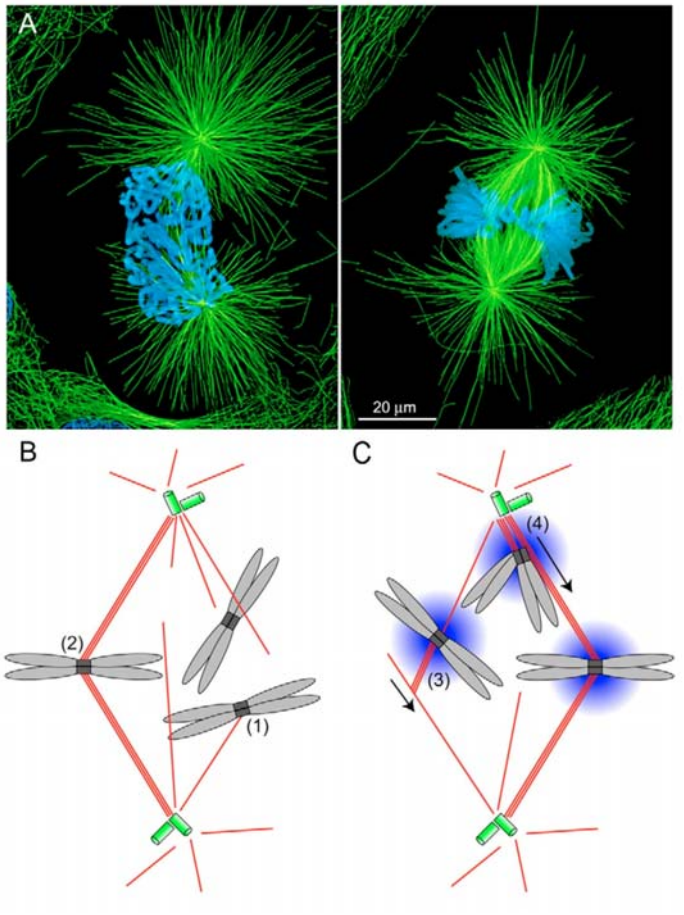

Figure 10. The process of mitotic spindle formation. (A) Immunofluorescence pictures of newt lung cells. MTs are shown in green and DNA in blue. The centrosomes with the two MT arrays of astral (left) and metaphase spindle (right) are illustrated. (B) Original search-and-capture models of chromosome congression. (1) Successive capture events of MTs on sister KTs (2) lead to bi-orientation and congression (2). (C) Additional mechanisms of spindle assembly. (3) KT-fibres nucleated at KTs via a Ran-GTP gradient (blue) elongate toward the periphery and capture astral MTs. (4) Chromosomes attached to only one pole use K-fibres of already bi-oriented chromosomes. This results in congression before bi-orientation (4). Illustration adapted from (O'Connell and Khodjakov, 2007)

4. The spindle checkpoint and anaphase entry

The events of early mitosis, spindle assembly and chromosome congression, bring the cell to metaphase. The progression through the metaphase-to-anaphase transition is restrained by the spindle assembly checkpoint (SAC) until all sister-chromatids have undergone proper bipolar attachment to the spindle. As soon as this prerequisite is satisfied anaphase onset begins with the simultaneous cohesin cleavage by separase and separation of all sister chromatids.

4.1. The spindle assembly checkpoint

The SAC plays a key role in ensuring the fidelity of chromosome segregation. It monitors bipolar attachment of sister chromatids and tension that is exerted at KTs upon bipolar attachment, it delays mitotic progression until all chromosomes have become bi-oriented on the metaphase plate and thus prevents premature sister chromatid separation. The first components of the SAC were identified by two genetic screens in *Saccharomyces cerevisiae*, including the MAD (mitotic-arrest deficient) genes Mad1, Mad2 and Mad3 (BubR1 in humans) and the Bub (budding uninhibited by benzimidazole) gene Bub1. Mad and Bub mutant strains of *S. cerevisiae* failed to properly arrest their cell cycles at mitosis in response to spindle poisons (Hoyt et al., 1991; Li and Murray, 1991). These genes are conserved in all eukaryotes and their products are components of the SAC.

The SAC targets the APC/C co-factor Cdc20 and thereby blocks its function as APC/C activator (Hwang et al., 1998; Kim et al., 1998; Peters, 2006). The precise *in vivo* form of the APC/C^{Cdc20} inhibitor is still an issue of debate but the mitotic checkpoint complex (MCC) that contains three SAC proteins, Mad2, BubR1/Mad3 and Bub3, as well as Cdc20 has emerged in recent years as a possible SAC effector (Fang et al., 1998; Hardwick et al., 2000; Morrow et al., 2005; Sudakin et al., 2001). The MCC inhibits the capability of APC/C^{Cdc20} to ubiquitinate securin, the inhibitory subunit of separase, (see also chapter 4.2 of introduction), and cyclin B1, the activatory subunit of Cdk1, and thereby prevents their degradation by the 26S proteasome and mitotic exit (Peters, 2002; Peters, 2006) (Figure 11). Besides the MCC, additional components of the SAC exist. Among them are the Aurora B, Bub1 and the Mps1 kinases, which are involved in amplifying the SAC signal and might stimulate directly the formation of the MCC, but the mechanistic details are still unclear (Abrieu et al., 2001; Hauf et al., 2003; Kallio et al., 2002b; Morrow et al., 2005; Tang et al., 2004). The Ndc80/Hec1 complex is required for Mad1 and Mad2 binding to KTs and thus for sustaining the checkpoint (DeLuca et al., 2003). Additional proteins that are involved in SAC signalling are $p31^{comet}$, which antagonizes the function of Mad2 (Xia et al., 2004), and the motor proteins dynein and CENP-E (Chan et al., 1999; Howell et al., 2001; Mao et al., 2005). It has been demonstrated that the dynein-dynactin complex transports the Mad1, Mad2 and other proteins away from the KT to the poles upon the attachment of MTs and thus is involved

in checkpoint silencing (Howell et al., 2001; Wojcik et al., 2001). CENP-E has been implicated in checkpoint signalling through binding to the mitotic checkpoint kinase BubR1 and monitoring KT-MT interactions. This makes CENP-E a possible candidate for being a link between attachment and SAC signalling (Chan et al., 1999; Jablonski et al., 1998; Yao et al., 2000).

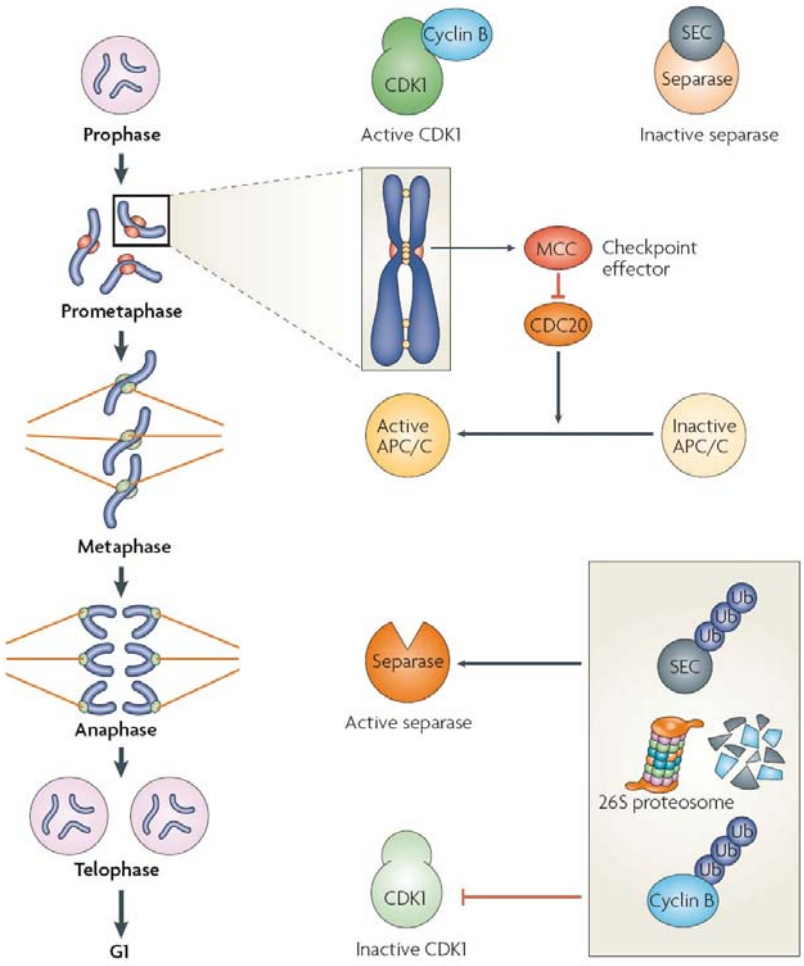

Figure 11. The SAC and the cell cycle. Illustration adapted from (Musacchio and Salmon, 2007).

During prometaphase, Cdc20 and all SAC proteins are bound to unattached KTs (Cleveland et al., 2003; Maiato et al., 2004) and then released upon bipolar attachment, suggesting that they are directly involved in the generation of a signal that blocks anaphase onset, the 'wait anaphase' signal (Chen et al., 1998; Chen et al., 1996; Taylor et al., 1998; Taylor and McKeon, 1997). In fact, it was shown that a single unattached KT

acts as source of a diffusible signal that is sufficient to block anaphase onset (Rieder et al., 1995). Fluorescence recovery after photobleaching (FRAP) demonstrated that Bub1, Mad1 and one pool of Mad2 are stable KT components unlike BubR1, Bub3, Cdc20 and a second pool of Mad2, which are proteins with fast turnover at KTs (Howell et al., 2000; Howell et al., 2004; Kallio et al., 2002a; Shah et al., 2004). These observations suggest that there is a stable catalytic platform at the KT that senses lack of MT attachment and activates Mad2, Bub3 and BubR1 to form the MCC with Cdc20.

Two related but distinct models of Mad1-assisted activation of Mad2, the 'two-state Mad2' and the 'Mad2 template' models have been proposed (De Antoni et al., 2005; Luo et al., 2004; Yu, 2006). These models describe the essential role of Mad1 in promoting binding of Mad2 to Cdc20, not involving BubR1 and Bub3. They depict the Mad1-assisted activation of Mad2, but still there are numerous open questions. Is the interaction between Mad2 and Cdc20 alone sufficient to explain how the SAC keeps the APC/C inactive? How does the MCC form and how does it bind and inhibit APC/C? How do other checkpoint proteins fit into this model? Thus many aspects of the model require further investigation.

4.2. Separase and anaphase entry

As described previously (introduction, chapter 4.1) entry into anaphase depends on all chromosomes being attached in a bipolar manner. Once this is achieved, sister chromatid separation is triggered by separase, a cysteine endopeptidase, which cleaves the cohesin subunit kleisin Scc1/Rad21 (see also introduction, chapter 3.2) (Uhlmann et al., 2000; Waizenegger et al., 2000). Separase is inhibited by its chaperone securin, which prevents access of substrates to the active site of separase (Waizenegger et al., 2002). In vertebrate cells separase activity is also suppressed by Cdk1/cyclin B1 mediated phosphorylation on serine 1126 followed by binding of cyclin B1 (Ciosk et al., 1998; Gorr et al., 2005; Holland and Taylor, 2006). Cdk1/cyclin B1 and securin bind separase in a mutually exclusive manner, which indicates that these two mechanisms may play redundant roles in inhibiting separase during mitosis (Gorr et al., 2005; Holland and Taylor, 2006). Destruction of both securin and cyclin B1 after ubiquitinylation by APC/C (see also introduction, chapter 2.2 and 4.1) results in the activation of the protease activity of

separase. In humans active separase undergoes self-cleavage, resulting in a 65 kDa C-terminal fragment (Papi et al., 2005; Waizenegger et al., 2002). Self-cleavage of separase in anaphase of the previous cell cycle is supposed to effect mitotic entry and progression through early mitosis (Papi et al., 2005). Furthermore, it was shown that upon degradation of securin in anaphase, vertebrate separase can act as a direct inhibitor of Cdk1. This implies that separase could assist the APC/C in inactivating Cdk1 and promoting mitotic exit (Gorr et al., 2005). In line with that, *S. cerevisiae* separase has a well established role in mitotic exit that does not depend on protease activity (Stegmeier et al., 2002). Taken together, the protease activity of separase is essential for sister chromatid cohesion and anaphase onset. Moreover, recent discoveries indicated that human separase has additional functions, for instance, it is involved in centrosome disengagement (introduction, chapter 3.1) (Gorr et al., 2005; Tsou and Stearns, 2006c). However, further functions of separase and the mechanisms of separase activation and regulation remain to be established.

AIM OF THE WORK

The MT associated protein (MAP) astrin was identified in the course of a mass spectrometry-based analysis of proteins associated with MTs in a mammalian mitotic extract. Except for a large predicted coiled-coil domain in its C-terminal region it lacks any known functional motifs (Mack and Compton, 2001). It has been indicated that astrin is required for spindle organization and mitotic progression, since astrin depletion results in highly disordered spindles and mitotic arrest (Gruber et al., 2002; Mack and Compton, 2001). Despite these initial reports, very little was known about astrin's function during mitosis. Therefore, the aim of this study was to characterize the requirements for astrin's KT and spindle localization, to identify interaction partners and to reveal the function of human astrin in mammalian cells.

RESULTS

1. Initial characterization of astrin

Astrin has previously been described as a spindle-associated protein involved in mitotic progression (Chang et al., 2001; Gruber et al., 2002; Mack and Compton, 2001). To explore the role of astrin during mitosis, a polyclonal rabbit antibody was raised against astrin. After having established its specificity, the anti-astrin antibody was used for the characterization of astrin.

1.1. Astrin is a mitotic spindle and outer kinetochore protein

To analyse astrin a polyclonal rabbit antibody was raised against the N-terminus (aa 1-481) and affinity purified. Moreover an affinity purified antibody raised against the C-terminus (aa 1014-1193) was used (a kind gift from Ulrike Grüneberg). Both purified antibodies show the same results in Western blot (Figure 13A and B) and immunofluorescence and are specific for astrin. As shown in Figure 13F the affinity-purified antibodies recognized a double band of ca. 135/120 kDa on Western blots of whole HeLa cell lysates, which disappeared upon siRNA-mediated depletion of astrin (Figure 12A, B and C). In line with that, immunofluorescence analysis demonstrated that the staining obtained with the anti-astrin antibody disappeared upon RNAi mediated depletion of astrin (Figure 13B).

In order to confirm that both bands recognized by the antibodies in Western blot are astrin, mass spectrometric (MS) analysis was performed (by Roman Körner and Xiumin Li) on astrin immunoprecipitations (IPs). HeLa cells were synchronized in mitosis by release from an aphidicolin block into nocodazole. The cells were harvested by mitotic shake off and released for 30 min in order to rebuild the mitotic spindle. Astrin was immunoprecipitated (IPed) from the mitotic extracts with anti-astrin antibodies and protein G beads and loaded on a gradient NuPAGE gel. Distinct bands specific for astrin (Figure 12D) were cut from the gel, in-gel digested with trypsin and analysed by MS. Besides the two astrin bands, additional bands were apparent in the astrin IP (Figure 12D). These could be candidate interactors but they could not yet be identified by MS analysis. IPed astrin revealed that the upper band corresponds to full-length astrin,

whereas the lower band lacks approximately 200 amino acids of the N-terminus, presumably due to either internal initiation or post-translational proteolytic processing (see Figure 12E and F for peptide coverage of slow and fast migrating band). Since our data indicate that the smaller of the two isoforms lacks approximately 200 amino acids of the N-terminus, which contains many potential serine or threonine phosphorylation sites, functional differences between the two isoforms might be expected. The nature of these and the question of how the smaller of the two astrin isoforms is generated require further investigation.

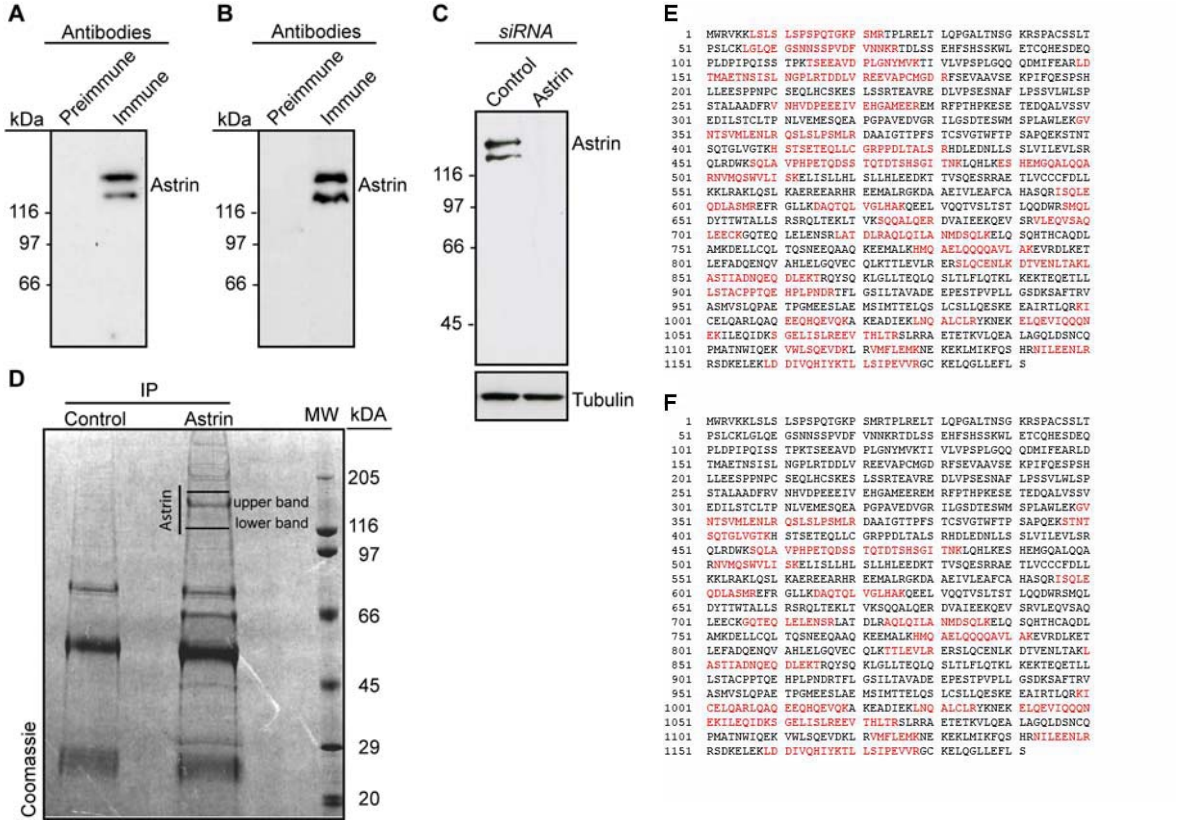

Figure 12. Initial characterization of astrin. (A and B) Antibodies raised against the N-terminus (aa 1-481) or the C-terminus (aa 1014-1193), respectively, were tested in Western blot analysis on whole cell lysates. (A) The antibody raised against the N-terminus recognized two bands of ca. 135/120 kDa (left lane), there was no signal detected for the preimmune serum. (B) The antibody raised against the C-terminus recognized two bands of ca. 135/120 kDa, there was no signal detected for the preimmune serum. (A and B) Both antibodies show the same result in Western blot analysis. (C) Whole cell lysates were prepared form HeLa cells depleted of astrin or control (Gl2). Equal amounts of cell lysates were separated by SDS-PAGE and probed after Western blotting with the indicated antibodies. (D) HeLa cells were synchronized by a sequential aphidicolin/nocodazole block release protocol. Cells were released from nocodazole for 30 min until the majority had reached metaphase before being lysed. Mitotic lysates were incubated with protein G beads and either with anti-astrin antibody or preimmune-sera as control. The beads of the respective IPs were loaded on a NuPAGE gradient gel, which was stained with Coomassie Blue, and indicated protein bands were cut out, followed by MS analysis. (E and F) Peptide coverage of the (E) slow-migrating and the (F) faster-migrating form of astrin. Peptides identified by mass spectrometry are indicated in red.

Immunofluorescence analysis of astrin localization throughout the cell cycle revealed centrosome localization in prophase and prominent spindle pole staining upon spindle formation. Astrin localized to KTs in prometaphase, leading to strong KT and reduced spindle staining in metaphase. This was retained into early anaphase, with a small pool of the protein transferring to the central spindle area. In telophase, the KT staining was lost and astrin concentrated in the spindle midzone (Figure 13A). The localization observed with the rabbit anti-astrin antibody was confirmed by transient transfection of Myc-astrin (Figure 13C). Taken together, these data show that astrin is a mitotic spindle and KT associated protein, confirming earlier reports (Gruber et al., 2002; Mack and Compton, 2001).

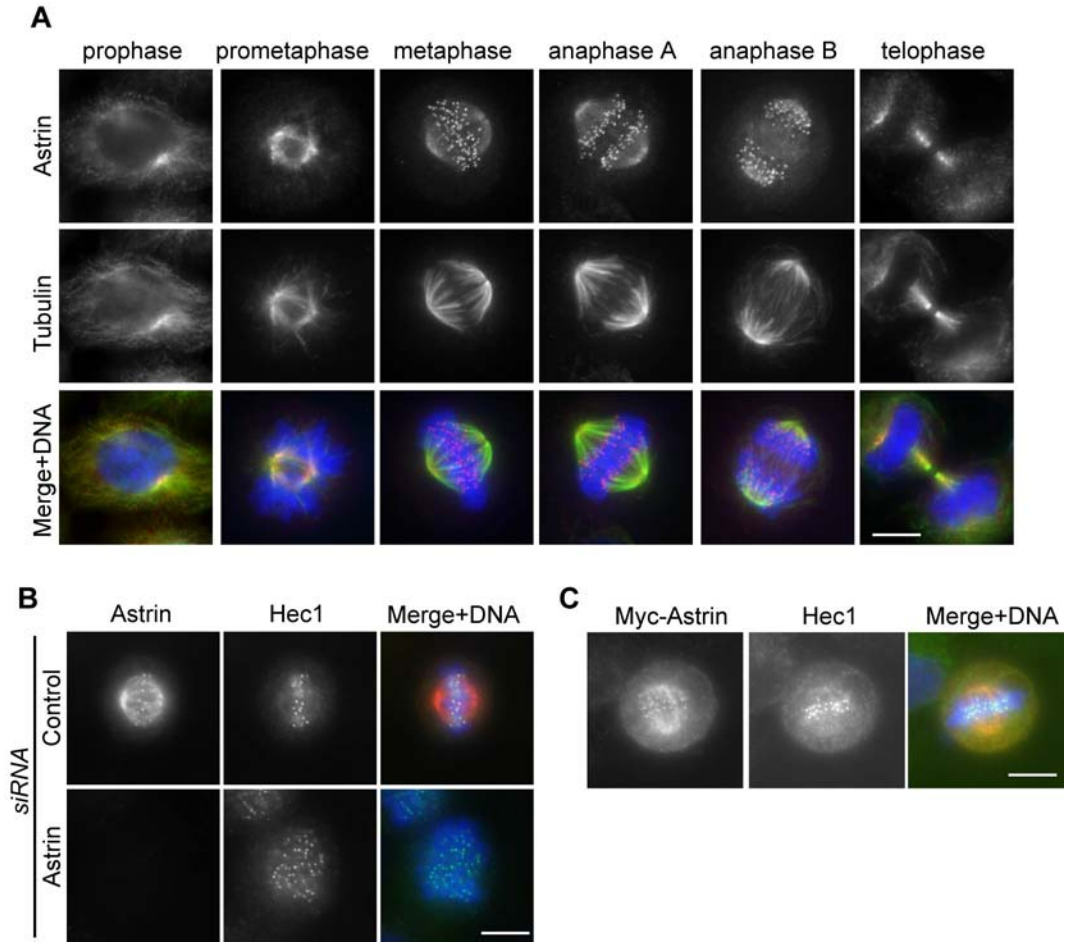

Figure 13. Antibody characterization and localization of astrin. (A) HeLa cells in different stages of the cell cycle were fixed and stained with antibodies against astrin (red) and tubulin (green). (B) Cell were depleted of astrin or Gl2 (control), cells were fixed after 48 h and stained with antibodies against astrin (red) and Hec1 (green) (C) Myc-astrin was transiently transfected into HeLa cells, after 30 h the cells were fixed and stained with antibodies against Hec1 (green), an outer KT protein, and Myc (red). (A, B, C) DNA (blue) was stained with DAPI. Bar, 10 µm.

For a closer analysis of astrin's localization, a co-staining with either centrosomal or KT markers was performed. During prophase and prometaphase a centrosomal pool of astrin was diffusely localized to the pericentriolar material and MTs emanating from the centrosome, overlapping with but distinct from the areas stained by antibodies against Polo like kinase 1 (Plk1), γ-tubulin and centrin (Figure 14A). A second chromosome-associated pool of astrin partially overlapped with the outer KT components Hec1 and CENP-E and the MT tip-binding protein EB1, but was discrete from other KT proteins such as Plk1, and the centromeric markers Aurora B and CENP-A (Figure 14B). This second pool of astrin is therefore most likely associated with the outer KT. The dual localization of astrin to both centrosomes and the KTs indicates that astrin is required for spindle formation and chromosome segregation.

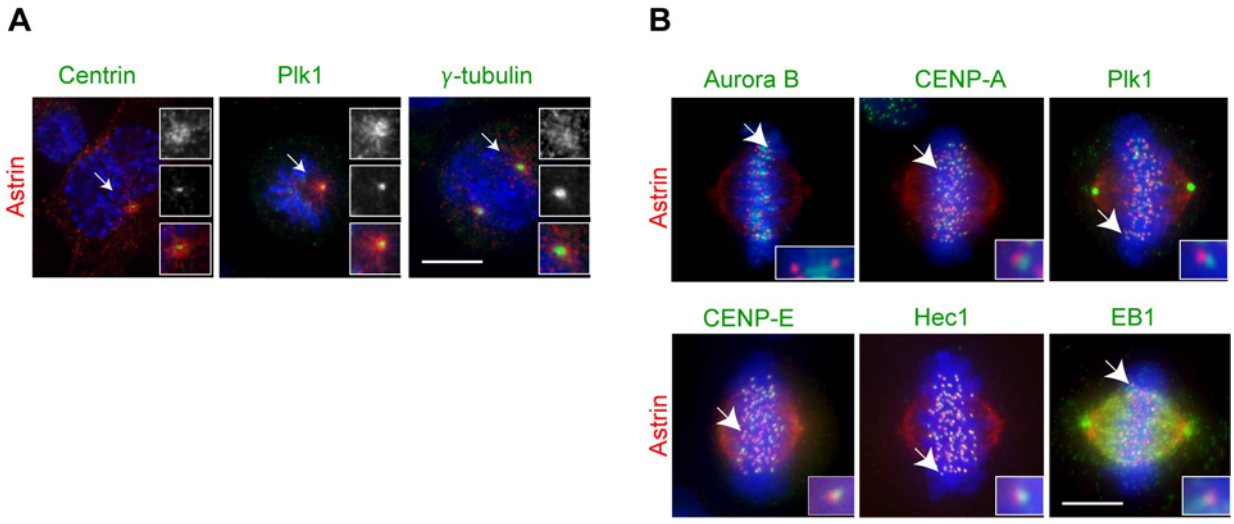

Figure 14. Astrin is an outer KT protein and localizes diffusely to the centrosome. (A) Pro- and prometaphase HeLa cells were stained with antibodies against astrin and centrin, Plk1 or γ-tubulin. Indicated centrosomes are shown enlarged on the right side. Bar, 10 µm. (B) Metaphase HeLa cells were processed for immunofluorescence using antibodies against astrin and Aurora B, CENP-A, Plk1, CENP-E, Hec1 or EB1. The indicated KTs are shown enlarged in the right hand corners of the images. Bar, 10 µm.

1.2. The kinetochore localization of astrin depends on stable MT-KT interactions

It was observed previously that astrin only binds to aligned chromosomes (Mack and Compton, 2001). To further explore these published data we analysed the factors that are required for astrin's localization to the outer KT. As a first approach, Hec1, an outer KT protein required for stable MT-KT interactions (DeLuca et al., 2005; Liu et al., 2007), was depleted by siRNA. The depletion of Hec1 resulted in the loss of astrin from the KTs but not the spindle (Figure 15). In contrast to that, the depletion of Bub1, another outer KT protein (Jablonski et al., 1998), did not influence astrin's localization. This result suggests that astrin is either directly recruited by Hec1, or that the transport of astrin from the spindle onto the KT requires stable MT-KT connections.

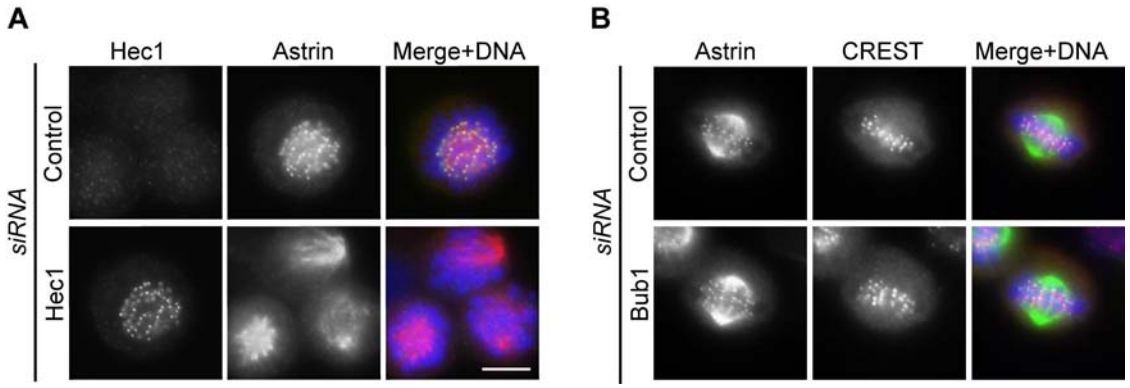

Figure 15. Astrin is lost from the KT after depletion of Hec1. (A) Cells were depleted of Hec1, required for stable MT-KT interactions, fixed and stained with antibodies against Hec1 (green) and astrin (red). (B) As control cells were depleted of Bub1, fixed and stained with antibodies against astrin (green) and CREST (red). (A and B) DNA was stained with DAPI. Bar, 10 μm.

To test the role of MT stability and dynamics in astrin localization we used different drugs that act on MTs and MT associated motors. In order to analyse whether the transport of astrin from the spindle onto the KT requires stable MT-KT interactions, we used nocodazole, a MT depolymerising drug. MT disassembly induced by nocodazole abolished KT, mitotic spindle and pole localization of astrin, and recovery of MTs following washout quickly re-established their localization (Figure 16A). Moreover, the addition of the MT stabilizing drug taxol impaired astrin's localization to KTs (Figure 16B). In the case of monastrol, an inhibitor of the kinesin related motor Eg5 (Mayer et al., 1999), which induces the formation of monopolar spindles, astrin is concentrated at the pole and only some KTs are positive for astrin. This result further supports the idea

that astrin localizes only to fully attached and aligned chromosomes of a bipolar spindle. Consistent with this, it was observed that in cells treated with noscapine, a chemical compound which interferes with MT dynamics and induces chromosome misalignment (Ye et al., 1998; Zhou et al., 2002), only aligned chromosomes stained positive for astrin (Figure 16C), confirming a previous report (Mack and Compton, 2001). Furthermore, costaining of astrin and pBubR1, a phosphospecific antibody which only recognizes BubR1 at chromatids that lack tension (Elowe et al., 2007), revealed that astrin does not localize to such chromatids but instead only binds to chromatids that do not show pBubR1 staining (Figure 16D). Taken together these data show that astrin requires intact MTs to localize to KTs and is thus not a constitutive KT component. It associates with KTs of only those sister chromatids that are aligned at the metaphase plate and under tension. Thus it would be attractive to speculate that astrin could contribute to generate a signal for the metaphase to anaphase transition.

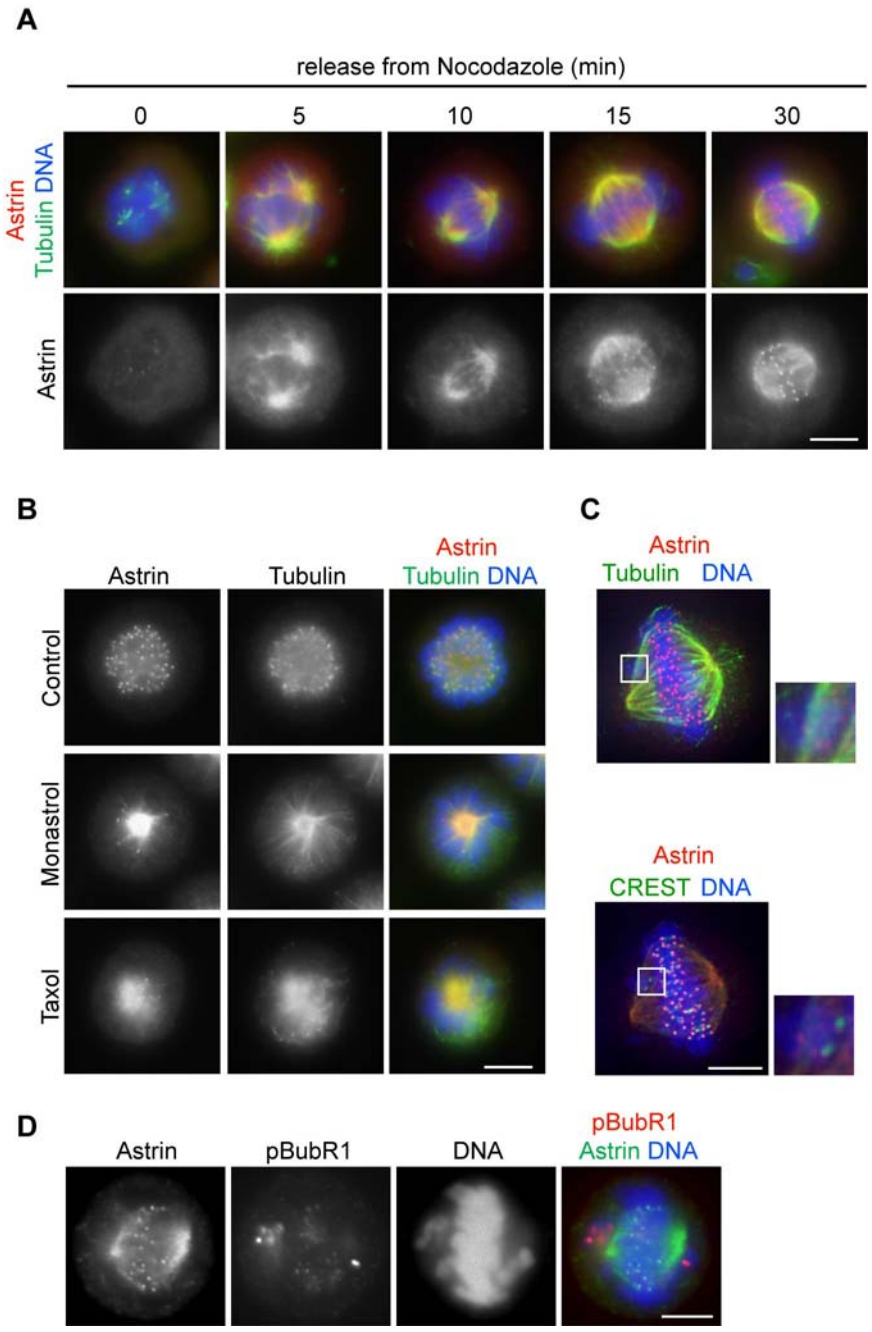

Figure 16. Astrin's localization to the KT is dependent on stable MT-KT interactions. (A) HeLa cells were treated with nocodazole for 14 h and released for the indicated periods, fixed and stained with antibodies against astrin and α–tubulin. (B) HeLa cells were treated with Taxol, Monastrol or DMSO (control) for 12 h, fixed and stained for the indicated proteins. (C) Noscapine treated cells (14 h) were fixed and stained with antibodies against astrin, α-tubulin and CREST. The inset highlights an unaligned chromosome that lacks astrin. (D) Cells were treated as in (C) and stained with antibodies against astrin (green) and pBubR1 (red). (C and D) Note astrin localizes only to aligned chromosomes. (A-D) DNA was stained with DAPI. Bar, 10 μm.

1.3. Astrin does not bind directly to microtubules

The nocodazole release experiment suggests (Figure 16A) that astrin is transported from the spindle pole to the KT and that its localization on these structures is dependent on MTs. To analyse a potential physical interaction between astrin and MTs *in vitro*, we tested whether astrin co-pellets with taxol-stabilized MTs (Gaglio et al., 1995). The assay was performed with bacterially expressed astrin (full-length) or MPP1, a plus-end-directed kinesin-related motor protein, which exhibits MT binding in vitro (Abaza et al., 2003) as positive control (a kind gift from Stefan Hümmer). The recombinant proteins were incubated with taxol stabilized MTs or buffer (control) and the protein samples were centrifuged through a glycerol cushion. The pellet fractions and the supernatants were recovered and analysed by Western blotting**.** Astrin did not co-pellet with MTs in contrast to MPP1, which associated with the MT pellet fraction (Figure 17A and B).

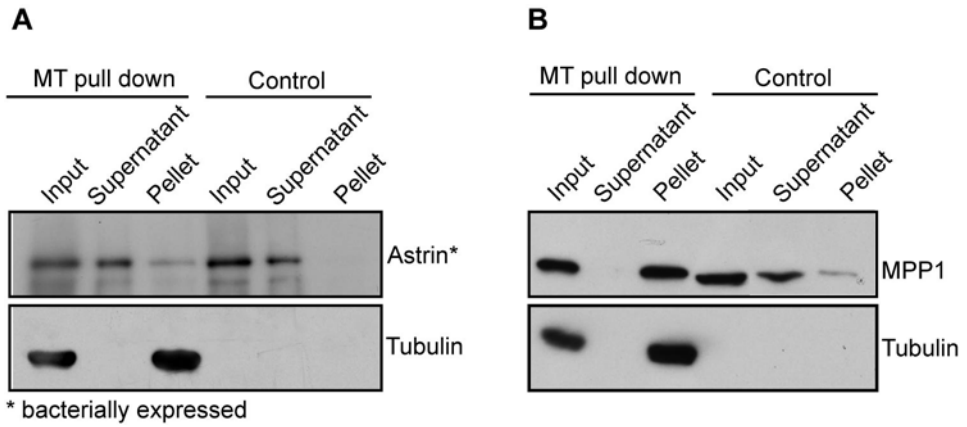

Figure 17. MT co-sedimentation assay. Bacterially expressed astrin (A) or MPP1 (B) were incubated with taxol stabilized MTs (5mM final concentration) or with buffer (control) for 15 minutes at 25° C. The protein solution was centrifuged through a glycerol cushion (20 min, 55.000 rpm, 25° C). Pellet and supernatant were recovered, loaded on a SDS-PAGE gel and probed after Western blotting with the indicated antibodies. To detect MPP1 an antibody against the His-tag was used.

This result indicates that astrin does not bind directly to MTs, suggesting that either an unknown linker protein or specific modifications of astrin are needed for astrin's localization to MTs. To test the latter hypothesis, MT co-sedimentation assays were performed with mitotic and interphase extracts (Mishima et al., 2002) instead of purified proteins. Interphase extracts were used because astrin does not bind to MTs in interphase (see immunofluorescence in Figure 13). Astrin of the mitotic samples should possess these specific modifications necessary for MT binding. However, Figure 18 shows that

astrin from mitotic cell extract did not co-pellet with MTs in contrast to the control protein PRC1, a MT binding protein (Mollinari et al., 2002). These data imply that an unknown linker protein or a motor protein is required to localize astrin to MTs.

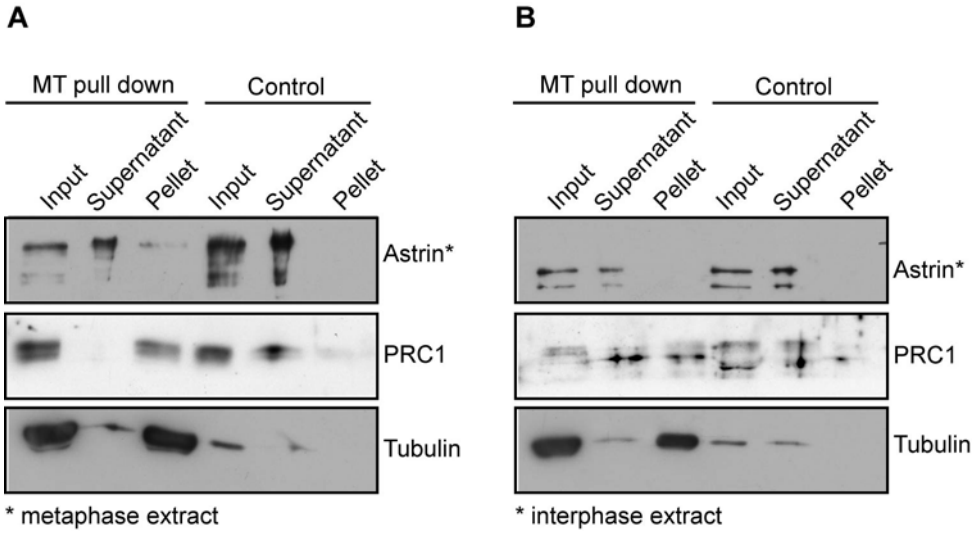

Figure 18. MT co-sedimentation assay. Metaphase (A) or interphase extracts (B) were incubated with taxol stabilized MTs (5mM final concentration) or with buffer (control) for 15 minutes at 25° C. The protein solution was centrifuged through a glycerol cushion (20 min, 55.000 rpm, 25° C). Pellet and supernatant were recovered, loaded on a SDS-PAGE gel and probed after Western blotting with the indicated antibodies. PRC1 was used as a positive control.

1.4. Search for motor proteins that localize astrin to the spindle or kinetochore

In the nocodazole release experiment astrin was first observed at the spindle poles and subsequently, as the spindle reformed it became more evident at the spindle and at the attached KTs (Figure 16A). This redistribution could be the consequence of an active motor-dependent transport from the poles to the KTs along MTs. Obvious candidate proteins for carrying astrin are plus-end directed motors like Kif18, Eg5 and CENP-E (Blangy et al., 1995; Mayr et al., 2007; Wood et al., 1997). Their influence on astrin localization was tested by RNAi depletion assays (Blangy et al., 1995; Mayr et al., 2007; Wood et al., 1997). MCAK was included as a control, since it is not motile but instead depolymerizes MTs (Desai et al., 1999; Hunter et al., 2003). As expected, siRNA mediated MCAK depletion did not impair astrin's localization (Figure 19A). Cells depleted of Kif18, a motile MT depolymerase (Mayr et al., 2007), showed diffuse astrin

staining at the KT compared to control cells (Figure 19B). This is most likely an indirect effect, since Kif18 depletion results in impaired MT dynamics and spindle morphology. However, we cannot exclude a direct role for Kif18 in localizing astrin. As shown in chapter 1.2 the inactivation of the motor activity of Eg5 by monastrol leads to the concentration of astrin at the pole, which is most likely also an indirect effect, since chromosomes are not aligned and not under tension in this situation. Depletion of CENP-E, a motor protein that transports cargo toward the MT plus ends and is concentrated at KTs during prometaphase (Wood et al., 1997; Yao et al., 1997), results in a mitotic arrest and congression defects (McEwen et al., 2001; Schaar et al., 1997). As shown in Figure 19C astrin was lost from the KTs in cells depleted of CENP-E, whereas spindle pole and spindle staining were not influenced. These results suggest either that astrin's localization to the KT depends directly on CENP-E or that the observed phenotype is indirect, since astrin's localization to the KT is dependent on stable MT-KT interactions, which are impaired in cells depleted of CENP-E (Yao et al., 1997).

One caveat of the siRNA based assays was that all of the motor proteins analysed either alter MT-KT interactions and/or spindle formation. Therefore it is difficult to decide whether effects on astrin localization are direct or indirect. In summary, our results indicate that among the tested plus-end directed motor proteins CENP-E is the most promising candidate responsible for astrin's localization to the KT, since in contrast to Kif18 RNAi or Eg5 motor activity inhibition, astrin was completely lost from the KT in cells depleted of CENP-E. In line with this we observed physical interaction between astrin and CENP-E (results, chapter 2.2).

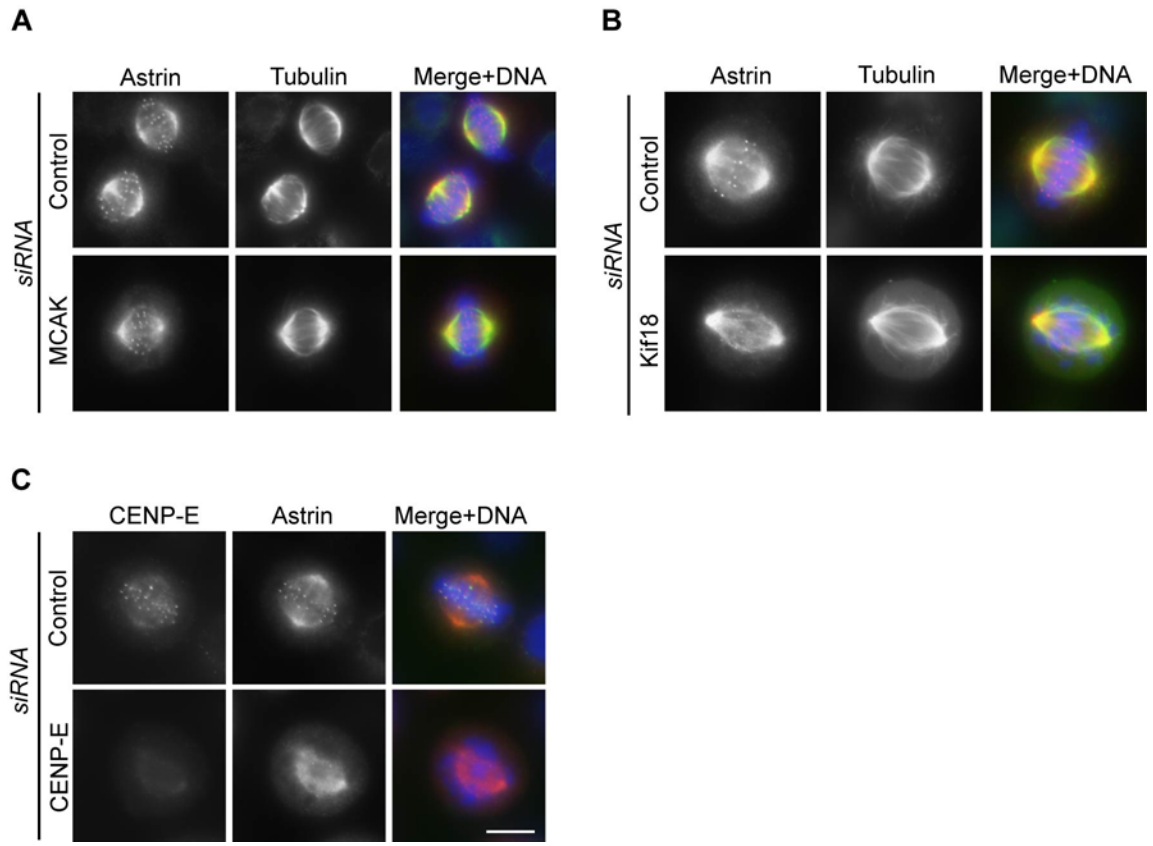

Figure 19. Astrin's localization to the KT is lost after CENP-E depletion. Cells were depleted of the plus end directed motor proteins (A) MCAK, (B) Kif18 or (C) CENP-E, fixed with (A) MeOH or (B and C) PTEMF, and stained with antibodies against astrin (red) and tubulin (green). DNA was stained with DAPI (blue). Bar, 10 μm.

2. Search for astrin interactors

Since astrin is a KT and mitotic spindle associated protein, plausible interactors might themselves localize to these structures. Two different approaches were considered to identify binding partners of astrin: yeast-two hybrid analysis and RNAi-based bi-dependency analysis. Since all astrin constructs of suitable length for yeast-two hybrid screens were autoactivatory in preliminary yeast-two hybrid experiments (Figure 20), we concentrated on the second approach.

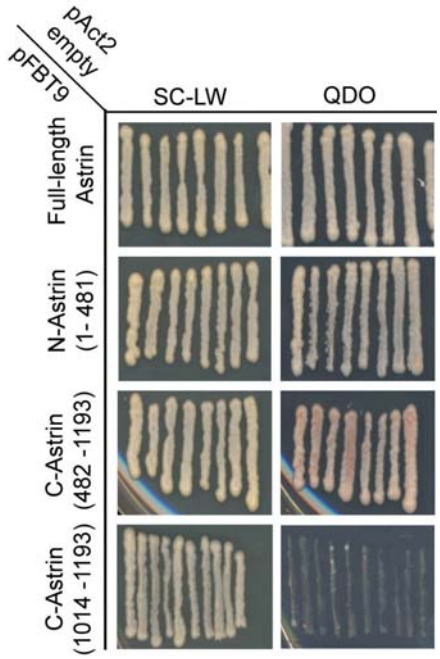

Figure 20. Full-length astrin, an N-terminal (aa 1-481) and a C-terminal (aa 482-1193) fragment of astrin cloned into the bait vector pFBT9 are all auto-activatory. Auto-activation was tested with the full-length, N-terminus (1-481), C-terminus (482-1193) and very C-terminus (1014-1193) of astrin, cloned into pFBT9, expressing as a binding domain fusion, along with the empty pAct2 vector, expressing the activating domain. Auto-activation was reflected by growth on selective medium (QDO, right panels). For control, growth on non-selective plates is also shown (SC-LW, left panels). Only the very small C-terminal fragment (1014-1193) is not auto-activatory but was considered to be too small for an yeast-two hybrid screen.

2.1. Bi-dependency analysis

As a second approach to finding interaction partners siRNA based bi-dependency analyses were performed. To reveal which proteins might be required for the localization of astrin to the KT and the spindle-pole, several KT and spindle-pole associated proteins were depleted by siRNA. Moreover it was tested, which proteins are affected by the loss of astrin. A summary of the results is given in Figure 21. Of all proteins tested, the depletion of the outer KT proteins CENP-E (Figure 19C and Figure 21I), Hec1 (Figure 15 and Figure 21) and Plk1 (Figure 21H) clearly reduced the concentration of astrin at the KT. Since Hec1 is necessary for stable KT-MT interactions it is difficult to decide whether the loss of astrin from the KT in Hec1 depleted cells is a direct or indirect effect. Moreover, astrin depletion resulted in a loss of CENP-E and its interaction partner CENP-F (Chan et al., 1998) from the KT (Figure 21 G and H), of hCdc14A from the

spindle poles (Figure 21A and I) and of Plk1 from both the KT and the centrosomes (Figure 21C and I). The spindle pole levels of Aurora A and its MT associated interaction partner TPX2 (Eyers and Maller, 2004; Kufer et al., 2002) were also reduced (Figure 21I), but this could be a consequence of the absence of Plk1 at the centrosomes. The observed mutual dependency between astrin and both the mitotic kinase Plk1 and the plus-end directed motor CENP-E suggests that these proteins could physically interact with astrin. Likewise, the mitotic phosphatase hCdc14A is affected by the loss of astrin and Ulrike Grüneberg found astrin as an interacting protein in a yeast-two hybrid screen with hCdc14A as bait (personal communication). Therefore its relation to astrin was also further analysed (see below, chapter 3.4). Taken together, the bi-dependency analysis allowed the identification of CENP-E, hCdc14A and Plk1 as three interesting candidates for being interactors of astrin. Below we explore the possible physiological relevance of these proteins for the function of astrin (chapters 2.2 and 3).

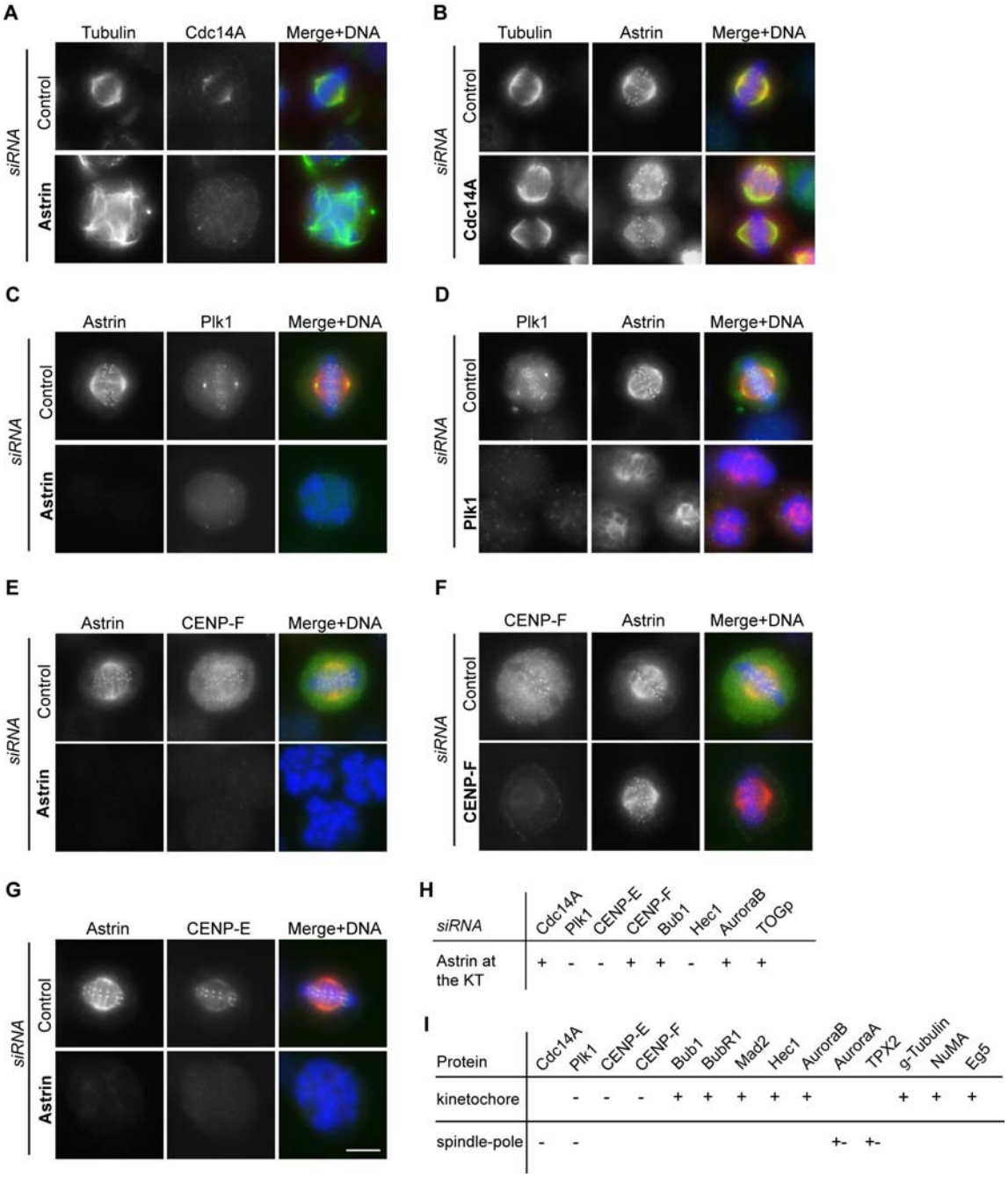

Figure 21. Astrin KT localization requires Hec1, CENP-E and Plk1. Astrin depletion results in a loss of CENP-E and CENP-F from the KT, of hCdc14 from the spindle pole and of Plk1 from the KT and centrosome. (A and B) HeLa cells were treated with control, astrin or hCdc14A specific siRNA oligos, fixed and stained with antibodies against α-tubulin (green), (A) cdc14 (red) or (B) astrin (red). (C and D) HeLa cells were treated with control, astrin or Plk1 specific siRNA oligos, fixed and stained with antibodies against astrin (red) and Plk1 (green) (E and F) HeLa cells were treated with control, astrin or CENP-F specific siRNA oligos, fixed and stained with antibodies against astrin (red) and CENP-F (green). (G) HeLa cells were treated with control or astrin specific siRNA oligos, fixed and stained with antibodies against astrin (red) and CENP-E. (A-F) DNA was stained with DAPI. Bar, 10 μm. (H) HeLa cells were depleted of various KT and spindle-pole components and the effects on astrin localization were analysed. The results are shown in the table. (I) HeLa cells were treated with control or astrin specific siRNA oligos, fixed and then the localization of KT and spindle-pole components was analysed. The table summarizes the observed effects.

2.2. Characterization of the relationship between CENP-E and astrin

As a first approach to explore the relationship between astrin and CENP-E in more detail, an endogenous astrin IP from mitotic cells was performed. For this experiment cells were synchronized with noscapine in order to trap them in a metaphase like state but maintain the MT network (Ye et al., 1998). CENP-E was not efficiently co-precipitated with endogenous astrin under these conditions (Figure 22A). It is possible that the relation between astrin and CENP-E is either indirect or very weak. It could also be that the antibody-astrin interaction sterically prevented the interaction of astrin with CENP-E. Overexpression of a Myc-tagged astrin followed by an IP using the rabbit anti-Myc antibody should, however, bypass this possible interference. For this purpose, Hek293T cells were transfected with either Myc-astrin or the empty Myc-plasmid as control. After precipitation with anti-Myc-antibodies, endogenous CENP-E but not the outer KT protein Hec1 was co-immunoprecipitated (co-IPed) with astrin (Figure 22B). In summary, these results and the bi-dependency of astrin and CENP-E in localization to the KT indicate that astrin and CENP-E interact. However, since CENP-E does not co-IP with endogenous astrin it is still possible that the association between astrin and CENP-E is either weak or requires an unknown interaction partner.

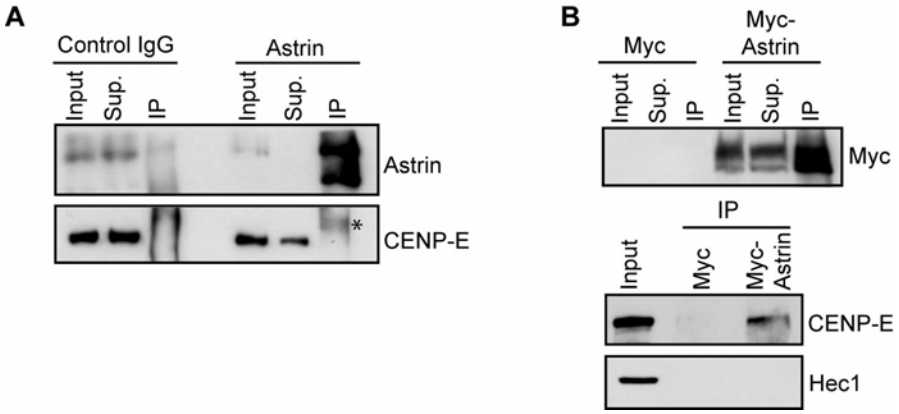

Figure 22. CENP-E co-IPs with over-expressed but not endogenous astrin. (A) IPs with either astrin or control IgG were performed from mitotic lysates. Inputs, supernatants (Sup.) and IPs were loaded onto a SDS-gel, followed by Western blot analysis using the indicated antibodies. Endogenous astrin IPed efficiently (upper panel), but CENP-E did not co-IP. *Asterisk indicates an unspecific band; however, this could also be a phosphorylated form of CENP-E. (B) Hec293T cells were transfected with Myc-astrin or the empty Myc-vector as control for 40 h. Cells were treated with noscapine for the last 16 h. Extracts were used for Myc-IP. Inputs, supernatants (Sup.) and IPs were separated by SDS-PAGE, followed by Western blot analysis with anti-Myc-antibodies. The input, the Myc-IP and the Myc-astrin IP were also loaded onto a SDS-PAGE, followed by Western blot analysis with the indicated antibodies. CENP-E but not Hec1 co-precipitates with Myc-astrin.

3. Analysis of astrin phosphorylation and functional insight into Plk1 astrin interaction

The mitotic kinase Plk1 was identified as a possible candidate protein for an astrin interactor in the bi-dependency analysis (chapter 2.1, Figure 21). Since astrin localizes to the same structures to which Plk1 is targeted in the course of mitosis, KTs, centrosome and midzone (Barr et al., 2004), it is likely that Plk1 and astrin influence each other. Thus the functional relationship between astrin and Plk1 was further analysed.

Plks are characterized by a C-terminal noncatalytic region containing two tandem Polo boxes, termed the Polo-box domain (PBD), which targets the substrate in a phospho-dependent manner (Elia et al., 2003b). It has been suggested that these priming sites are most likely created by Cdk1/cyclin B1 (Elia et al., 2003b). Thus it was also investigated if astrin is phosphorylated during mitosis and if it is a substrate of Cdk1/cyclin B1.

3.1. Astrin is highly phosphorylated in mitosis

In order to analyse if astrin is mitotically phosphorylated, cell extracts were prepared from cells either arrested in G1 by double thymidine block, or in a prometaphase-like state by release from a thymidine block into nocodazole. Western blotting of these extracts with anti-astrin antibodies revealed that both forms of astrin (see chapter 1) are highly upshifted in prometaphase compared to the two distinct bands in G1 (Figure 23A). The upshift could be reversed by treatment with alkaline phosphatase indicating that it is caused by phosphorylation rather than by any other post-translational modification (Figure 23B). To analyse the phosphorylation pattern of astrin more precisely, Western blot analysis was performed on HeLa cell lysates, which were released from a nocodazole block and harvested at different time points (the samples were a kind gift from Herman Sillje). The Western blot analysis revealed that astrin is expressed at near constant levels throughout the cell cycle. Astrin was highly phosphorylated in nocodazole arrested cells and then dephosphorylated concomitantly with cyclin B1 degradation, suggesting that the key mitotic kinase Cdk1/cyclin B1 might be responsible for phosphorylating astrin (Figure 23C). To test this, we examined whether a recombinant MBP-tagged N-terminal fragment of astrin (aa 1-481), which is rich in serine and threonine residues (Gruber et al.,

2002), could act as a substrate of Cdk1/cyclin B1 (Upstate) in an *in vitro* kinase assay. As positive control Histone H1 (H1), as negative control MBP and a recombinant His-tagged C-terminal fragment of astrin (aa 1014-1193) (a kind gift from Ulrike Grüneberg) were used. The autoradiogram (^{32}P) showed that astrin is phosphorylated in vitro by Cdk1/cyclin B1 (Figure 23D), confirming published data (Chang et al., 2001). These results indicate that astrin's function in mitosis might be regulated by phosphorylation. Cdk1/cyclin B1 might be the main kinase phosphorylating astrin and could therefore create Plk1 docking sites on astrin.

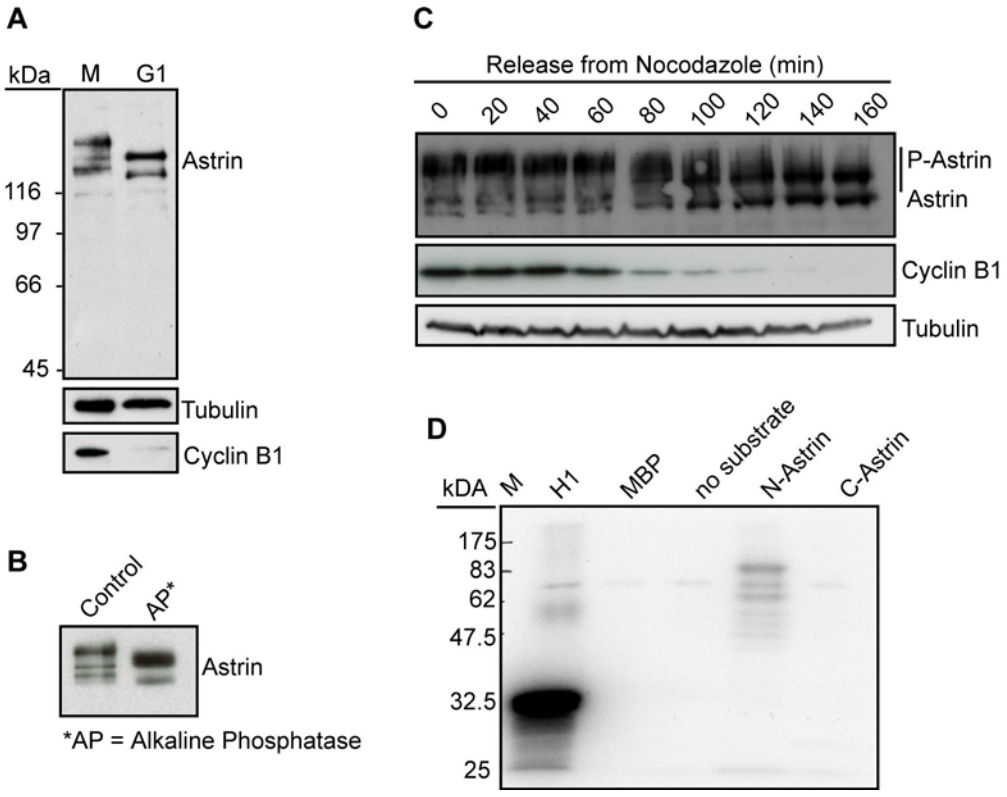

Figure 23. Phosphorylation of astrin. (A) Cell extracts were prepared from HeLa cells synchronized in G1 or M phase by drug treatment. (B) The upshifted astrin forms are sensitive to alkaline phosphatase treatment. IPed astrin of HeLa lysates from nocodazole arrested cells was either incubated with alkaline phosphatase (AP) or left untreated (control) for 1 h at 30°C. Equal amounts of cell lysates were separated by SDS-PAGE and probed after Western blotting with the indicated antibodies. (C) HeLa cells were synchronized by a sequential aphidicolin/nocodazole block release protocol. After nocodazole release samples were taken every 20 min. Equal amounts of cell extracts were separated by SDS-PAGE and probed after Western blotting with the indicated antibodies. (D) An in vitro kinase assay with MBP-astrin (aa 1-481) was performed, Histone H1 (H1) was used as positive controls, MBP and His-astrin (aa 1014-1193) as negative control, since there are no SP/TP sites in the very C-terminus of astrin. Panel shows the autoradiogram (^{32}P). Equal amounts of protein (300 ng of recombinant astrin) were loaded.

3.2. Plk1 interacts with astrin via its polo-box binding domain

The observed mutual dependency between astrin and Plk1 (see chapter 2.1, Figure 21) suggests that these proteins physically interact. In order to test this possibility astrin was precipitated from mitotic cell extracts with anti-astrin antibodies, using rabbit IgG as control. Under these conditions Plk1, but not the outer KT protein Hec1 or the spindle pole associated motor protein Eg5 (Sawin et al., 1992), was efficiently co-precipitated with endogenous astrin (Figure 24A). As mentioned previously it has been suggested that the Plk1 priming sites are most likely created by Cdk1/cyclin B1 (Elia et al., 2003b). To test this possibility with regard to astrin, which is an *in vitro* substrate of Cdk1/cyclin B1, full-length GFP-astrin (which expresses better than Myc-astrin) was expressed in Hek293T cells and half of the cells were treated with nocodazole prior to harvest in order to increase the mitotic index and Cdk1 activity in these extracts. After precipitation with anti-GFP antibodies endogenous Plk1 and also CENP-E (as shown before with Myc-astrin, see chapter 2.2, Figure 22), but not the control proteins γ-tubulin or Hec1, could be detected in the IPs (Figure 24B). The interaction between astrin and Plk1 was markedly increased by the presence of nocodazole, probably due to a combination of increased Plk1 levels in the cell lysate and enhanced Cdk1 phosphorylation of astrin.

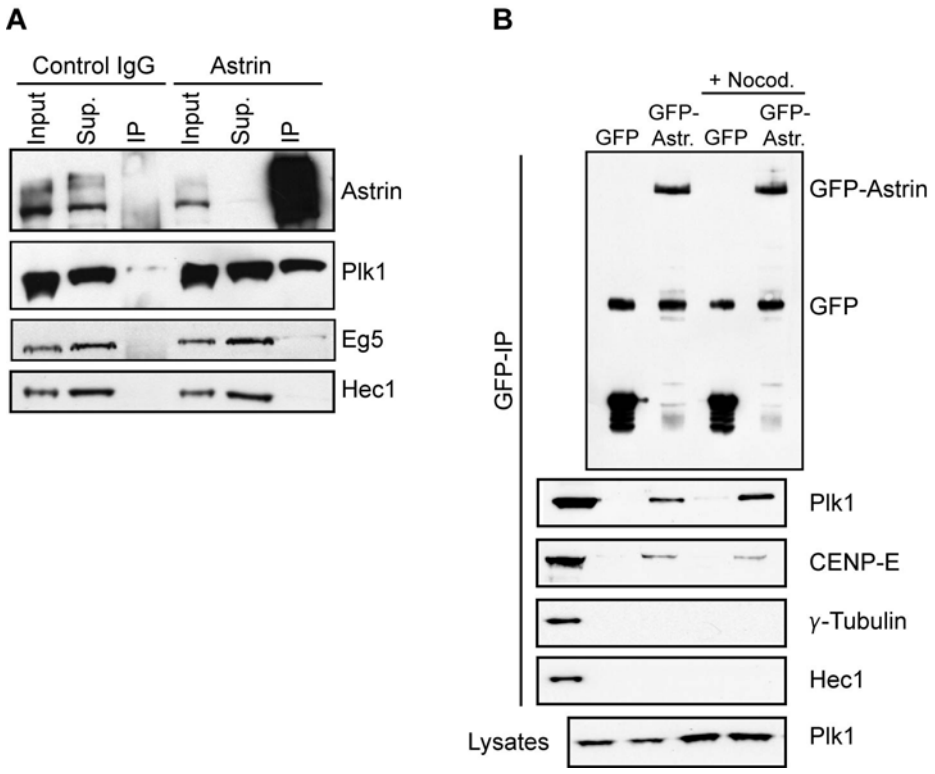

Figure 24. Plk1 interacts biochemically with astrin. (A) HeLa cells were pre-synchronized with aphidicolin, released and then arrested in mitosis with noscapine. IPs with either astrin or control IgG were performed from mitotic lysates. Inputs, supernatants (Sup.) and immune complexes (IP) were loaded onto a SDS gel, followed by Western blot analysis using the indicated antibodies. (B) Hec293T cells were transfected with GFP-astrin or the empty GFP-vector as control for 40 h. Cells were treated with nocodazole for the last 16 h. Extracts were used for GFP-IP. Input and IPs were separated by SDS-PAGE, followed by Western blot analysis with the indicated antibodies.

To further examine whether Plk1 interacts with astrin via its PBD IPs of endogenous astrin were overlayed with GST-PBD (a kind gift from Rüdiger Neef). GST-PBD bound efficiently to precipitated astrin but not to control precipitates (Figure 25A) and consistent with a requirement for phosphorylation it bound only to the upshifted species of astrin. In line with this, astrin precipitated with PBD-pull-downs from cells stably expressing wild type PBD (PBD-wt) but not from cells stably expressing a mutated PBD (PBD-AA), lacking residues critical for phospho-peptide binding (Hanisch et al., 2006) (Figure 25B). The samples were a kind gift from Anja Hanisch. Taken together the results demonstrate that the interaction between astrin and Plk1 is mediated via the PBD.

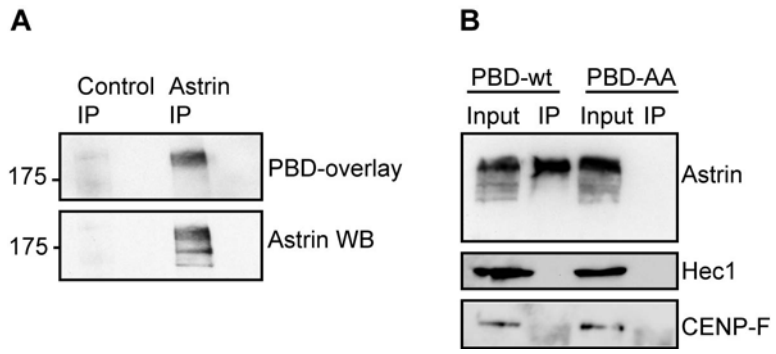

Figure 25. Plk1 interacts with astrin via its PBD. (A) HeLa cells were pre-synchronized with aphidicolin, released and then arrested in mitosis with noscapine. IPs were performed using affinity-purified anti-astrin antibodies. IPs obtained were overlayed with GST-PBD, and GST-PBD-binding was visualized with antibodies against GST. Note that only the slower migrating forms of astrin bound GST-PBD in this assay. (B) Myc-IPs from HeLa cells stably expressing Myc-PBD-wt or Myc-PBD-AA carrying mutations in residues critical for phosphopeptide binding (H538A, K504A) (Hanisch et al., 2006) were analysed for the presence of astrin, Hec1 and CENP-F.

3.3. The interaction of astrin and Plk1 is dependent on the Cdk1 phosphorylation site at Thr 111

As the optimal phosphopeptide binding motif for PBD docking the amino acid sequence S-[pS/pT]-P/X was identified (Elia et al., 2003b). Analysis of the astrin amino acid sequence revealed three potential PBD docking sites conforming to this consensus motif (SS65/66 = PBD1; ST110/111 = PBD2; ST936/937 = PBD3). In order to examine which of these three sites mediates the binding to the PBD the putative phosphorylated residue of all three sites and the preceeding serine were simultaneously mutated to alanine. All Myc-astrin PBD mutants (Myc-astrin PBD1AA, PBD2AA, PBD1/2AA and PBD3AA) still localized like the wild type when transiently expressed in HeLa cells suggesting that the mutations did not introduce any severe structural changes into the proteins (Figure 26).

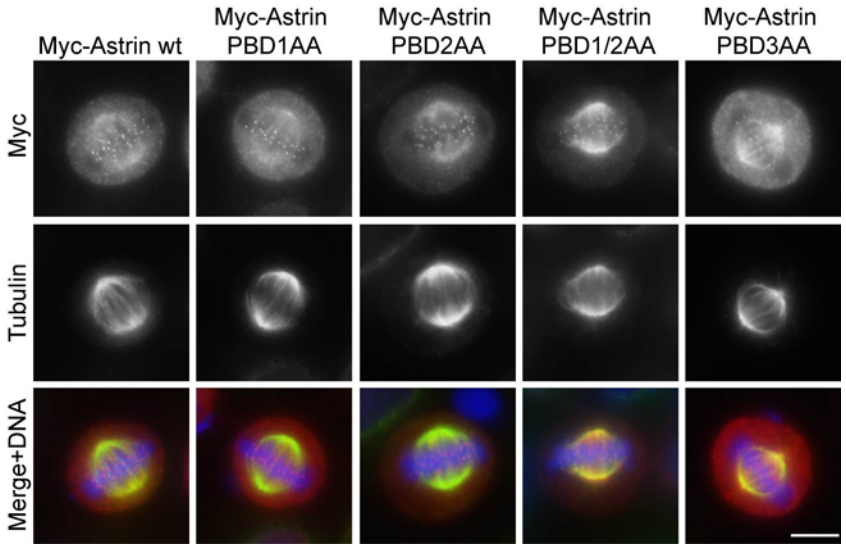

Figure 26. Transiently transfected Myc-astrin PBD mutants show normal localization. Myc-astrin wild type and PBD mutants were transiently transfected into HeLa cells. After 30 h the cells were fixed and stained with antibodies against tubulin (green) and Myc (red). DNA (blue) was stained with DAPI. Bar, 10 µm. Differences in intensity are most likely due to differences in expression levels.

Pull-down experiments precipitating the Myc-wt-astrin or the Myc-astrin mutants overexpressed in 293T cells demonstrated that Plk1 binding to astrin was reduced by approximately 50% when SS65/66 was mutated (Myc-astrin PBD1AA) and completely abolished after mutation of ST110/111 (Myc-astrin PBD2AA) or mutation of both sites (Myc-astrin PBD1/2AA) (Figure 27). No effect on Plk1 binding was observed with the Myc-astrin PBD3 mutant (Figure 27). Interestingly, the bands for the precipitated Myc-astrin PBD2AA and the Myc-astrin PBD1/2AA mutants were clearly less upshifted than the bands of the wild type Myc-astrin, the Myc-astrin PBD1AA and Myc-astrin PBD3AA mutants (Figure 27), suggesting that Thr111 is the main phosphorylation-site responsible for the mitotic upshift in astrin. Collectively, these results demonstrate that astrin interacts directly with Plk1 and that this interaction is dependent on the presence of the Cdk1 phosphorylation site at Thr 111 (PBD2) and, to a minor extent, on the presence of the Cdk1 phosphorylation site at Ser 66 (PBD1).

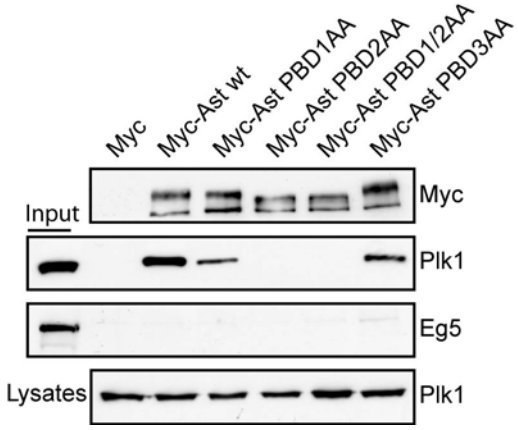

Figure 27. The direct interaction of Plk1 and astrin is dependent on the presence of the Cdk1 phosphorylation site at Thr 111 (PBD2). Myc, Myc-astrin wt and PBD mutants were expressed in 293T cells for 40 h. The cells were treated with nocodazole for the last 16 h and Myc-tagged proteins were precipitated. The IPs were analysed for the presence of the Myc-tagged proteins and co-precipitating Plk1 and Eg5 as control. Western blotting of the lysates with anti-Plk1 antibodies show equal loading. Note that the mutation of the putative PBD-binding site 2 (Myc-astrinPBD2AA) leads to altered running behaviour of the overexpressed protein in comparison to the control and the other two PBD mutants.

After having demonstrated that Plk1 binds to astrin it was obvious to ask whether astrin is a substrate of Plk1. In a first approach we tested whether astrin's localization was influenced in cells treated with the Plk1 kinase activity inhibitor TAL (Santamaria et al., 2007) or whether astrin's mitotic upshift was impaired in cells depleted of Plk1. Immunofluorescence analysis of cells treated with TAL for various time periods revealed that astrin's localization to the KT, the mitotic spindle and the spindle pole was only slightly affected. Since Plk1 kinase activity is required for the stabilization of MT-KT interactions, this is most likely an indirect effect (Santamaria et al., 2007). Moreover, Western blot analysis revealed that the mitotic upshift in cells depleted of Pk1 was only impaired to a limited extent, compared to mitotically arrested control cells. Taken together, these results demonstrate that the loss of Plk1 kinase activity only mildly influences astrin's localization. This indicates either that Plk1 does not phosphorylate its binding partner astrin but instead an unknown interactor of astrin, or that the Plk1 phosphorylation of astrin is not involved in astrin's localization. The slight influence on astrin's mitotic upshift could either be due to the fact that Plk1 does not phosphorylate astrin or that its phosphorylation is only partly responsible for the mitotic upshift, which might be caused mainly by Cdk1.

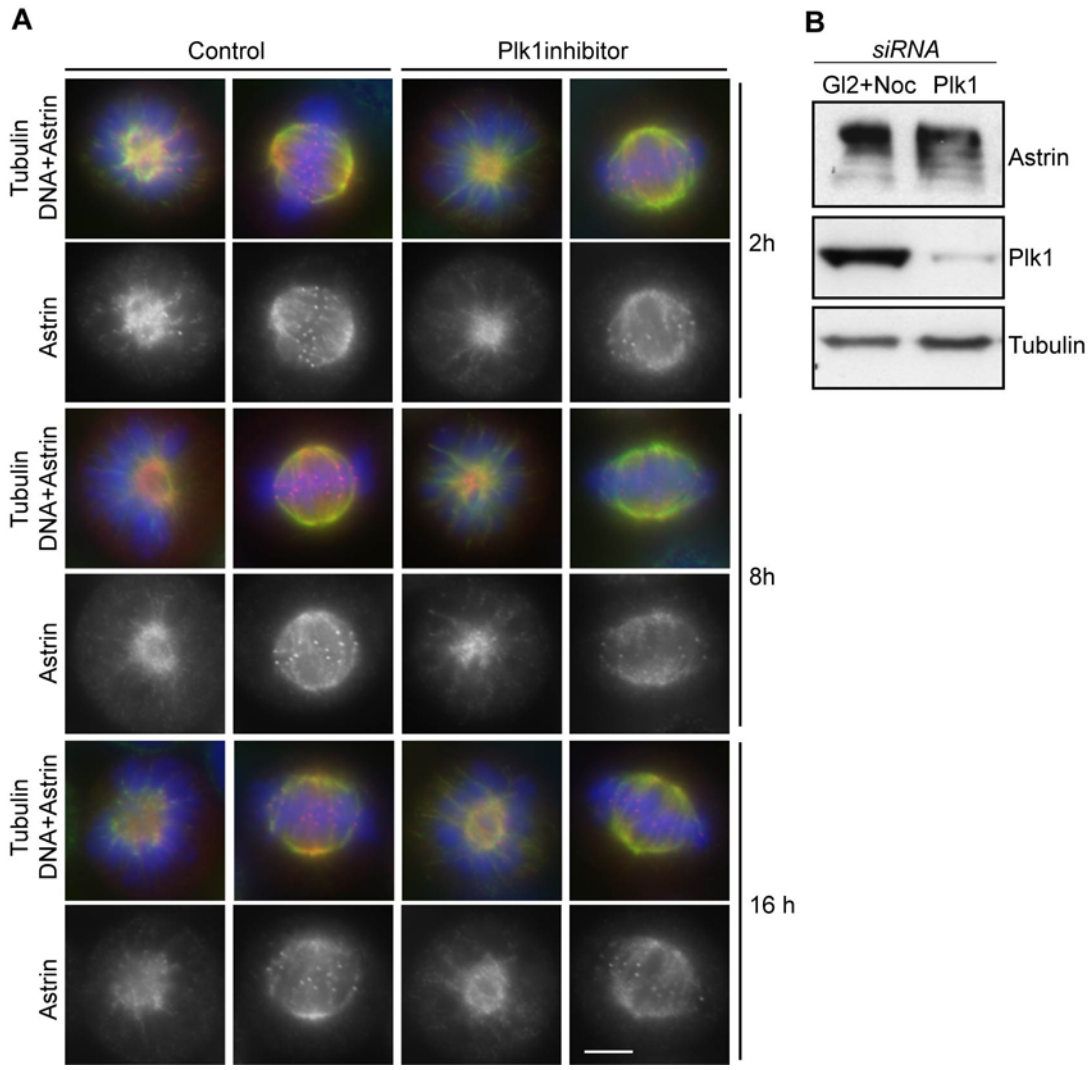

Figure 28. Inhibition of Plk1 kinase activity only slightly influenced astrin's localization and astrin's mitotic upshift in cells depleted of Plk1 is only slightly impaired. (A) Asynchronous cells were treated with Plk1 inhibitor (TAL) for various time periods, then fixed and stained with antibodies against astrin (red) and α- tubulin (green). DNA was stained with DAPI. Bar, 10 μm. (B) Cells were either depleted of Plk1 by siRNA or treated with control (Gl2) oligos. 12 h prior to mitotic shake off control cells were treated with nocodazole to mitotically arrest them. Then cells were harvested by mitotic shake off and lysed. The cell lysates were analysed be Western blotting with the indicated antibodies.

To analyse when in mitosis astrin is phosphorylated on the PBD-binding site Thr111, a polyclonal antibody (p-astrin) directed against a peptide encompassing pThr111 was generated. The Western blot analysis of mitotic control and astrin depleted samples revealed that the p-astrin antibody recognized a band with an apparent molecular weight of ca. 140 kDa, which disappeared upon siRNA-mediated depletion of astrin (Figure 29A). Consistent results were obtained by immunofluorescence analysis. Whereas control cells exhibited strong KT and spindle pole staining with the anti-p-astrin antibody, cells

depleted of astrin showed no staining. By Western blotting on mitotic or interphase lysates, the p-astrin antibody only recognized a band in mitotic but not interphase samples (Figure 29B, left panel). Anti-p-astrin reactivity to this band was lost upon phosphatase treatment, confirming its specificity for phosphorylated astrin (Figure 29C, upper panel). Reprobing the membrane with anti-astrin antibody demonstrated that the band recognized by the p-astrin antibody corresponds exactly to the slowly migrating, phosphorylated form of astrin (Figure 29C, upper and lower panel). It should be noted also that the phosphospecific astrin antibody recognizes only the full-length form of astrin, since the smaller form lacks approximately 200 aa at the N-terminus and thus also Thr111 (Figure 12). Having established the specificity of the anti-p-astrin antibody, it was used to track the timing of astrin phosphorylation on the PBD-binding site. Analysis of asynchronously growing HeLa cells by immunofluorescence microscopy revealed that Thr111 phosphorylation was observed mainly in metaphase, when the cells showed strong KT and spindle pole staining. Phosphorylation was gradually lost in anaphase and no telophase cells were found to stain positive with the anti-p-astrin antibody (Figure 29E). Taken together, these results show that phosphorylation of astrin on Thr111 occurs predominantly during metaphase. The data showing that astrin and Plk1 interact directly via the PBD consensus motif centred on Thr111 and that phosphorylation of this residue occurs predominantly at metaphase are a good basis for future studies of the function of the interaction between Plk1 and astrin.

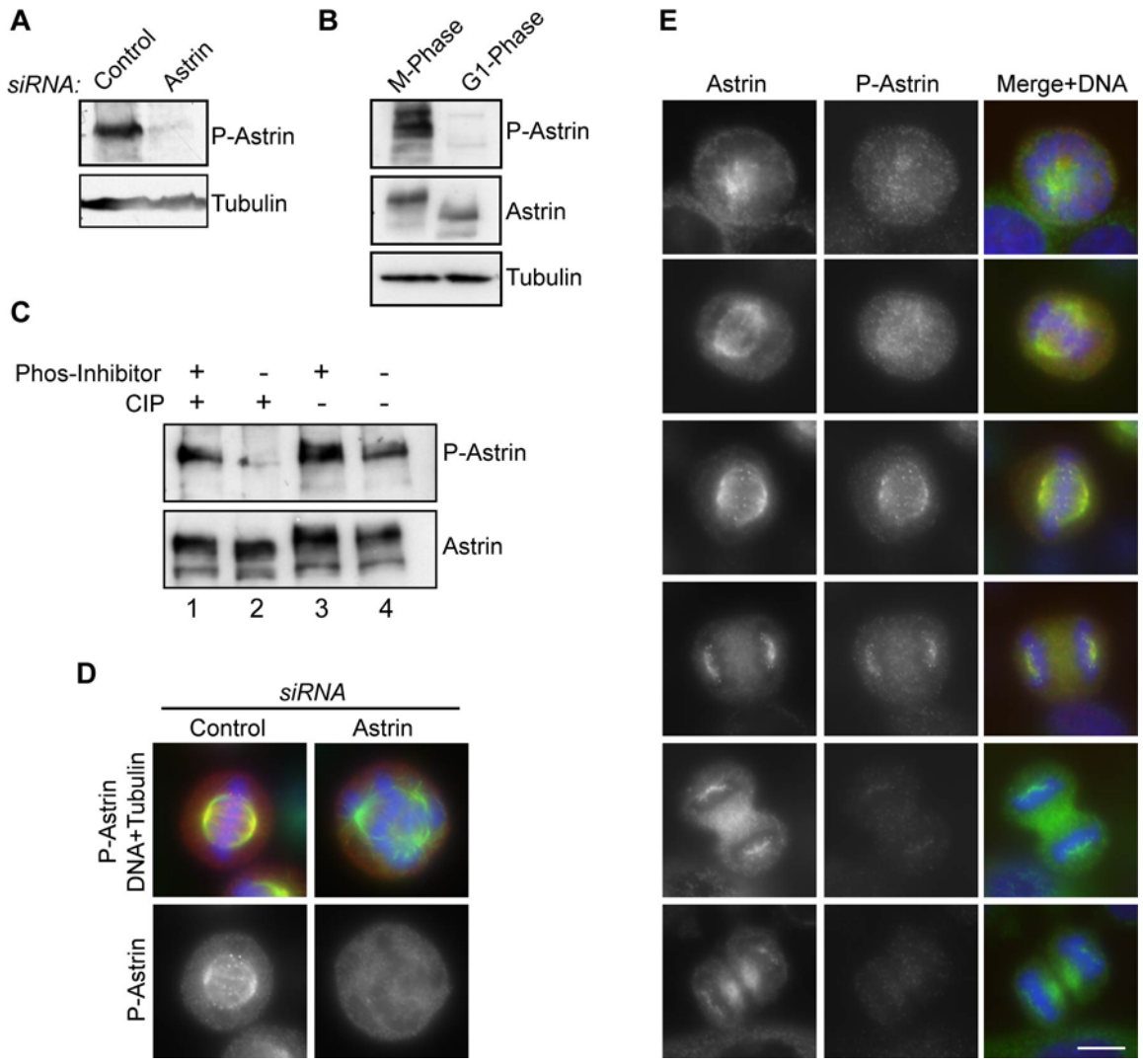

Figure 29. Thr111 is phosphorylated mainly in metaphase. (A) Mitotic cell lysates were prepared form HeLa cells depleted of astrin or control (Gl2). (B) Cell extracts were prepared from HeLa cells synchronized in G1 or M phase by drug treatment. (A and B) Equal amounts of cell lysates were separated by SDS-PAGE and probed after Western blotting with the indicated antibodies. (C) Mitotic extracts of synchronized cells either incubated with Calf Intestinal Phosphatase (CIP) (lane 1 and 2) or left untreated (lane 3 and 4) for 1 h at 30°C with (lane 1 and 3) or without (lane 2 and 4) phosphatase inhibitor (Phos-Inhibitor). Note that the phosphatase inhibitor was not absolutely efficient, because astrin in the first lane (treated with CIP and phosphatase inhibitor) is a little bit down-shifted compared to the samples that were not treated with CIP (lanes 3 and 4). Equal amounts of cell lysates were separated by SDS-PAGE and probed after Western blotting with the anti-astrin antibody (upper panel). The same blot was reblotted with anti-astrin antibodies (lower panel), which also shows equal loading. (D) HeLa cells were treated with control or astrin specific siRNA oligos, fixed and stained with antibodies against α-tubulin (green) and p-astrin (pThr111) (red). (E) Asynchronous HeLa cells were fixed and stained with rat-anti-p-astrin antibody (green) and rabbit-anti-p-astrin antibody (red). (D and E) DNA was stained with DAPI. Bar, 10 μm.

3.4. Initial analysis of the relationship between hCdc14A and astrin

Budding yeast Cdc14p is a serine-threonine phosphatase that was identified as a essential protein for antagonizing Cdk activity and inducing mitotic exit (Bardin and Amon, 2001; Jaspersen et al., 1998; Visintin et al., 1998). Mammalian cells express two homologs of Cdc14, termed hCdc14A and hCdc14B, which are both functional homologs of yeast Cdc14 (Vazquez-Novelle et al., 2005). Recent evidence points to isoforms-specific roles in centrosome separation/maturation and spindle stability, with the possibility of additional roles in mitotic exit and cytokinesis (Trinkle-Mulcahy and Lamond, 2006). Astrin was identified as an interactor of hCdc14A in our laboratory (Ulrike Grüneberg, unpublished). These data were confirmed with a direct yeast-two hybrid analysis. HCdc14A, but not hCdc14B, interacts specifically with the C-terminus of astrin (aa 1014-1193) (Figure 30A and B). To further analyse the interaction of hCdc14A and astrin, IP experiments were performed. On the one hand endogenous astrin was immuno-precipitated from mitotic cells, arrested with noscapine. On the other hand Hek293T cells were transfected with either Myc-astrin or the empty Myc-plasmid as control and astrin was pulled down with anti-Myc antibodies. HCdc14A did not co-IP with endogenous astrin, but with overexpressed-astrin (Figure 30C and D). This result indicates that the interaction between hCdc14A and astrin is either very weak or indirect, or that the antibody interferes with the interaction. As shown above, astrin is highly phosphorylated during mitosis and dephosphorylated concomitantly with cyclin B1 degradation, suggesting that the key mitotic kinase Cdk1/cyclin B1 phosphorylates astrin. Since it has been suggested that Cdc14A reverses the modifications introduced by Cdks hCdc14 could be the phosphatase that dephosphorylates astrin when cells exit mitosis.

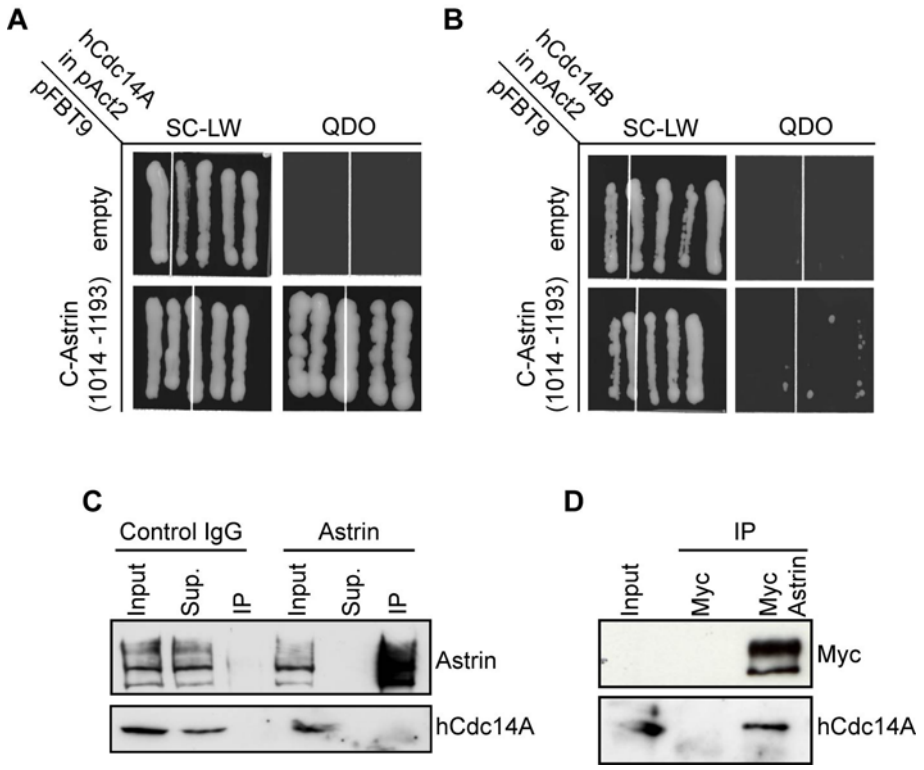

Figure 30. HCdc14A interacts with the C-terminus of astrin and co-IPs with over-expressed but not endogenous astrin. (A and B) Direct yeast-two hybrid analysis with either hCdc14A (A) or hCdc14B (B), cloned into pAct2 and a C-terminal fragment of astrin (aa 1014-1193) cloned into pFBT9. Interaction was reflected by growth on selective medium (QDO, right panels). For control, growth on non-selective plates is also shown (SC-LW, left panels). (C) IPs with either astrin or control IgG were performed from mitotic lysates. Inputs, supernatants (Sup.) and immune complexes (IP) were loaded onto a SDS gel, followed by Western blot analysis using the indicated antibodies. HCdc14 does not co-IP with endogenous astrin. (D) Hec293T cells were transfected with Myc-astrin or the empty Myc-vector as control for 40 h. Cells were treated with noscapine for the last 16 h. Extracts were used for Myc-IP. Input and IPs were separated by SDS-PAGE, followed by Western blot analysis with the indicated antibodies. HCdc14A does co-precipitate with Myc-astrin.

In budding yeast it has been shown that Cdc14 regulates the yeast INCENP-Aurora B complex, Sli15-Ipl1 (Pereira and Schiebel, 2003). Sli15 is partially dephosphorylated during anaphase in a Cdc14-dependent manner and human INCENP can also be dephosphorylated by human Cdc14A (Gruneberg et al., 2004). To test whether hCdc14 dephosphorylates astrin, a phosphatase assay with recombinant hCdc14A and hCdc14A phosphatase dead (hCdc14A PD) was performed, INCENP was used as a positive control substrate. The enzymes were a kind gift from Ulrike Grüneberg. For the phosphatase assay INCENP and astrin were IPed from mitotically arrested cells with either antibodies against Aurora B, the interaction partner of INCENP, or against astrin, respectively, and protein G-Sepharose beads. The IPed proteins coupled to protein G-Sepharose were

resuspended in 1x phosphatase buffer, aliquoted and treated with different amounts of recombinant hCdc14A (wt: 50 and 500 ng, PD: 500 ng). For control, aliquots were either left untreated for 30 min at 30°C (control 1) or left on ice (control 2). Equal amounts of protein were separated by SDS-PAGE. Western blot analysis revealed that the mitotically phosphorylated astrin was dephosphorylated by hCdc14A (Figure 31B) but not as efficiently as the positive control INCENP (Figure 31A). After separating the proteins on a 6 % gel, the down shift of astrin was more obvious (Figure 31 B, lane 4). However, compared to the Western blot analysis shown above for the Alkaline Phosphatase treatment (Figure 23B), astrin is not completely dephosphorylated. These results indicate that hCdc14A only dephosphorylates specific phosphorylation sites on astrin and that there might be another phosphatase besides hCdc14A which dephosphorylates astrin. In summary, hCdc14A is an attractive candidate for a regulator of astrin function.

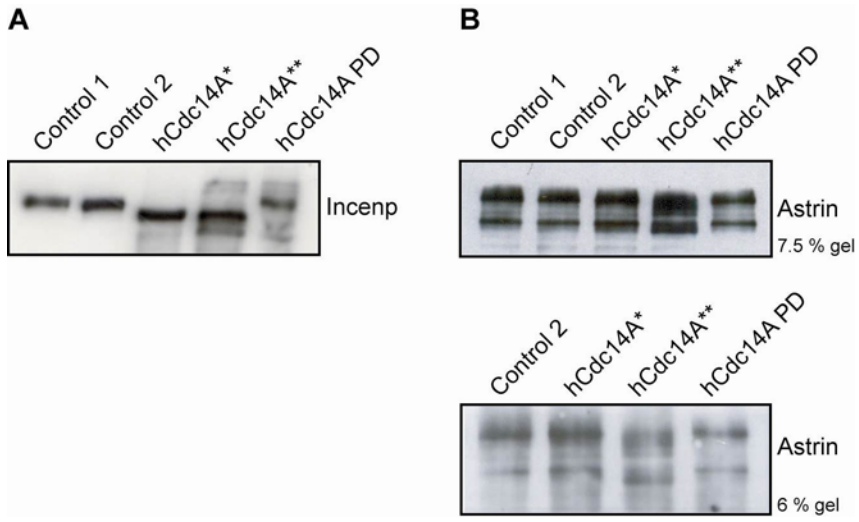

Figure 31. Astrin is dephosphorylated by hCdc14A. (A and B) For the phosphatase assay mitotically phosphorylated INCENP or astrin was IPed from mitotic lysates with either anti-Aurora B (to IP INCENP) or anti-astrin antibodies and Protein G-Sepharose. The protein-coupled beads were resuspended in 1x phosphatase buffer, aliquoted and treated with different amounts of recombinant hCdc14A wt (*50 ng, **500ng) or hCdc14A PD (500ng) or left untreated for 30 min at 30°C (control 1) or on ice (control 2). The phosphatase reaction was stopped by addition of sample buffer followed by boiling. Equal protein amounts were loaded on and separated by SDS-PAGE, followed by Western blot analysis with the indicated antibodies.

4. Astrin acts at different steps in cell division

The dual localization of astrin to both centrosomes and KTs (Figure 13) and its possible interaction with the KT associated motor CENP-E, the mitotic phosphatase hCdc14A and the mitotic kinase Plk1 indicates that it may act at different steps in cell division. To analyse astrin's role in mitosis, loss-of-function experiments were performed.

4.1. Depletion of astrin results in an increase in mitotic index and cell death by apoptosis

To study the functional consequences of astrin depletion, HeLa cells were treated with astrin siRNA and examined by immunofluorescence microscopy 48 h later. Analysis of the resulting mitotic cells revealed that most of the cells were multipolar and showed disorganized DNA (Figure 32A). To test whether the siRNA phenotype was specific we used two approaches, antibody microinjection and siRNA rescue experiments. For microinjection experiments purified astrin antibodies, or rabbit IgG as a control, were microinjected into the cytoplasm of HeLa cells. 24 h after injection cells were fixed, co-stained with secondary anti-rabbit antibodies to visualize injected cells, and with anti-α-tubulin antibodies to monitor the mitotic spindle (Figure 32B). Cells injected with anti-astrin antibodies displayed multipolar spindles with disorganized DNA, whereas control injection of purified rabbit IgG did not give any obvious phenotypes (Figure 32B). For rescue experiments the siRNA-resistant Myc-astrin plasmid or the empty Myc-vector as a control were transfected 24 h prior to the transfection of siRNA duplexes targeting astrin. The cells were fixed and analysed 42 h later. The defects caused by siRNA mediated depletion of astrin were efficiently rescued by Myc-astrin. Taken together, these data show that the siRNA based phenotype is specific to astrin. The loss of astrin results in multipolarity and disordered DNA, indicating that the loss of astrin's function interferes with centrosome integrity and chromosome congression.

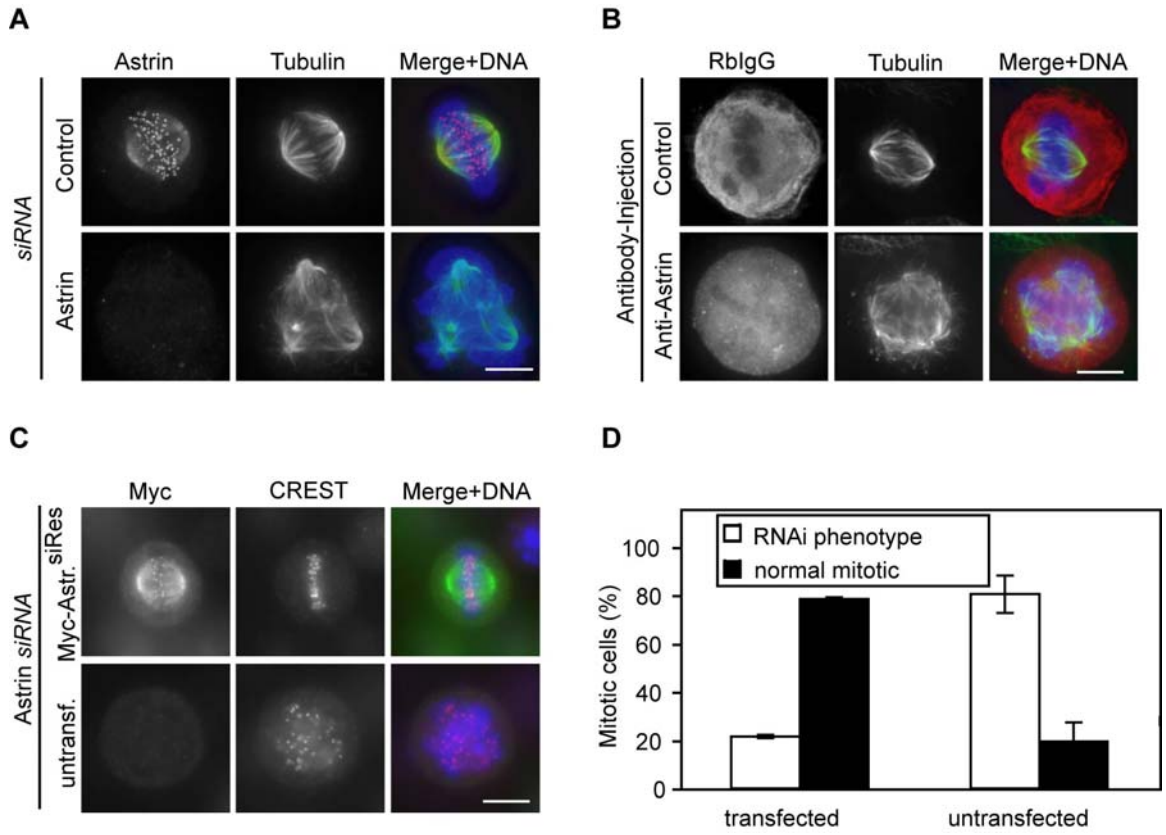

Figure 32. Astrin depletion results in multipolarity and uncongressed chromosomes. (A) HeLa cells were treated with control or astrin siRNA oligos, fixed after 48 h and stained for astrin and α-tubulin. (B) Interphase HeLa cells were injected with purified rabbit anti-astrin antibodies or control rabbit IgG, fixed after 24 h and stained with antibodies against tubulin (green) and secondary anti-rabbit antibodies (red). (C) HeLa cells were transfected with Myc-astrin constructs, containing five silent mutations in the sequence targeted by the astrin siRNA oligo, 24 h prior to transfection with astrin siRNA oligos, and stained with CREST antiserum (red) and antibodies against Myc (green). (A,B and C) DNA was stained with DAPI (blue). Bar, 10 µm. (D) The percentage of transfected and untransfected cells displaying the astrin depletion phenotype was scored in two independent experiments.

Closer analysis of the siRNA phenotype by a time course (cells were examined after 24, 36 and 48 h) revealed that the depletion of astrin resulted in an increase in mitotic index and in multipolarity. Concomitantly, increased cell death by apoptosis was observed (Figure 33) as described previously (Gruber et al., 2002). Taken together, these results demonstrate that astrin is essential for progression through mitosis, confirming a previous report (Gruber et al., 2002).

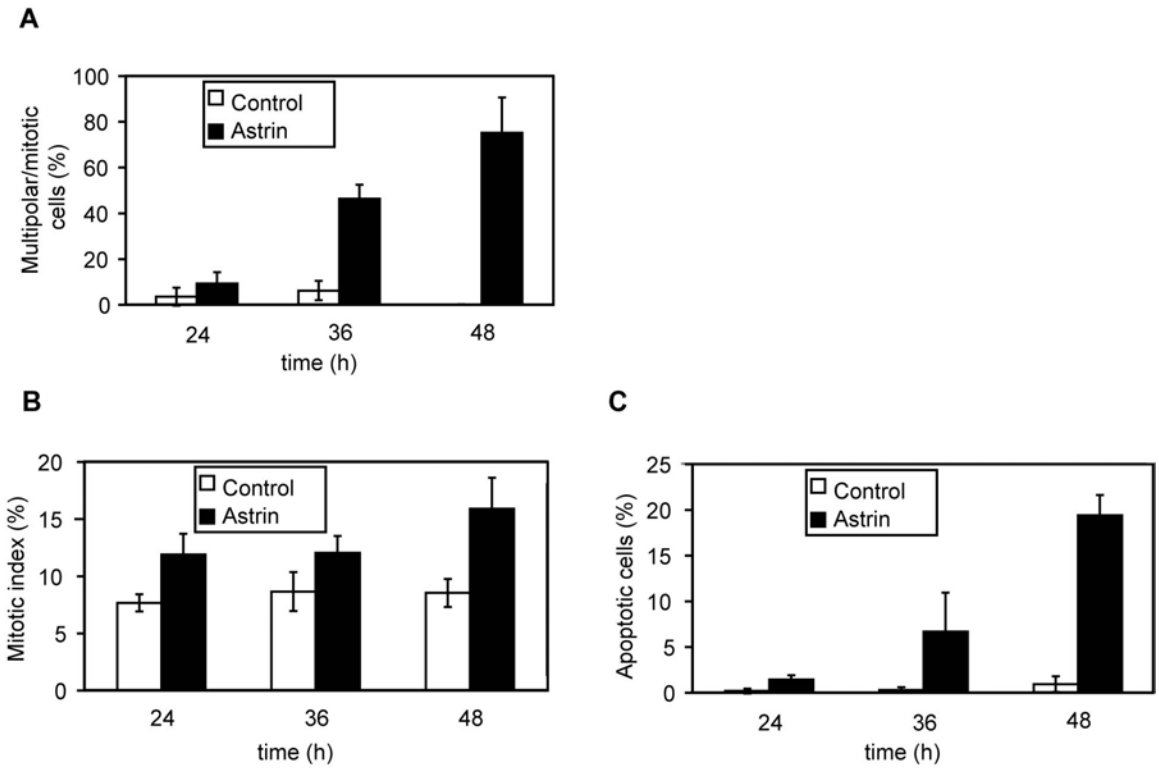

Figure 33. Astrin depletion by siRNA results in an increase in mitotic index, multipolarity and apoptosis. SiRNA treated cells were fixed and analysed after 24, 36 and 48 h. (A) The percentage of mitotic cells with multipolar spindles, (B) the mitotic index, (C) and the percentage of apoptotic cells were scored in control and astrin depleted HeLa cells. The graphs represent triplicate experiments. For each time point 200 cells were counted.

4.2. Astrin is required for efficient chromosome alignment and spindle pole integrity

To investigate the mitotic phenotype in more detail, time-lapse video microscopy was performed on HeLa cells that stably express a histone H2B-GFP fusion protein (Figure 34). These experiments showed that astrin depleted cells exhibited a profound chromosome alignment defect (Figure 34). They required significantly more time to assemble a metaphase plate than control cells (63.9 +/- 28.5 mins in comparison to 27.0 +/- 8.0 mins) (Figure 34) and 60% of the cells never accomplished full alignment of all the chromosomes (Figure 34). Once metaphase chromosome alignment was achieved, chromosomes were lost again from this structure (Figure 34, t = 104' and t = 160') and cells remained arrested in a metaphase-like state for prolonged periods of time, up to 10 h, and eventually died by apoptosis. While most astrin depleted cells (8/9) initially formed a bipolar spindle, after several hours of mitotic arrest (194.4 +/- 46.5 min)

bipolarity was lost, and a multipolar spindle was formed (Figure 34, t = 252'). In the one remaining case, a multipolar spindle was formed immediately without a preceding period of bipolarity. Together, these data suggest that astrin has functions at both spindle poles and KTs, and that the lack of astrin leads to a prolonged mitotic arrest.

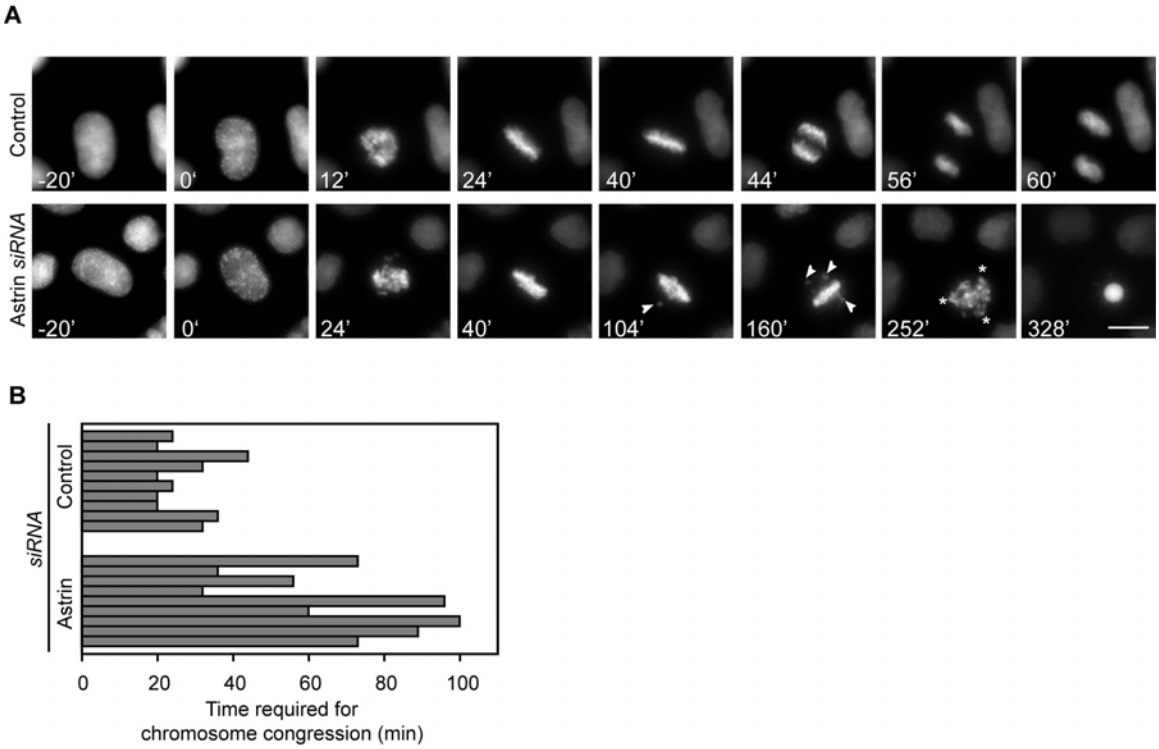

Figure 34. Live cell imaging reveals astrin depletion results in chromosome congression defects and multipolarity. (A) Stills of representative movies of control and astrin depleted cells. Bar, 10 μm. Time is indicated in mins. All astrin depleted cells analysed (n=10) exhibited delayed chromosome congression (compare t = 24' in control and astrin siRNA cells) and unstable metaphase plates. Note unaligned chromosomes in astrin siRNA at t = 104' and t = 160' (arrowheads). The depicted astrin depleted cell is initially bipolar but forms a multipolar spindle (asterisks indicate spindle poles) during the mitotic arrest. (B) Control or astrin depleted HeLa cells expressing histone-H2B-GFP were followed by live cell analysis. The time required for chromosome congression was plotted.

4.3. Astrin depleted cells are spindle checkpoint arrested

The observed mitotic arrest in cells depleted of astrin suggests that the SAC is activated and cannot be satisfied. Consistent with this idea, cells lacking astrin displayed Mad2 and strongly BubR1-positive KTs (Figure 35). As the KT association of BubR1 and Mad2 usually (albeit not invariably; (Martin-Lluesma et al., 2002) correlate with an active SAC, this observation indicates that astrin depleted cells failed to turn off the SAC. Indeed, the

mitotic arrest induced by astrin depletion could readily be overcome by co-depletion of Mad2, or treatment of astrin depleted cells with Aurora B inhibitor ZM447493 confirming its dependency on the SAC (Figure 35).

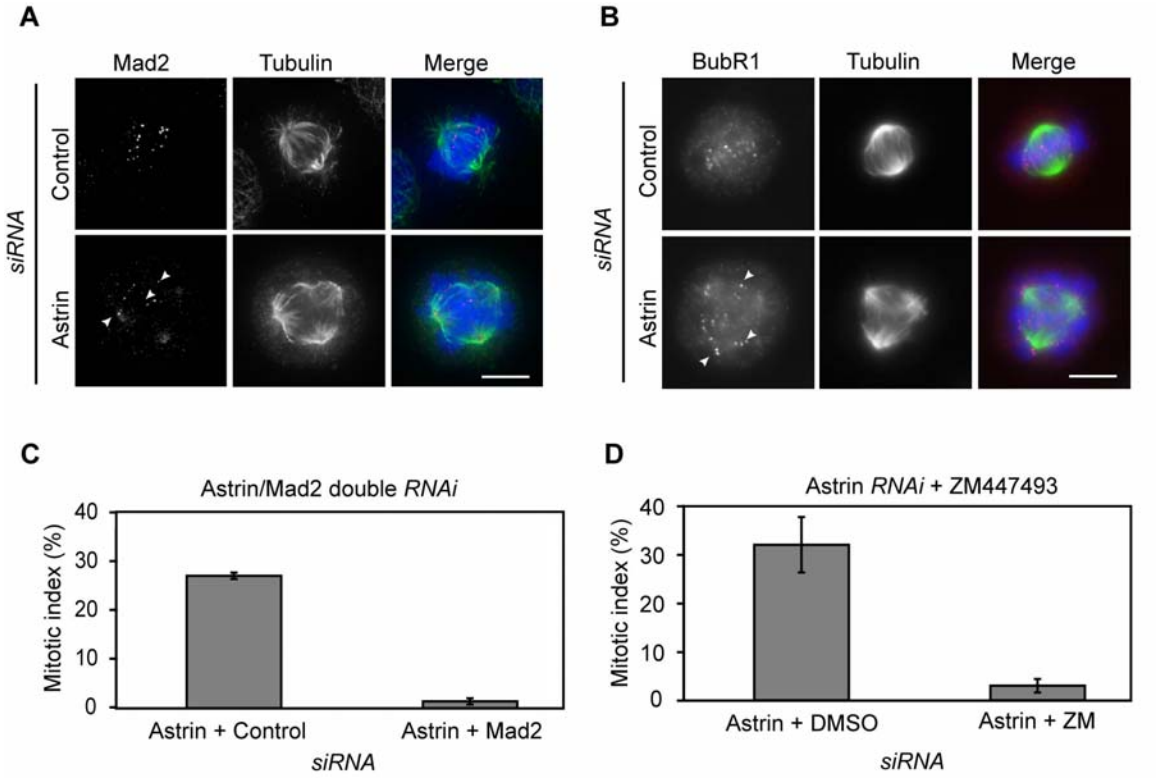

Figure 35. Astrin depleted cells are spindle checkpoint arrested. (A and B) Control or astrin depleted HeLa cells were stained with antibodies against α-tubulin (green) and either Mad2 or BubR1 (red). (C) HeLa cells were transfected with astrin siRNA and 16 h later with Mad2 or control siRNA oligos for an additional 24 h. The mitotic index was scored. (D) Control and astrin depleted cells were treated with DMSO or 10 μM ZM447493 for 3 h, and the mitotic index was scored.

Consistent with the previous results, extracts prepared from astrin depleted cells had levels of cyclin B1, securin and phospho-histone H3(Ser10) comparable to control nocodazole arrested cells (Figure 36 C). Cells lacking astrin stained brightly for cyclin B1 and securin (Figure 36 A and B). To analyse the securin staining in astrin depleted and control cells more precisely, the levels of securin staining were measured in four independent experiments using ImageJ software. The mean pixel intensities of astrin depleted and control cells were similar (Figure 36 D). Taken together, these data further confirm that cells lacking astrin are SAC arrested.

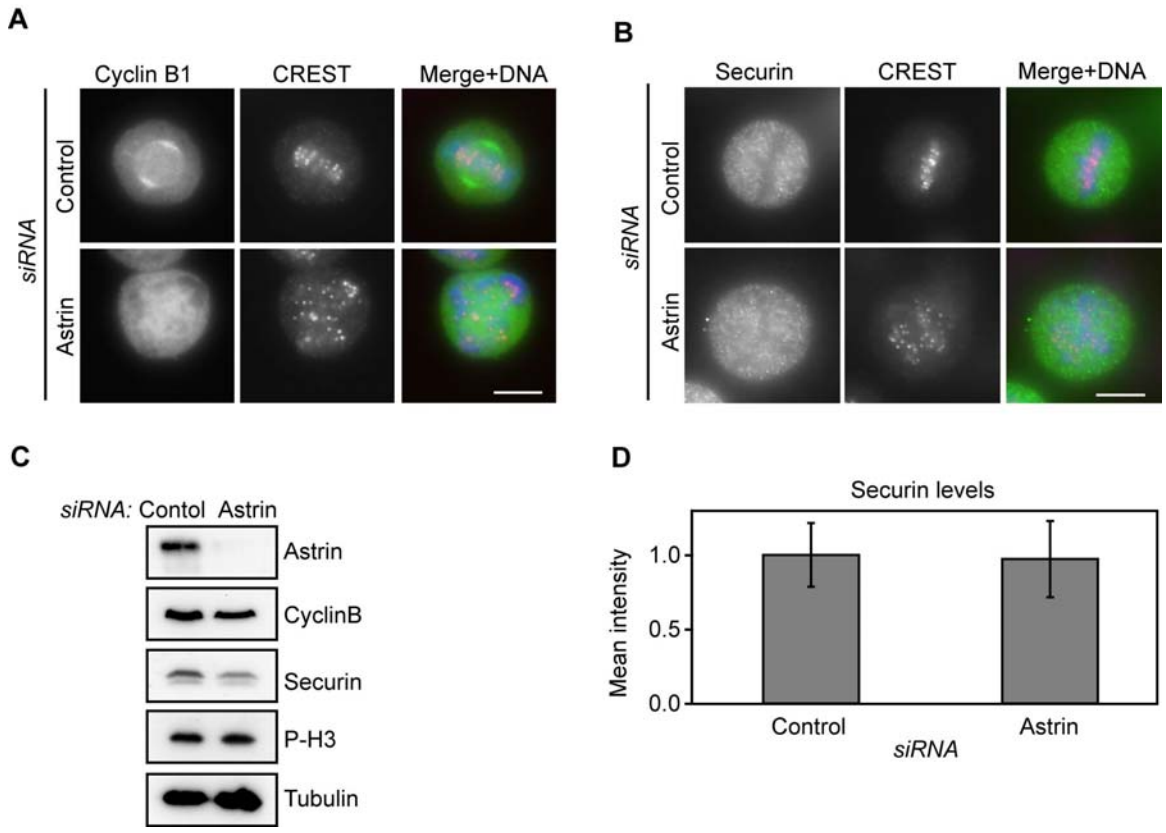

Figure 36. Securin and cyclin B1 are stable in cells lacking astrin. (A and B) Control or astrin depleted HeLa cells were stained with antibodies against CREST (red) and either cyclin B1 or securin (green), respectively. DNA was visualized with DAPI. Bar, 10 μm. (C) Lysates of mitotic control and astrin depleted HeLa cells harvested by mitotic shake-off were immunoblotted with antibodies against the indicated proteins. The two astrin bands appear as one because of a higher percentage SDS gel used**.** (D**)** The levels of securin staining in control or astrin depleted mitotic cells were measured in four independent experiments using ImageJ software, analysing 15-20 cells of each kind per experiment.

4.4. Cells lacking astrin have unstable microtubule kinetochore interactions

The persistent activation of the SAC (chapter 4.3), together with the chromosome congression defect (Figure 32), suggested that MT-KT interactions are impaired in cells lacking astrin. To test this idea, cells were analysed after cold treatment (Rieder, 1981) or pre-extracted prior to fixation to differentially preserve KT fibres (Holt et al., 2005). Under both conditions, astrin depleted cells displayed many unattached KTs and fewer stable KT-MTs than control cells, although the phenotype was not as drastic as the one observed in Hec1 depleted cells (Figure 3A and B) (DeLuca et al., 2002). The KTs that were MT associated often appeared to be attached laterally rather than end-on in cells lacking astrin (Figure 37B, lower panel, insets).

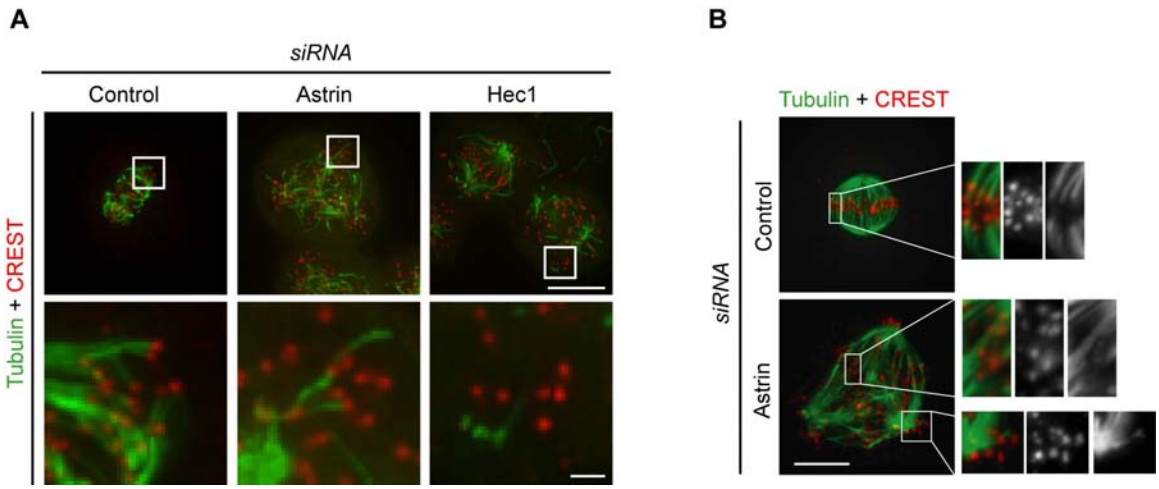

Figure 37. MT-KT interactions are unstable. (A) HeLa control cells and astrin or Hec1 depleted cells were incubated on ice for 20 minutes prior to fixation. Cold-stable K-fibre MTs were revealed by KT staining with CREST serum and antibodies against α-tubulin. The indicated areas are shown blown-up in the bottom panel. Note the presence of unattached KTs in astrin depleted cells. Bars, 10 µm in top panel, 1 µm in bottom panel. (B) Control or astrin depleted HeLa cells were pre-extracted prior to fixation and MT-KT interactions were visualized as above. Bar, 10 µm.

As shown above in chapter 2.1 the core KT protein Hec1 and the spindle checkpoint kinase Bub1 were unaffected (Figure 21), the KT-resident motor protein CENP-E (Yen et al., 1992) and its interaction partner CENP-F (Chan et al., 1998) were delocalized from the KT in the absence of astrin (Figure 21). These data suggest that the presence of astrin is required for the KT recruitment or maintenance of CENP-E and CENP-F. Moreover, it has been suggested that Plk1 is required for stabilization of MT-KT attachments (Elowe et al., 2007; Lenart et al., 2007; Matsumura et al., 2007). This, in combination with the lack of CENP-E, CENP-F and astrin itself, may cause unstable MT-KT interactions, unaligned chromosomes and persistent activation of the SAC. However, these finding do not explain why multipolar spindles are formed in cells lacking astrin.

5. Astrin is required for maintenance of centrosome integrity and sister chromatid cohesion

To analyse the molecular basis of the multipolar spindle phenotype in more detail, the localization of centrin, a marker for individual centrioles (Paoletti et al., 1996) was investigated in astrin depleted cells. Multipolar spindles can arise by a number of different routes that can be distinguished by the number of centrioles found at the individual poles. Failure of cytokinesis will lead to multiple spindle poles with two

centrin-positive centrioles at each pole. Aberrant centriole disengagement, in contrast, will cause the formation of multipolar spindles with single centrioles at individual spindle poles (Keryer et al., 1984; Sluder and Rieder, 1985). A further possible cause for the loss of spindle bipolarity is the loss of MT anchoring at the centrosome as observed, for instance, upon TOGp depletion (Cassimeris and Morabito, 2004; Holmfeldt et al., 2004).

5.1. The absence of astrin results in centriole disengagement

In contrast to the bipolar spindles of control cells, which displayed two centrin dots at each pole, the multipolar spindles in cells lacking astrin often displayed single centrin dots at each pole (Figure 38A). For a further, quantitative comparison the number of centrin dots per pole in multipolar cells depleted of Aurora B, known to be required for correct chromosome segregation and progression through cytokinesis (Honda et al., 2003), or TOGp, a protein important for maintaining intact spindle poles (Cassimeris and Morabito, 2004; Gergely et al., 2003; Holmfeldt et al., 2004) was evaluated (Figure 38C). This approach revealed that 79.2% of multipolar spindles in Aurora B depleted cells displayed two centrin-positive dots per pole (Figure 38B and C), consistent with the idea that these spindles had arisen from a previous cytokinesis failure. Multipolar spindles in TOGp depleted cells often showed poles with no centrin staining in addition to two "normal" poles with two centrin dots, and therefore contained the highest number of acentriolar poles (43.9%, Figure 38B and C). Strikingly, and in contrast to both Aurora B and TOGp depletion, in astrin depleted cells 55.4% of poles had single centrioles suggestive of aberrant centriole disengagement (Figure 38C). In line with these data, Aurora B and astrin depleted cells generally displayed pericentrin staining at all poles of multipolar spindles, whereas TOGp depleted cells often possessed multipolar spindles with only two pericentrin-positive poles, confirming published results (Holmfeldt et al., 2004) (Figure 38D). Taken together, these results suggest that the formation of multipolar spindles upon astrin depletion is mainly caused by an untimely loss of the connection between the two centrioles of each centrosome.

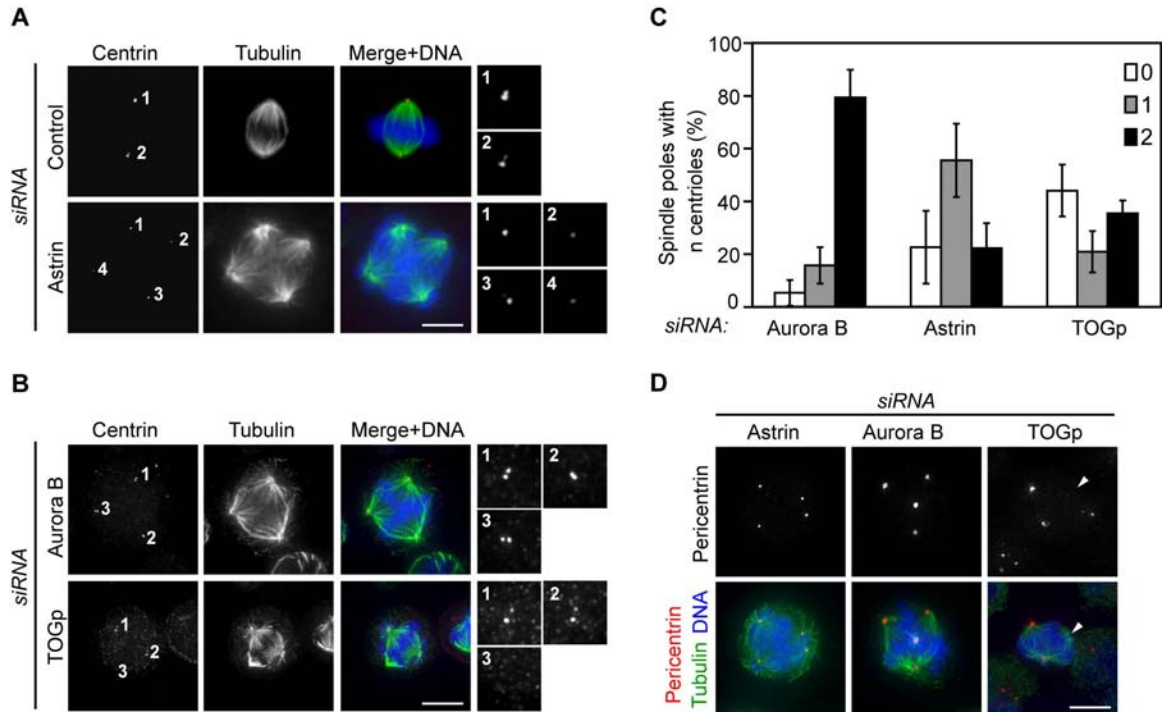

Figure 38. Astrin depletion causes loss of centriole cohesion. (A) Control or astrin depleted cells were stained with antibodies against centrin (red) and α-tubulin (green). DNA was visualized with DAPI (blue). Individual centrosomes are shown enlarged on the right hand side. (B) HeLa cells depleted of Aurora B or TOGp were stained as in (A). (C) Quantitative analysis of the centriole number at the poles of multipolar spindles in cells depleted of astrin, Aurora B or TOGp. The number of poles containing no, one, or two centrin stainings was plotted as a percentage of the total number of poles. The cells were analysed double blind by three different researchers. The graphs represent triplicate experiments of at least cells, each. Bars, 10 µm. (D) Astrin, Aurora B and TOGp depleted cells were stained with antibodies against pericentrin (red) and α-tubulin (green). The arrowhead indicates an acentriolar spindle pole in the TOGp depleted cell. Bar, 10 µm.

5.2. Sister chromatid cohesion is prematurely lost in astrin depleted cells

In normal cells, the connection between the two centrioles is lost at the end of mitosis or early G1 phase, when the two centrioles are disengaged. It has recently been demonstrated that this disengagement of the two centrioles is dependent on the activity of separase (Tsou and Stearns, 2006b), a protease that also controls cohesion cleavage between sister chromatids (Uhlmann et al., 2000). One possible explanation for the formation of multipolar spindles in cells depleted of astrin could therefore be an inefficient inhibition of separase during the checkpoint arrest, leading to premature disengagement of the centrioles. In this case one would predict that cohesion between sister chromatids would also be affected. Consistent with this idea, immunofluorescence

analysis of cells or single chromosomes showed that the chromosomes of mitotically arrested astrin depleted cells displayed single dots of CREST staining, indicative of separated sister chromatids, in comparison to paired dots in metaphase control cells (Figure 39A and B). Furthermore 65.0% of mitotic chromosomes in chromosome spreads prepared from astrin depleted cells displayed separated sister chromatids, compared to less than 1.0% of control cell spreads, 97.7% of chromosome spreads of Sgo1 depleted cells, known to display loss of sister chromatid cohesion (McGuinness et al., 2005), and 9.3% of spreads of CENP-E depleted cells (Tanudji et al., 2004) (Figure 39C and D). This loss of cohesion was not caused by lack of the centromeric protectors Sgo1 or the associated B56-containing subtype of PP2A phosphatase (Kitajima et al., 2006; McGuinness et al., 2005) (Figure 39E and F).

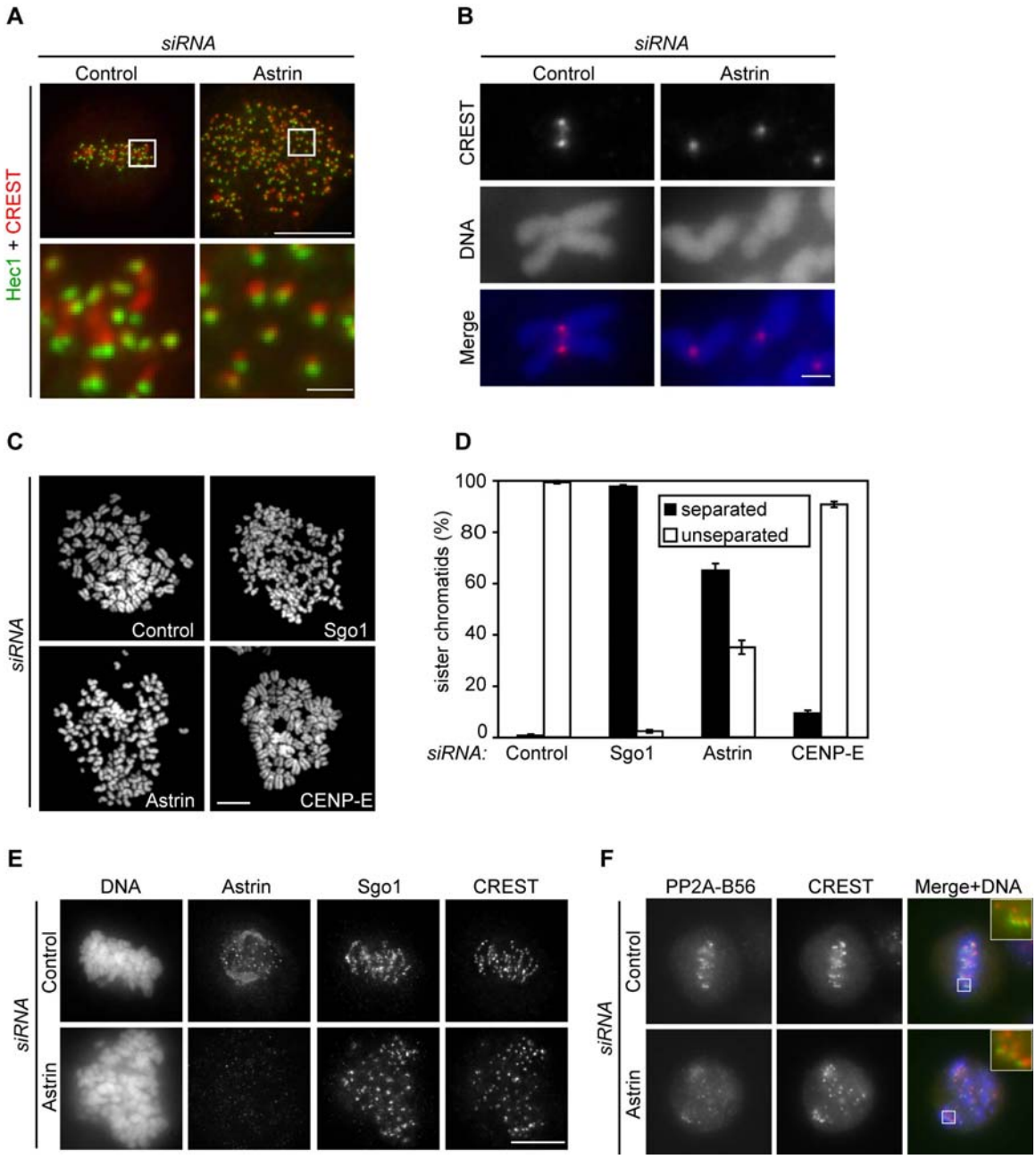

Figure 39. Astrin depletion causes loss of centriole cohesion. (A) Control and astrin depleted HeLa cells were fixed and stained with CREST serum (red) and with antibodies against Hec1 (green). DNA was stained with DAPI (blue). The indicated areas are shown enlarged in the bottom panel. Bar, 1 µm. Note that in astrin depleted cells single Hec1-CREST pairs are observed. (B) Chromosome spreads of mitotically arrested control or astrin depleted cells were stained with CREST serum. Bar, 1µm. (C) Chromosome spreads were prepared from mitotic HeLa cells depleted of Gl2 (control), CENP-E (both 48 h RNAi), Sgo1 and astrin (both 40 h RNAi). Representative pictures of each sample are shown. (D) Quantitation of the chromosome spreads shown in (E). Each bar represents triplicate experiments. 100 cells of each sample were counted per experiment. (E and F) Control and astrin depleted HeLa cells were fixed and stained with CREST serum and antibodies against (E) astrin and Sgo1 or (F) PP2A-B56 (green) and CREST (red). Bar, 10 µm.

To investigate the chromosome cohesion defect in more detail, time-lapse video microscopy was performed on astrin depleted cells expressing YFP-tagged CENP-A. This revealed that these cells established and maintained cohesion normally in early mitosis through to the formation of (imperfect) metaphase plates but lost cohesion during subsequent mitotic arrest, on average 89.6 +/- 42.3 mins (n = 10) after forming a metaphase(like) plate (Figure 40). In summary, the data obtained from imaging histone H2B-GFP (Figure 34) or CENP-A-YFP (Figure 40) expressing astrin depleted cells indicate that loss of sister chromatid cohesion precedes loss of centrosome integrity in these cells but that both events occur after the formation of an imperfect metaphase plate.

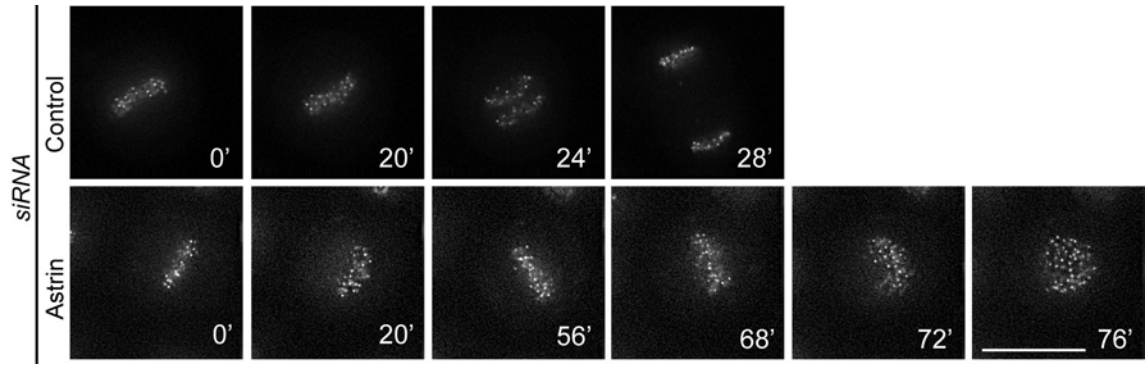

Figure 40. CENP-A-YFP expressing astrin depleted cells indicate that loss of sister chromatid cohesion precedes loss of centrosome integrity. Control or astrin depleted HeLa CENP-A-YFP cells were followed through mitosis by live cell imaging. Time is indicated in min. Like control cells, astrin depleted cells formed a metaphase (like) plate with well-cohesed sister chromatids (visible as paired YFP-CENP-A dots, see t = 0). During the ensuing mitotic arrest astrin depleted cells lost sister chromatid cohesion visible as single YFP-CENP-A dots), on average 896 +/- 42.3 mins (n = 10) after reaching a metaphase (like) state (see lower panel 72 and 76 mins).

To clearly demonstrate that loss of sister chromatid cohesion and centrioles disengagement were specific for cells depleted of astrin, we compared astrin depleted cells to pre-synchronized and then nocodazole arrested cells and additionally also to CENP-E depleted cells. Both treatments resulted in a mitotic arrest of at least 10 h, similar to what is observed upon astrin depletion (Yao et al., 2000). Nevertheless, the amount of multipolar cells observed under these conditions was far less than in astrin depleted cells (23.0 +/- 2.0% and 12.8 +/- 3.7%, respectively, compared to 67.3 +/-21%). Furthermore, closer analysis of the multipolar cells formed under these conditions demonstrated that in nocodazole arrested and released cells a high proportion of multipolar cells contained acentriolar poles, suggesting loss of MT anchoring, and that

CENP-E depleted multipolar cells mostly displayed two centrioles per poles, which is indicative of failed cell division and re-entry into the cell cycle. Both situations are therefore clearly distinct from the multipolar cells observed in astrin depleted cells, in which the majority of poles possess only one centriole, suggesting premature centriole disengagement. Moreover, and again different from astrin depleted cells, neither CENP-E depleted nor nocodazole arrested cells displayed any significant loss of sister chromatid cohesion. In summary, the data presented here confirm that astrin depletion causes unique defects (67.3 +/- 2.1% multipolar mitotic cells, 65.0 +/- 2.6 % separated sister chromatids) that cannot be phenocopied by forcing cells into extended mitotic arrest by other means.

Table 1. Analysis of centrosome integrity and sister chromatid cohesion in spindle checkpoint – arrested cells

Treatment	**Separated chromatids**	**Mitotic index**	**Multipolar/ mitotic cells** [A]	**Poles with a single centriole** [B]
Astrin siRNA [C]	**65.0** +/- 2.6 %	**16.2** +/- 2.0 %	**67.3** +/- 2.1%	**55.4** +/- 13.9 %
CENP-E siRNA	**9.3** +/- 1.2 %	**26.3** +/- 3.2 %	**12.8** +/- 3.7 %	**16.3** +/- 4.8 %
Nocodazole (16h) [D]	**0.3** +/- 0.6%	**52.7** +/- 2.9 %	**23.0** +/- 2.0 %	**28.7** +/- 10.2 %

A: Mitotic cells = 100 %

B: Percentage of poles with a single centriole relative to all poles in multipolar spindles

C: Live cell imaging shows that mitotic arrest lasts for approximately 10 h before apoptosis occurs.

D: Cells were synchronized with aphidicolin for 16 h, released for 6 h and then blocked in mitosis for 16 h by adding nocodazole. For immunofluorescence analysis of mitotically arrested cells, the cells were released into fresh medium for 40 min in order to allow formation of a mitotic spindle.

5.3. Separase is prematurely activated in cells depleted of astrin

The separation of the sister chromatids in cells lacking astrin would be consistent with premature activation of separase. This hypothesis was tested by exploiting the fact that active separase undergoes self-cleavage, resulting in a 65 kDa C-terminal fragment (Waizenegger et al., 2002). Extracts prepared from mitotically arrested, or mitotically arrested and released cells, were used to create situations in which separase was either

inactive (mitotic arrest) or active (release from mitotic arrest). Immunoblotting revealed the presence of a C-terminal cleavage product only in the control cells that had been released from the mitotic block (Figure 42, compare lanes 1 and 2). Significantly, in extracts prepared from astrin depleted cells the C-terminal separase cleavage product was present at ca. 30% of the level observed in the released control cells (Figure 42, lane 3). These data suggest that a fraction of separase is active in mitotic astrin depleted cells.

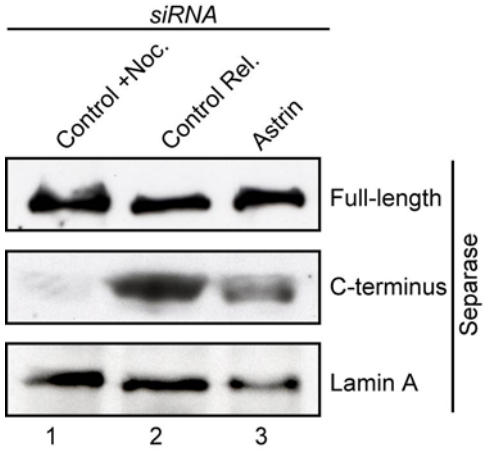

Figure 41. Separase is prematurely activated in cells depleted of astrin. (A) Extracts prepared from nocodazole arrested HeLa control cells (lane 1); control cells that had been released from a nocodazole block for 100 mins (lane 2) or astrin depleted cells harvested by mitotic shake-off (lane 3) were immunoblotted with mouse anti-C-separase antibodies and mouse-anti-lamin A as a loading control. The blot shown is a representative example of five independent experiments.

To directly test the involvement of separase in the astrin phenotype, cells were simultaneously depleted of astrin and separase. Immunofluorescence and Western blot analysis showed that both proteins could be efficiently depleted, either singly or together (Figure 42A and B). Cells lacking both separase and astrin displayed a similarly elevated mitotic index in comparison to cells depleted only of astrin (15.5 +/- 3.7% in the double depletion in comparison to 16.2 +/- 3.0% in astrin depletion) (Figure 42C). However, in contrast to astrin depletion alone, cultures depleted of both astrin and separase contained significantly fewer cells with multipolar spindles (16.9 +/- 6.0% in the double depletion versus 68.8 +/- 11.5% in the astrin RNAi) (Figure 42D). Importantly, chromosome spreads of these cultures showed that sister chromatid cohesion was restored in cells in which both astrin and separase expression had been repressed (Figure 42E). In contrast, no effect on the TOGp phenotype was observed upon the additional depletion of

separase. The depletion of TOGp and separase resulted in a similar mitotic index compared to cells depleted only of TOGp (20.8 +/- 1.1% in the double depletion in comparison to 22.0 +/- 3.7% in TOGp depletion) and the percentage of multipolar spindles was similar in both cases (45.5 +/- 11.3% in the double depletion in comparison to 40.5 +/- 3.7% in TOGp depletion). Taken together, these data show that both the aberrant centriole disengagement and the premature loss of sister chromatid cohesion observed in astrin depleted cells involve separase.

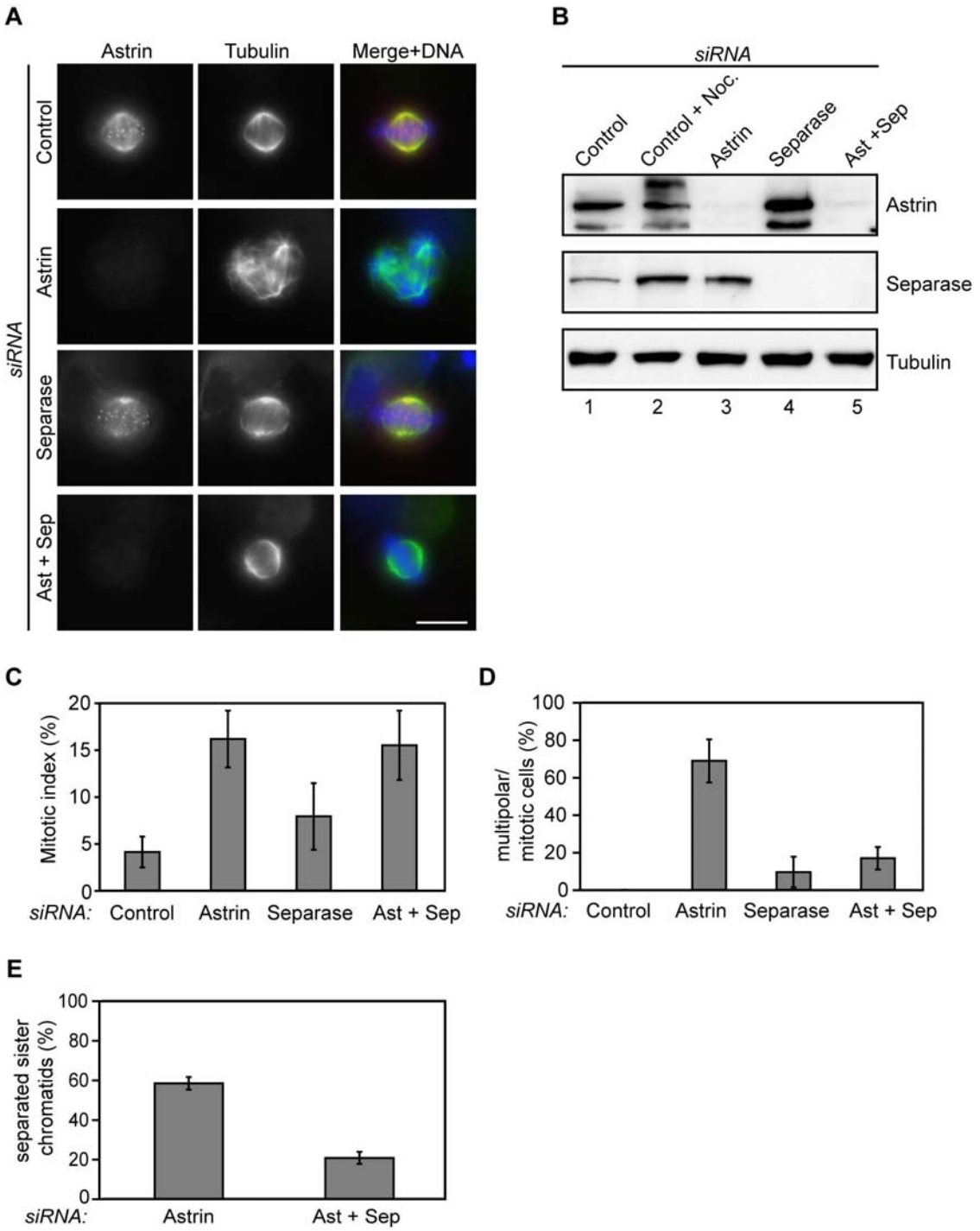

Figure 42. Separase-dependent formation of multipolar spindles and loss of sister chromatid cohesion in cells depleted of astrin. (A) HeLa cells were depleted of astrin and separase individually, or together (for 48 hours). Extracts from these and control cells were blotted for astrin and separase, and tubulin as a loading control. Note that astrin depleted cells (lane 3) contain more separase than asynchronous (lane 1), but similar amounts to nocodazole arrested control cells (lane 2), because of the elevated mitotic index. (B) Cells treated as in (A) were stained with antibodies against astrin (red) and α-tubulin (green). Representative images of each cell population are shown. Bar, 10 μm. (C), (D) and (E) Quantitation of the mitotic index, percentage of multipolar of mitotic cells and degree of sister chromatid separation observed in astrin-, separase- or double depleted cells and control cells.

DISCUSSION

During mitosis one cell is divided into two genetically identical daughter cells. To ensure equal segregation of chromosomes into the two daughter cells, progression through mitosis has to be tightly regulated. Here the functional analysis of the mitotic spindle and KT associated protein astrin is described. Astrin was originally identified in a mass spectrometric analysis of proteins associated with mitotic MTs and it has been indicated that astrin is required for progression through mitosis (Gruber et al., 2002; Mack and Compton, 2001).

1. Two isoforms of astrin were identified

Mass spectrometry based characterization of IPed astrin revealed two forms of astrin, which differ in size. The smaller of the two isoforms lacks approximately 200 amino acids of the N-terminus (aa 1-481), which is rich in potential serine and threonine phosphorylation sites. It has also been shown that astrin is highly phosphorylated in mitosis (Figure 23A, B and C) and that astrin is an *in vitro* substrate of Cdk1 (Figure 23D and Chang et al., 2001). These data indicate that astrin's function is regulated by phosphorylation. Since the smaller form of astrin lacks a part of the N-terminus, there could be functional differences between the two isoforms of astrin, which needs further investigation.

2. Analysis of factors that influence astrin's localization

Since astrin localizes to the mitotic spindle and spindle poles, MT binding assays were performed to test whether astrin directly binds to MTs. Our results showed that astrin does not co-pellet with MTs, suggesting that modifications, e.g. phosphorylation or binding to an interactor are responsible for astrin's association with MTs. Since neither treatment with the Cdk1 inhibitor roscovitin (data not shown) nor with the Plk1 inhibitor TAL (Santamaria et al., 2007) (Figure 28) influences astrin's localization to MTs, it is very unlikely that this association is regulated by phosphorylation. We therefore favour the hypothesis that a so far unknown interactor is responsible for astrin's localization to MTs.

Release from nocodazole reestablished astrin's localization simultaneously with the recovery of MTs. Astrin was first observed at the poles and subsequently, as the mitotic spindle reformed, it became more and more apparent at the KTs (Figure 16A). This redistribution could be the consequence of astrin's transport from the pole to the KT by a plus-end directed MT motor protein, such as Kif18, CENP-E or Eg5 (Blangy et al., 1995; Mayer et al., 1999; Mayr et al., 2007; Yao et al., 1997). In contrast to both Kif18 depletion and Eg5 inhibition, depletion of CENP-E results in a complete loss of astrin from the KT. Since astrin's localization to the KT depends on stable MT-KT interactions, which are impaired in cells depleted of CENP-E, it is possible that the observed effect on astrin localization is indirect. However, the overlap of astrin and CENP-E at the KT (Figure 14), the bi-dependency of astrin and CENP-E in localization to the KT and the fact that they biochemically interact, strongly suggest that astrin's localization to the KT is directly dependent on CENP-E.

However, CENP-E did not influence astrin's localization to the spindle or the spindle pole, which suggests that CENP-E is not the plus-end directed motor responsible for astrin's transport from the pole to the KT. In fact, none of the proteins we depleted so far impaired astrin's localization to these structures. Thus further studies are required to identify the motor protein that transports astrin from the spindle pole along the mitotic spindle to the KT. A possible approach to identify this motor could be the optimisation of astrin IP followed by mass spectrometric analysis.

3. Bi-dependency analysis revealed Plk1 as an astrin interactor

The siRNA based bi-dependency analysis revealed that astrin is lost from the KT in cells depleted of Plk1 while spindle staining of astrin was not influenced (Figure 21D and H). Vice versa, depletion of astrin resulted in complete delocalization of Plk1; it was lost from the KT and the centrosome (Figure 21C and I). Since astrin and Plk1 localize to the same structures during mitosis: KTs, centrosome and midzone (Barr et al., 2004), it is likely that Plk1 and astrin influence each other. Indeed, we have shown that astrin interacts directly with Plk1 in a PBD dependent manner. However, so far we have been unable to demonstrate unequivocally that astrin is a Plk1 substrate.

Recent studies indicated that Plk1 is involved in checkpoint signalling by generating the 3F3/2 phospho-epitopes, which are involved in tension-sensing by being only present at unattached or unaligned KTs and released as soon as tension is established between the sister chromatids (Ahonen et al., 2005; Wong and Fang, 2006). It has been suggested that Plk1 phosphorylation of SAC components is involved in proper MT-KT attachments (Elowe et al., 2007). In line with that it has been shown that Plk1 is involved in the stabilization of MT-KT interactions and chromosome congression (Elowe et al., 2007; Hanisch et al., 2006). However it is still not known how Plk1 contributes to chromosome congression. Plk1 is delocalized in cells depleted of astrin and chromosome congression as well as MT-KT interactions are impaired in these cells, suggesting that the loss of Plk1 contributes to this phenotype. Moreover it is tempting to speculate that astrin is part of a protein complex at the outer KT, which is involved in chromosome congression and MT-KT interactions. Plk1 could regulate this complex by phosphorylation.

Plk1 and astrin do not co-localize at the outer-KT (Figure 14), indicating that it is unlikely that astrin is a structural binding partner of Plk1 at the KT. Nevertheless, Plk1 might regulate astrin by phosphorylating a specific pool of astrin at the KT. Alternatively, since both proteins show overlapping localization to the spindle pole, it might be the case that the interaction of astrin and Plk1 takes place at the spindle pole.

The serine-threonine phosphatases hCdc14A, which we identified here as a potential astrin interactor also localizes to the spindle pole. HCdc14A counteracts Cdk1 activity (Visintin et al., 1998). Thus it could be speculated that hCdc14A dephosphorylates Thr111 and thereby regulates the binding of Plk1 to astrin. However, because the functions of hCdc14 in mitosis are not well understood, it is difficult to speculate about how hCdc14 regulates astrin's function in mitosis (Kaiser et al., 2002; Mailand et al., 2002).

4. Astrin is an outer KT protein which localizes to aligned chromosomes and is involved in the stabilization of MT-KT interactions

Immunofluorescence analysis of astrin's localization showed a centrosomal pool of astrin and an outer-KT-associated pool (Figure 14). The dual localizations of astrin together with depletion studies by siRNA indicate that astrin is involved in proper spindle

formation and chromosome segregation (Figure 14 and Figure 32). Moreover, live-cell imaging studies of cells depleted of astrin demonstrated that the absence of astrin resulted in a chromosome alignment defect. Once chromosome alignment was achieved, chromosomes were lost again from this structure. Thus depletion of astrin leads to an arrest in a metaphase-like state characterized by increasing loss of chromosomes and a persistent activation of the SAC. Taken together, these data indicate that astrin is required for the maintenance of chromosomes in a fully aligned metaphase plate. Our results concerning astrin's localization to the KT demonstrated that astrin's association with the outer KT requires intact KT-MT attachments. Thus it is plausible that after being recruited to KTs astrin is involved in the stabilization and maintenance of attachments.

Furthermore, we found that depleting astrin by siRNA resulted in many unattached KTs and fewer stable KT-MTs than in control cells. Moreover, in cells depleted of astrin CENP-E, its interaction partner CENP-F and Plk1, which are all involved in stabilization of MT-KT interactions and chromosome congression (Chan et al., 1998; Elowe et al., 2007; Kapoor et al., 2006; Yen et al., 1991), were lost from KTs (Figure 21). This, in combination with the lack of astrin itself, may cause unstable MT-KT interactions, chromosome congression defects and a persistent activation of the SAC. Since bi-dependency analysis and IPs suggest that Plk1 and CENP-E are astrin interactors, it is tempting to speculate that astrin is part of a complex with other proteins of the outer KT, such as CENP-E and possibly also CENP-F and other so far not identified proteins. This complex could be regulated by phosphorylation by Cdk1 and Plk1 (which binds astrin and might phosphorylate other binding partners) and by dephosphorylation of Cdc14A and possibly other mitotic phosphatases, such as PP2A or PP1. This complex could be involved in stabilization of MT-KT interactions and chromosome congression (see model Figure 43).

5. Astrin as a potential regulator of the metaphase to anaphase transition

Live cell imaging studies of cells depleted of astrin demonstrated that in the absence of astrin early mitotic events, besides chromosome congression, were not impaired (Figure 34 and Figure 40). Cells depleted of astrin arrested in a metaphase like state and did not

exit mitosis. Interestingly, astrin associated with KTs of only those sister chromatids that were aligned at the metaphase plate of the bipolar spindle and under tension. Hence, in metaphase, when all KTs are attached to the bipolar spindle and under tension, they were also positive for astrin. At this timepoint the spindle assembly checkpoint is satisfied and cells enter into anaphase. Thus it is tempting to speculate that astrin is an important signal for the metaphase to anaphase transition. The metaphase arrest together with the involvement of astrin in the regulation of separase, which becomes active as soon as the spindle assembly checkpoint is satisfied and cells enter into anaphase, further supports the idea that astrin is involved in the regulation of the metaphase to anaphase transition. However, astrin is clearly not a component of the spindle assembly checkpoint pathway, since the depletion of astrin results in an activation of the spindle assembly checkpoint. In contrast to components of the spindle assembly checkpoint (e.g. BubR1 and Mad2), which localize to unattached KTs and are released upon bipolar attachment (Cleveland et al., 2003; Maiato et al., 2004), astrin behaves just the opposite. On the basis of these results, one could speculate that astrin senses bipolar attachment of sister chromatids. Thus, like CENP-E or together with CENP-E astrin could be involved in the coupling of MT attachments and the SAC (Yao et al., 2000) (see model Figure 43).

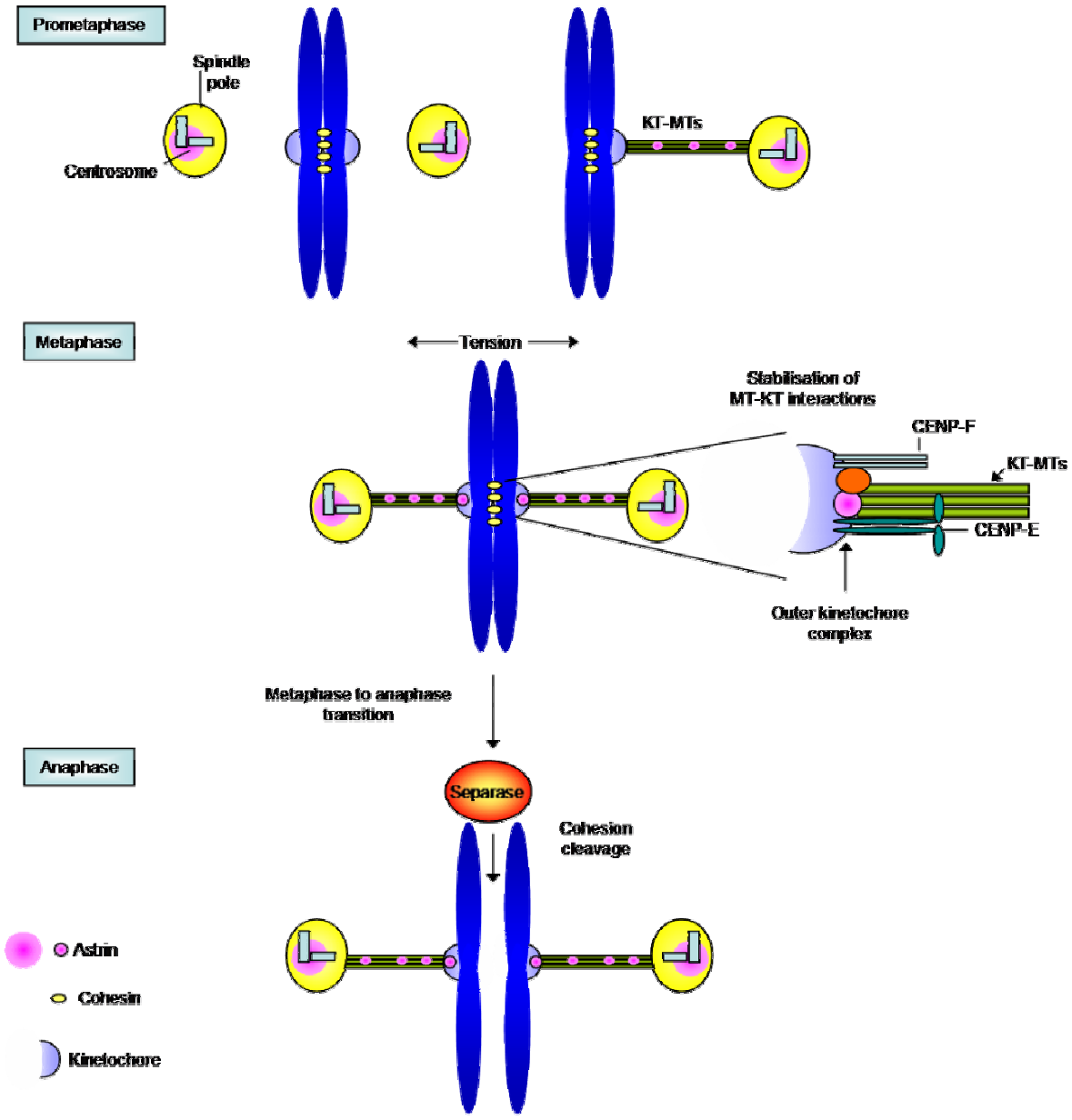

Figure 43. Illustration of astrin's localization during mitosis. Astrin associates with the spindle pole upon spindle formation and localizes only to KTs that are attached to the bipolar spindle and under tension. Our data suggest that astrin contributes to the regulation of the metaphase to anaphase transition. Moreover, astrin might be part of an outer KT complex together with CENP-E, CENP-F and other so far not identified proteins, which contributes to the stabilization of MT-KT interactions and to chromosome congression. Moreover, our data suggest that astrin contributes to the regulation of the metaphase to anaphase transition.

6. Astrin contributes to the tight regulation of separase activity

The cleavage of sister chromatid cohesion by separase is subject to multiple layers of control, involving the regulation of the enzymatic activity of separase by cyclin B1 and securin, both targets of the spindle assembly checkpoint (Ciosk et al., 1998; Gorr et al., 2005; Holland and Taylor, 2006; Waizenegger et al., 2002). This surveillance mechanism prevents premature chromosome segregation by delaying sister chromatid separation until all chromosomes have achieved attachment to the bipolar spindle (Musacchio and Salmon, 2007). The SAC targets Cdc20, the activatory subunit of the APC/C, an E3 ubiquitin ligase, which polyubiquitinates securin, the inhibitory subunit of separase and cyclin B1, the activatory subunit of Cdk1, and thereby initiates their destruction by the 26S proteasome (Peters, 2006). As soon as the SAC is satisfied the APC/C is activated and thereby separase inhibition by securin and cyclin B1 is released. Active separase cleaves sister chromatid cohesion, chromosomes segregate and cells exit mitosis. During exit from mitosis the activity of separase is also involved in centrioles disengagement, a mechanism, which license the centrosome duplication to one per cell cycle (Tsou and Stearns, 2006c).

Our experiments demonstrated that cells depleted of astrin arrest in mitosis due to an activation of the SAC. In line with that, securin and cyclin B1 are stable and unattached KTs are positive for the checkpoint proteins BubR1 and Mad2. In contrast to expectation however, the loss of astrin leads to a premature activation of ca. 30% of separase, resulting in the loss of sister chromatid cohesion and centriole disengagement. Live cell imaging of histone H2B-GFP and CENP-A-YFP (Figure 34 and Figure 40) expressing cells showed that astrin depleted cells were bipolar in early stages of mitosis and reached prometaphase with unseparated sister chromatids to allow the formation of imperfect metaphase plate. In addition, the data also show that loss of sister chromatid cohesion and of centrosome engagement occur after the formation of an imperfect metaphase plate. Taken together, our observations clearly indicate that a subpopulation of separase can be activated even though the general mitotic arrest of the cells is maintained. It has been suggested that cells, which cannot satisfy the SAC and arrest in mitosis for prolonged periods of time escape mitosis (Rieder and Maiato, 2004). However, the mechanisms that lead to this escape are not known, but clearly must include Cdk1

inactivation. Cells depleted of astrin exhibit premature separase activity but the APC/C is still inhibited, since securin and cyclin B1 are stable (Figure 36).

By comparing the effects of astrin depletion with the phenotype observed in consequence of prolonged mitotic arrest induced by either nocodazole treatment or depletion of CENP-E, we demonstrated that astrin depleted cells display a unique phenotype that is not caused by an extended mitotic arrest. However, it is very unlikely that astrin acts directly as an inhibitor of separase, since separase was not detected in astrin IPs and subsequent mass spectrometry analysis. Moreover, only ca. 30% of separase was active in cells depleted of astrin; if astrin was a novel inhibitor of separase one would have expected a nearly complete activation of separase after loss of astrin.

There are two possible scenarios, outlined below, to explain our findings. One model would evoke localized APC/C and separase activation in the absence of astrin, whereas the other model would posit a direct regulation of separase (or its regulators) by astrin.

Model A: As mentioned previously, the activity of the APC/C, which depends on co-activators, such as Cdc20 and Cdh1, is essential for mitotic exit (Peters, 2006). APC/C^{Cdc20} is already active during prophase, after the phosphorylation of some of its subunits by Cdk1 and Plk1 (Golan et al., 2002; Kraft et al., 2003; Kramer et al., 2000). Its ability to ubiquitinate securin and cyclin B1 is blocked by the SAC in a substrate specific manner. However, a few substrates, notably Nek2A or cyclin A, are destroyed in early mitosis in an APC/C^{Cdc20} dependent manner (den Elzen and Pines, 2001; Geley et al., 2001; Hames et al., 2001). Since Cdk1 phosphorylation of Cdh1 restrains its interaction with the APC, APC/C^{Cdh1} does not become active until Cdk1 activity decreases due to APC/C^{Cdc20} mediated destruction of cyclin B1 and phosphates are removed by protein phosphatases such as Cdc14 (Kramer et al., 2000; Visintin et al., 1998; Yamaguchi et al., 2000; Zachariae et al., 1998). Recently it has been suggested that anaphase entry is also controlled by a balance in the ubiquitination of substrates by the APC/C on the one hand and the deubiquitination by UPS44 on the other hand (Stegmeier et al., 2007). However, it is still unclear how the balance between ubiquitination and deubiquitination is controlled and how this influences the transition from the inhibited to the active APC/C upon bipolar attachment. One possibility could be the phosphorylation dependent activation of USP44 by mitotic kinases, thus its deubiquitination activity would be high

during mitosis and low when cells exit mitosis (Stegmeier et al., 2007). In addition it has been suggested that the APC/C and the degradation of its substrates is regulated spatially, since it has been shown that the APC/C is recruited to unattached KTs (Acquaviva et al., 2004; Wakefield et al., 2000). Since we demonstrated that astrin localizes to various structures during mitosis and interacts with the mitotic kinase Plk1 and the mitotic phosphatase hCdc14A, it is tempting to speculate that the loss of astrin might affect the phosphorylation state and/or the localization of the APC/C. This may result in the activation of a pool of separase.

Model B: Separase activity is controlled by different mechanisms. As mentioned before, it has been shown that securin inhibits separase activity (Waizenegger et al., 2002). Due to the fact that securin knockout mice only showed slight phenotypes (Mei et al., 2001), it was presumed that additional mechanisms exist. One of them is the binding of cyclin B1 upon previous phosphorylation of separase by Cdk1/cyclin B1 (Ciosk et al., 1998; Gorr et al., 2005; Holland and Taylor, 2006). Moreover, it has been shown that the effects of non-degradable cyclin B1 are dose-dependent (Hagting et al., 2002; Stemmann et al., 2001; Wolf et al., 2006). It has been demonstrated that sister chromatid separation is only inhibited by high expression levels of non-degradable cyclin B1, whereas levels, which are approximately as high as endogenous cyclin B1, result in a anaphase-like arrest and sister chromatid separation (Wolf et al., 2006). In the latter case endogenous securin and cyclin B1 are degraded, which indicates that the APC/C is active. In contrast, Chang and co-workers suggested that already a low level of non-degradable cyclin B1 blocks anaphase onset (Chang et al., 2003). These controversial data demonstrate that the exact function of cyclin B1 in maintaining sister chromatid cohesion is still controversial (Chang et al., 2003; Wolf et al., 2006). Our results suggest that additional layers of separase control exist.

Recently it has been shown that besides Cdk1 phosphorylation also binding of the phosphatase PP2A is involved in the regulation of separase activity (Holland et al., 2007; Holland and Taylor, 2006). Moreover it has been proposed that PP2A is involved in the regulation of securin degradation, which is triggered by phosphorylation (Gil-Bernabe et al., 2006). Since it has been indicated that securin and separase are subject to phosphorylation dependent control, it is possible that the loss of astrin, which interacts

with mitotic kinases and at least one phosphatase, results in an impaired balance between phosphorylation and dephosphorylation. Initial studies concerning the contribution of hCdc14A to the astrin RNAi phenotype, revealed that cells depleted of hCdc14A arrest in mitosis, display bipolar spindles, uncongressed chromosomes and premature loss of sister chromatid cohesion (Ulrike Grüneberg, unpublished data). Hence our data indicate that astrin and hCdc14A interact and there are some similarities between the astrin and hCdc14 RNAi phenotype. Thus it might be that the phenotype observed upon astrin depletion is linked to the one observed upon loss of hCdc14A phosphatase activity. However, the function of hCdc14A during mitosis is still unclear. Thus additional studies are required to reveal hCdc14A's function during mitosis and its possible contribution to separase activity control.

To understand the mechanisms of astrin's role in the regulation of separase activity, two aspects will be important to explore. In the first place, additional mechanisms of separase activity regulation have to be revealed. Secondly, it will be essential to elucidate the functional relationship between astrin and hCdc14A on the one hand and to identify other astrin interacting proteins, which may contribute to the regulation of separase activity, on the other hand.

MATERIAL AND METHODS

1. Cloning procedures

All cloning procedures were carried out according to standard techniques as described in Molecular Cloning, A Laboratory Manual, 2nd edition, Sambrook, J., Fritsch, E.F., Maniatis, T., Cold Spring Harbor Laboratory Press, 1989 and Current Protocols in Molecular Biology, Wiley, 1999. Restriction enzyme reactions were performed as specified by the suppliers (NEB, Ipswich, MA) and ligation reactions were done using T4 DNA Ligase (Roche Diagnostics, Indianapolis, IN) or a Rapid Ligation Kit (Roche). Extraction of DNA from agarose gels and preparation of plasmid DNA were performed using kits from Qiagen (Hilden, Germany) according to the manufacturer's instructions. For PCR reactions, Pfu DNA polymerase was used as recommended by the manufacturer (Stratagene) and reactions were carried out in a RoboCycler Gradient 96 (Stratagene, La Jolla, CA). PCR products were checked by sequencing at Medigenomix (Martinsried, Germany) or by an in-house sequencing service.

Astrin was amplified by Dr. Ulrike Grüneberg from a human testis cDNA (CLONTECH Laboratories, Inc.) library using a two-round nested PCR strategy. For the first round, the following primer pair was used: 5'-GAGACGTGATAGGCCT GCCTTCTGGTTGAAG-3' (forward) and 5'-GAGGTGAAGCAGATTCTGGCTTTCA GTTTC-3' (reverse). In the second round XhoI and KpnI sites on either sites of the coding sequence were introduced by using the primers 5'-GAGGTGAAGCAGA TTC TGGCTTTCAGTTTC-3' (forward, XhoI) and 5'-GGCCTCGAGTTAGCTCAGAAA TTCCAGCAATCCCTGT AG-3' (reverse, KpnI). The resulting PCR product was TA-cloned into pCRII-TOPO (Invitrogen, Carlsbad, CA). This construct (UG59) was sequenced and found to match the published astrin sequence except for 7 amino acid changes. These could all be found in the EST database. The astrin-TOPO construct was the source for further PCR-mediated subcloning of astrin or astrin fragments (for further constructs see Table 1).

Astrin full-length was cloned in-frame by PCR in either pEGFP-C3 (Clontech Mountain View, CA) by using primers 5'-GGCCTCGAGATGTGGCGAGTGAAAAAA

CTGAGCCTCAGC-3' and 5'-GGCCTCGAGTTAGCTCAGAAA TTCCAGCAATCCC TGTAG-3'. Astrin was excised from UG59 with KpnI and XhoI and cloned into pcDNA3.1 (+) (KpnI/XhoI) or in a pcDNA3.1 (KpnI/XhoI) vector encoding an N-terminal 3xMyc-tag (Invitrogen).

The RNAi resistant Myc-tagged astrin constructs in the pcDNA3.1.-3xMycA vector were generated by introducing six silent point mutations in the RNAi targeting sequence using primers 5'-GAGTCGGTCCCGACAgttaACtGAaAAACTCACAGTC AAG-3' and 5'-CTTGACTGTGAGTTTtTCaGTtaacTGTCGGGACCGACTC-3'. The Myc-tagged astrin (SS65/66AA) mutants, the Myc-tagged astrin (ST110/111AA) mutants and the Myc-tagged astrin (ST936/937AA) mutants were made by site-directed mutagenesis using the following primers, respectively: 5'-GAAGGCAGCAACAACG CAGCTCCAGTGGATTTTGTA-3' and 5'-TACAAAATCCACTGGAGCTGCGTTGT TGCTGCCTTC-3', 5'-ATTCCCCAAATTAGCGCTGCTCCTAAAACGTCTGAG-3' and 5'-CTCAGACGTTTTAGGAGCAGCGCTAATTTGGGGAAT-3', 5'-GATGAAG AGCCAGAAGCAGCTCCTGTGCCCTTGCTT-3' and 5'-AAGCAAGGGCACAGGA GCTGCTTCTGGCTCTTCATC-3'. The astrin fullength constructs were cloned in-frame by PCR in the pFBT9 vector, a version of pGBT9 modified to encode kanamycin resistance (Clontech Laboratories, Inc.; a kind gift from F. Barr) by using the primers 5'-GGCCTCGAGGGATGTGGCGAGTGAAAAAACTGAGCCTCAGC-3' and 5'-GGCC TCGAGTTAGCTCAGAAATTCCAGCAATCCCTGTAG-3'. The C-terminal astrin fragment spanning residues 482-1193 was cloned in-frame by PCR into either pFBT9 (Clontech) or pACT2 (Clontech) by using the primers 5'-GCCCTCGAGGGATGAA TAAACTTCAGCATCTTAAGGAG -3' and 5'-GCCCTCGAGTTAGCTCAGAAAT TCCAGCAATCCCT-3'. The C-terminal astrin fragment spanning residues 482-1193 was cloned in-frame by PCR either into pEGFP-C2 (Clontech) or pcDNA3.1-3xMycA (Invitrogen) by using either the primers 5'-GCCCTCGAGGATGAAACTTCAGCA TCTTAAGGAGAGC-3' and 5'-GCCCTCGAGTTAGCTCAGAAATTCCAGCAAT CCCT-3' or the primers 5'-GCCGGTACCTATGAAACTTCAGCATCTTAAGGAG AGC-3' and 5'-GGCCTCGAGTTAGCTCAGAAATTCCAGCAATCCC-3'. The N-terminal astrin fragment spanning residues 1-481 was cloned in-frame by PCR either into pEGFP-C2 (Clontech), pcDNA3.1-3xMycA (Invitrogen), pFBT9 (Clontech) or pACT2

(Clontech) by using the primers 5'-GCCGGATCCTTATGTGGCGAGTGA AAAAACTGAGCC-3' and 5'-GGCCTCGAGTTAAGTTATCCCACTGTGAGATGTG TC-3'. For gene-fusion with hexa-histidine tag (His-tag) or MBP-tag this N-terminal astrin was cloned into the pQE vector (QIAGEN) or pMaLtFN (modified from pMAL-c2x, NEB).

2. Expression and purification of recombinant proteins

For production of recombinant His-tagged astrin (fullength) the plasmids UG61 (a kind gift from Ulrike Grüneberg) were transformed into *E. coli* (strain JM109-RIL), grown over night at 37°C under ampicillin selection and diluted 1:5 with fresh medium the next morning. The culture was grown until late log-phase (OD 600 of 0.5-08), when expression of the recombinant protein was induced with 0.1 mM IPTG at 18°C over night. Cells were pelleted the next morning by centrifugation and lysed in buffer [20 mM TrisHCl (pH 7.5), 300 mM NaCl, 1.5% N-laurosylsarcosin, 1% Triton X-100, 5 mM Imidazole, protease inhibitor tablets (-EDTA) (Roche), 1 mM Pefabloc, 0.5 mg/ml lysozyme (in 50 mM Tris-Cl, pH 8.0) and 0.1 mg/ml DNAse1] and incubated with Ni-NTA agarose (Qiagen) for 90 min at 4°C on a roller to allow binding of the expressed protein. After several washing steps with lysis buffer, wash buffer 1 [20 mM TrisHCl (pH 7.5), 300 mM NaCl, 0.5% Triton X-100, 20 mM Imidazole] and wash buffer 2 [20mM TrisHCl (pH 7.5), 300 mM NaCl, 0.1% TritonX-100, 20 mM Imidazole]. His-tagged astrin was eluted by incubating beads in elution buffer (20 mM Tris-HCl (pH 7.5), 300 mM NaCl and 200 mM Imidazole). Purified astrin was dialyzed over night at 4°C with 20 mM TrisHCl (pH 7.5) and 300 mM NaCl and then frozen as aliquots at -80°C.

3. Antibody production

In order to produce astrin specific antibodies, the astrin fragment spanning residues 1-481 cloned in pQE was expressed as a poly-histidine-tagged fusion protein in *E. coli* (strain JM109-RIL) and purified over a Ni^{2+}-column under denaturing conditions. Following further purification on a preparative 15 % SDS-PAGE gel. 200-250 µg of purified antigen was injected every four weeks, to a total of six injections, with Freund's adjuvant into New Zealand white rabbits (Charles River Laboratories, Romans, France) or into rats (in-

house animal facility, MPI of Biochemistry, Martinsried, Germany). The obtained sera from the rabbits were affinity purified using Activated Immunoaffinity Support (Biorad), which was coated with the respective MBP-tagged antigen according to the manufactors protocol. The obtained sera of the rats were used without purification.

In order to produce a phosphospecific astrin antibody against the Threonine 110 site, the following peptide H-CQISST(PO3H2)PKTS-OH was synthesized (Core facility, Martinsried, Germany), coupled to KLH (Pierce) according to the manufactors protocol. The coupling efficiency was tested by using Ellman's reagent. The immunization was performed as described above. The obtained sera were purified in two steps; firstly total IgG was isolated by using Protein A Sepharose (GE Healthcare, Uppsala, Sweden), secondly the isolated total IgG was affinity purified by using Sulfo-Link coupling gel (Pierce) according to the manufactors protocol.

4. Cell culture, synchronization and drug treatment

HeLa S3, HeLa H2B-GFP, HeLa CENP-A-YFP and HEK293T cells were cultured at 37°C in a 5% CO_2 atmosphere in Dulbecco's modified Eagle's medium (DMEM), supplemented with 10% heat-inactivated fetal calf serum and penicillin-streptomycin (100 IU/ml and 100 µg/ml, respectively, Gibco-BRL, Karlsruhe, Germany). For synchronization in G1/S phase HeLa S3 cells were treated for 14 h with 1.6 µg/ml aphidicolin (Sigma, A-6781). These cells were released for 12 h in fresh prewarmed medium, treated again with 1.6 µg/ml aphidicolin for 14 h and collected. For G2/M synchronization HeLa S3 cells were treated with aphidicolin as described above, released in prewarmed medium for 6 h, then 100 ng/ml nocodazole was added and culturing was continued for additional 14 h. Mitotic cells were collected by mitotic shake off. To prepare HeLa S3 cells for nocodazole release experiment, cells were treated as above. The cells were washed twice with PBS and incubated in fresh prewarmed medium after mitotic shake off. Cell samples were taken after various time points. In order to block HeLa S3 cells efficiently in mitosis without subsequent release final concentrations of 10 µM taxol (MT stabilization drug), 150 µM monastrol (Eg5 inhibitor) and 25 µM noscapine were added to the medium for 14 h, respectively. In order to block Aurora B or Plk1 kinase activity or proteasomal degradation, cells were incubated for 1 h with 10 µM

ZM44743 (Aurora-B kinase inhibitor), for various time intervals with TAL (Plk1 inhibitor), or for 3 h with MG132 (Proteasome inhibitor).

5. Transient transfection and siRNA-mediated protein depletion

Plasmid transfections in HeLa S3 cells and transfection of HEK293T cells were performed using Fugene6 reagent (Roche Diagnostics, Mannheim, Germany) or TransIT-LT1 transfection reagent (Mirus Bio, Madison,Wi) according to the manufacturers' protocol. SiRNA duplexes were transfected using Oligofectamine (Invitrogen) according to the manufacturer's protocol. The sequences of the siRNA duplexes (Qiagen) used in this study are listed in

Table 2. For rescue experiments the siRNA-resistant Myc-astrin plasmid (or the empty Myc-vector as a control) was transfected 24 h prior to the transfection of siRNA duplexes targeting astrin. The cells were fixed and analyzed 42 h later.

6. Microinjection

Purified anti-N-terminal and anti-C-terminal astrin antibody or control rabbit IgG was concentrated to 2 mg/ml using Ultrafree-0.5 centrifugal filters (Amicon Bioseparation, Millipore, Schwalbach, Germany), followed by centrifugation at 55,000 rpm for 30 minutes at 4°C in a TLA-55 rotor and an Optima ultracentrifuge (Beckman, Krefeld, Germany). For microinjection experiments HeLa S3 cells were seeded onto coverslips, arrested in G1/S phase for 14 h and then released into fresh prewarmed medium. After 2 h of release antibodies were injected into the cell cytoplasm using 0.5µm Femtotips glass needles with a micromanipulator 5171 coupled to a FemtoJet/InjectMan microinjection apparatus (Eppendorf, Hamburg, Germany). 24 h after microinjection cells were analyzed.

7. Cold treatment and K-fiber analysis

Cold treatment was performed in order to depolymerize preferentially unattached MTs in mitotic HeLa S3 cells. Medium was replaced by ice-cold medium, followed by placing the dishes on ice for 30 min before fixation. For the analysis of KT fibers cells were

washed twice in PBS and permeabilized for 90 seconds with PBS plus 0.1% Triton X-100 prior to fixation.

8. Mitotic chromosome spreads

HeLa S3 cells were treated with the respective siRNA oligo for the time determined for depletion of the targeted protein. Mitotic cells were collected by mitotic shake off, centrifuged for 4 min at 1000 rpm and resuspended in 40% DMEM culture medium (diluted with deionised water). The cells were allowed to swell at RT for 5 min before spinning and resuspending them in fixation solution (3:1 methanol: acetic acid). The fixed cells were incubated at 4°C for at least 20 min, washed twice with the fixation solution and diluted with fixation solution to $1x10^6$ cells/ml. 10 µl of each cell solution were dropped on an ice cold cover slip, which had been moistened before by breathing on to it. After drying of the cover slip on a wet Kleenex tissue over a 60°C heating block, spreads were stained for 5 min with 0.4 µg/ml DAPI and mounted. In order to perform chromosome spreads for immunostaining, mitotic cells were collected by shaking-off, centrifuged for 4 min at 1000 rpm and washed twice with 1x PBS. The cells were incubated in a hypotonic buffer [30 mM Tris (pH 8.0), 50 mM Sucrose, 17 mM Sodium citrate] for 8 minutes in order to swell, before spinning and resuspending them in 100 mM sucrose [in 10 mM TrisHCl (pH 8.0)] to a final concentration of $1x10^6$ cells/ml. 10 µl of the cell solution was dropped on a coverslips, which had been dipped in fixative solution [1% formaldehyde, 5mM Sodium borate (pH 9.2), 0.15% Triton X-100]. The coverslips were firstly dried in a humid chamber for 15 min at RT and secondly dried on a wet Kleenex tissue over a 37°C heating block, washed twice with PBS and processed for immunofluorescence microscopy.

9. Microtubule co-sedimentation assays

For the preparation of cell extracts suitable for MT co-sedimentation assays, HeLa S3 cells were arrested in metaphase or interphase by synchronization. Cells were lysed in ice-cold BRB80 (80 mM K Pipes, 1 mM $MgCl_2$, 1mM EGTA (pH 6.8) with 0.1% Triton X-100 (Mishima et al., 2002). The lysates were clarified by centrifugation at 10,000 x g for 15 min. The resulting supernatant was centrifuged at 25,000 x g for 20 min at 4°C in a

TLA-55 rotor and an Optima ultracentrifuge (Beckman, Krefeld, Germany). The lysates were frozen at -80°C. Prior to the MT co-sedimentation assay metaphase extracts, interphase extracts and bacterially expressed proteins were centrifuged at 100,000 g for 1 h at 4°C. The supernatants were incubated with taxol stabilized MTs (5mM final concentration) for 15 minutes at 25° C. The protein solution was centrifuged through a glycerol cushion at 55,000 rpm for 20 min at 25° C in a TLA-55 rotor and an Optima ultracentrifuge (Beckman, Krefeld, Germany). The original protein samples, the supernatant and the pellet fraction were resuspended with sample buffer and analyzed by immunoblotting.

10. Image acquisition and time-lapse microscopy

Cells were grown on coverslips and either fixed in paraformaldehyde at RT for 20 min followed by 10 min treatment with Quenching solution (50 mM NH_4Cl in PBS) and permeabilisation with 0.1 % Triton X-100, or in –20°C methanol for 4 min at 4°C or in PTEMF buffer (20 mM PIPES, pH 6.8, 4 % formaldehyde, 0.2 % Triton X-100, 10 mM EGTA, 1 mM $MgCl_2$) for 12 min at RT. After PTEMF fixation cells were incubated for 30 min at RT in blocking solution (PBS, 2% BSA, 0.1% Triton X-100). All antibody incubations were carried out for 1 h at RT in a humidified chamber, followed by three washes in PBS. Primary antibodies used in this study are listed in Table 3 with the respective dilutions for immunofluorescence indicated. Secondary antibodies were with Alexa-Fluor-488-(green) and Alexa-Fluor-555-(red) conjugated, donkey anti-mouse, anti-rabbit or anti-sheep IgGs, respectively, Alexa-Fluor-647-(far red) conjugated anti-rabbit IgGs (1:1000, Molecular Probes, Eugene, OR) or Cy2- and Cy3-conjugated donkey anti-human IgGs (1:1000, Jackson Immunoreasearch, West Grove, PA). DNA was stained with 2 µg/ml DAPI. Cover slips were mounted in phenylenediamine in 90% glycerol. IF microscopy was performed using a Zeiss Axioplan II microscope (Zeiss, Jena, Germany) with Apochromat 40x and 63x oil immersion objectives, respectively. Photographs were taken using a Micromax CCD camera (model CCD-1300-Y, Princeton Instruments, Trenton, NJ) and Metaview software (Visitron Systems GmbH, Puchheim, Germany). For high-resolution images and for time-lapse microscopy of HeLa H2B-GFP a Deltavision microscope on an Olympus IX71 (Deltavision; Applied Precision, Issaquah,

WA), equipped with Plan Apo 40x/0.95 and Plan Apo 60x/1.4 and Uplan Apo 100x/1.35 oil immersion objectives (Olympus) and a photometrics CoolSnap HQ camera (Photometrics), was used for collecting 0,15 μm-distanced optical sections in the z-axis. HeLa CENP-A-YFP cells were filmed on the same system at intervals of 4 mins, imaging 7 focal planes 2 μm apart, with an exposure of 0.8 sec, 100% ND. Images at single focal planes were processed with a deconvolution algorithm, and optical sections were projected into one picture using Softworx software (Applied Precision). Images were processed using Adobe Photoshop 7.0 and then sized and placed in figures using Adobe Illustrator CS (Adobe Systems, San Jose, CA).

11. Cell extracts and immunoprecipitation

In order to prepare whole cell lysate HeLa S3 cells of one 2 cm plate were harvested, washed three times in ice-cold PBS and lysed in SDS sample buffer. For mitotic lysates, mitotic HeLa S3 cells were collected by shake off, washed three times in ice-cold PBS and lysed in Lysis buffer [20 mM Tris-HCl, pH 7.5, 150 mM NaCl, 40 mM β-glycerolphosphate, 10 mM NaF, 0,3 mM Na-vanadate, 1mM EDTA, 1% [vol/vol] IGEPAL, 0.1% [vol/vol] deoxycholate, 2mM Pefabloc, 100 nM okadaic acid and protease inhibitor cocktail without EDTA (Roche Diagnostics)]. For the analysis of separase activity N-ethyl maleimide (2.5 mM final concentration, Sigma) was added to the lysis buffer. Protein concentrations in the cleared lysates were determined using the Dc protein assay (Bio-Rad Laboratories, Hercules, CA).

Endogenous astrin was IPed from HeLa S3 cells on 15-cm-diameter dishes presynchronized with aphidicolin and arrested for 14 h with noscapine. Cells were obtained by mitotic shake off, washed three times with ice cold PBS and lysed in lysis buffer. The cleared lysates were incubated with protein G-Sepharose beads (Pierce Biotechnology, Rockford, IL) and affinity purified antibody or the corresponding IgGs as control for 2h at 4°C on a rotating wheel. The immune-complexes bound to the beads were washed twice with IP buffer, once with wash buffer (20mM Tris-HCl, pH 7.5, 150 mM NaCl, 40 mM β-glycerolphosphate, 10mM NaF, 0.3 mM Na-vanadate, 1mM EDTA and 0.1% [vol/vol] IGEPAL) and then boiled in SDS sample buffer. For pull-down experiments HEK293T cells on 15 cm diameter dishes were transfected with 8 μg of the

required plasmid DNA and 24 µl Fugene-6 (Roche Diagnostics) according to the manufacture's instructions. After 40 h, cells were harvested, washed three times in ice-cold PBS and lysed in IP buffer (20mM Tris-HCl, pH 7.5, 150 NaCl, 1% [vol/vol] IGEPAL, 2mM Pefabloc, and protease inhibitor cocktail without EDTA). The lysates were incubated with protein G-Sepharose beads (Pierce) and tagged, transiently expressed proteins were precipitated using either antibodies against GFP or Myc. Beads were washed once with IP buffer and twice with IP buffer containing 0.1% [vol/vol] IGEPAL and then boiled in SDS sample buffer.

12. Immunoblotting and Far Western analysis

For Western blot analysis equal protein amounts of each sample were loaded on SDS-PAGE gels and separated. The proteins were transferred to nitrocellulose membranes (Schleicher & Schuell, Keene, NH) using a Hoefer semi-dry blotting apparatus (Amersham Biosciences, Little Chalfont, UK) and completed transfer was assayed by staining membrane bound proteins with Ponceau-red. For Western blot analysis membranes were incubated for 1 h at RT in blocking buffer (5% skimmed-milk powder in PBS, 0.1% Tween-20), probed with primary antibodies (name and dilution listed in Table 3) in blocking buffer for 1 h at RT or over night at 4°C or and detected by HRP-conjugated goat anti-mouse and anti-rabbit (1:10000, Pierce Biotechnology, Rockford, IL) and donkey anti-sheep IgGs (1:10000, Jackson Immunoresearch). Bound antibodies were detected by ECL (Pierce). Farwestern blots were performed in TBS-T (50 mM Tris-HCl, pH 7.4, 137 mM NaCl, 0.1% Tween 20) supplemented with 5% skim-milk powder. The blots were probed with 1µg/ml GST-PBD for 6 h at 4°C. Bound GST-PBD was detected using affinity-purified rabbit anti-GST antibody.

13. *In vitro* kinase assay

For *in vitro* kinase assays, MBP-tagged and His-tagged proteins were incubated with Cdk1/cyclin B1 (Upstate, Charlottesville, VA) in BRB80 buffer (80 mM Pipes, pH 6.8, 1 mM MgCl2, 1 mM EGTA) with 10µM DTT. Kinase reactions were carried out at 30°C for 30 min in this buffer supplemented with 10 µM ATP and 2 µCi [γ-32P] ATP (Amersham Corp.). Reactions were stopped by the addition of SDS sample buffer and

heating at 95°C for 5 min. Protein samples were separated by SDS–PAGE followed by Coomassie Blue staining. The gels were dried on filter paper and ^{32}P incorporation was visualized by autoradiography.

14. Phosphatase assay

For the phosphatase assays either cell extracts or IP was performed from prometaphase arrested cells (as described above). The IPed proteins coupled to protein G-Sepharose (GE Healthcare) were washed twice with Lysis buffer (see chapter 11) and one time with phosphatase buffer (Roche Diagnostics). The beads were then resuspended in 1x phosphatase buffer, either treated with 20 U Alkaline Phosphatase (Roche Diagnostics), or recombinant hCdc14A (wt or PD) (a kind gift from Ulrike Grüneberg) or left untreated for 30 min at 30°C. To obtain cell extracts, prometaphase cells were lysed with Lysis buffer (see chapter 11) either in the presence or in the absence of phosphatase inhibitors for 15 minutes on ice, pelleted and the supernatants of the lysates were treated with Calf Intestinal Phosphatase (CIP, 1:50 final concentration in lysate, Roche) or left untreated for 1 h at 30°C. The phosphatase reaction was stopped by addition of sample buffer followed by boiling. Equal protein amounts were loaded and separated on a SDS-PAGE gel followed by Western blot analysis.

15. *In vitro* coupled transcription translation

Proteins were produced by in vitro coupled transcription translation (IVT) in the presence of 35S-methionine using the TNT T7 Quick Coupled Transcription/Translation System (Promega, Madison, WI).

16. Yeast-two hybrid analysis

Different astrin fragments were cloned in frame into the two-hybrid prey vector pACT2 (Clontech Laboratories, Inc.) or the bait vector pFBT9 (a version of pGBT9 modified to encode kanamycin resistance; Clontech Laboratories, Inc.; a kind gift from F. Barr). The pFBT9 constructs were cotransformed with the empty pAct2 plasmid into the yeast strain PJ69-4A. In order to test for direct interactions, they were first plated onto non-selective medium lacking leucine and tryptophane (SC-LW), and then streaked out onto both non-

selective (SC-LW) and selective medium lacking leucine, tryptophane, histidine and adenine (QDO). Different pFBT9 and pACT2 constructs were used for a direct yeast-two hybrid analysis, by co-transfecting one pFBT9 construct with one pACT2 construct and tested for interaction as described above.

17. Chemicals and growth media

All chemicals were bought from Fluka, Sigma Aldrich Chemical Company (Buchs, Switzerland), Merck (Darmstadt, Germany) or Roth (Karlsruhe, Germany), unless otherwise stated. Components of growth media for E.coli or yeast were from Difco Laboratories or Merck.

APPENDIX

1. Table 1: Plasmids

List of plasmids: Several plasmids used were generated by Ulrike Grüneberg (UG).

Plasmid	Gene	Insert	Vector	Tag
KE3	Astrin	Full-length; wt	pEGFP-C3	GFP
KE6	Astrin	Aa 1-481; wt	pMaLtFN	GST
KE7	Astrin	Aa 1-481; wt	pQE-32	MBP
KE8	Astrin	Aa 1-481; wt	pEGFP-C2	GFP
KE9	Astrin	Aa 1-481; wt	pcDNA3.1-3xMycA	Myc
KE10	Astrin	Aa 1-481; wt	pFBT9	BD
KE11	Astrin	Full-length; wt	pcDNA3.1 (+)	
KE14	Astrin	Aa 482-1193; wt	pEGFP-C2	GFP
KE15	Astrin	Aa 482-1193; wt	pcDNA3.1-3xMycA	Myc
KE23	Astrin	Full-length; wt	pFBT9	BD
KE25	Astrin	Aa 482-1193; wt	pFBT9	BD
KE36	Astrin	Aa 1014-1193; wt	pFBT9	BD
KE41	Astrin	Aa 1-481; wt	pAct2	AD
KE43	Astrin	Aa 482-1193; wt	pAct2	AD
KE52	Astrin	Full-length; RNAi mutant	pcDNA3.1-3xMycA	Myc
KE53	Astrin	Full-length; SS65/66AA	pcDNA3.1-3xMycA	Myc
KE54	Astrin	Full-length; ST110/111AA	pcDNA3.1-3xMycA	Myc
KE55	Astrin	Full-length; SS65/66AA-ST110/111AAA	pcDNA3.1-3xMycA	Myc
KE56	Astrin	Full-length; ST936/937AA	pcDNA3.1-3xMycA	Myc
UG19	Cdc14A	Full-length, wt	pFBT9	BD
UG30	Cdc14B	Full-length, wt	pACT2	AD

UG31	Cdc14B	Full-length, wt	pFBT9	BD
UG32	Cdc14A	Full-length, wt	pACT2	AD
UG59	Astrin	Full-length; wt	pCRII-TOPO	
UG61	Astrin	Full-length; wt	pQE81L	His
UG60	Astrin	Full-length; wt	pCDNA3.1.-3xMycA	Myc
UG62	Astrin	Aa1014-1193	pCRII-TOPO	

2. Table 2: SiRNA oligos

List of siRNA oligos used in this study, together with the respective references of the published sequences.

Targeted gene	**siRNA oligo sequence**	**Reference**
Aurora B	5'-GGTGATGGAGAATAGCAGT-3'	(Honda et al., 2003)
Astrin	5'-TCCCGACAACTCACAGAGAAA-3'	
Bub1	5'- TAGGCTAATTGTACTGCTC-3'	
Cdc14	5'- AGGGACATTGATAGCCTGTTA-3'	
CENP-E	5'-ACTCTTACTGCTCTCCAGTTT-3'	(Stucke et al., 2004)
CENP-F	5'-AAGAGATGCTAATAGCAGT-3'	(Holt et al., 2005)
Eg5	5'-CTGGATCGTAAGAAGGCAG-3'	
Gl2	5'-CGTACGCGGAATACTTCGA-3'	(Elbashir et al., 2001)
Hec1	5'-GTTCAAAAGCTGGATGATC-3'	(Stucke et al., 2004)
Kif18	5'-AACCAACAACAGTGCCATAAA-3'	(Mayr et al., 2007)
Mad2	5'-GAGTCGGGACCACAGTTT-3'	(Stucke et al., 2004)
MCAK	5'-GCTATCTGCTGGCTCTAAA-3'	
Plk1	5'-CGAGCTGCTTAATGACGAG-3'	(Kraft et al., 2003)
Separase	5'-AAGCTTGTGATGCCATCCTG-3'	
Sgo1	5'-CAGTAGAACCTGCTCAGAA-3'	(McGuinness et al., 2005)
TOGp	5'-TGTCTTACTGGCCTGGCTG-3'	(Holmfeldt et al., 2004)

3. Table 3: Antibodies

List of antibodies used for IF or Western blot analysis in this study

Antigen	Species	MW (kDa)	Company	Dilution IF	Dilution WB
Astrin	Rabbit	134	In-house	1:1000	1:200
Astrin	Rat	134	In-house	1:1000	
Aurora-A	Mouse	45	BD Biosciences Pharmingen	1:1000	
Aurora-B	Mouse	41	BD Transduction Laboratories	1:500	1:250
Bub1	Mouse	130	In-house	1:5	
BubR1	Mouse	120	In-house	1:10	
Cdc14A	Rabbit	60	In-house	1:1000	1:1000
Cdc14A	Mouse	60	Santa Cruz		1:1000
CENP-A	Mouse	17	MBL	1:2500	
CENP-E	Mouse	310	Abcam	1:200	
CENP-E	Rabbit	310	Gift from T.Yen	1:1000	1:1000
CENP-F	Mouse	400	BD Transduction Laboratories	1:1000	
Centrin	Goat	20	In-house	1:250	
Cyclin B1	Mouse	60	Upstate	1:1000	1:1000
CREST	Human		Immunovision	1:5000	
EB1	Mouse	30	BD Transduction Laboratories	1:200	
Eg5	Rabbit	97	In-house		1:1000
Eg5	Mouse	97	BD Biosciences Pharmingen	1:1000	
GST	Rabbit		Gift from U. Grüneberg		1µg/ml
Hec1	Mouse	75	Abcam	1:1000	1:1000
His	Mouse		In-house		undiluted

INCENP	Rabbit	120	In-house	1:1000	1:500
LaminA	Mouse	75	In-house		1:10
Mad2	Rabbit	27	Bethyl	1:1000	
MCAK	Rabbit	75	In-house	1:2000	
Myc	Rabbit		Gramsch Laboratories	1:2500	1:2500
Myc/9E10	Mouse		In-house	1:10	1:10
NuMA	Mouse	200	Calbiochem	1:1000	
Pericentrin	Rabbit	220	Abcam	1:1000	
Plk1	Mouse	66	In-house	1:10	1:10
PP2A B56	Mouse	60	Zymed	1:1000	
PRC1	Rabbit	71	In-house		1:1000
Securin	Mouse	23	Abcam	1:500	1:500
Separase	Rabbit	220	Novus Biologicals		1:500
Sgo1	Mouse	72	Abnova	1:1000	
TOGp	Rabbit	212	Gift from Dr. X. Yan	1:500	
Tpx2	Mouse	100	Gift from O.Gruss	1:10	
α-Tubulin	Mouse	55	Sigma	1:1000	1:1000
γ-Tubulin	Mouse	50	Sigma	1:1000	

4. Abbreviations

All units are abbreviated according to the International Unit System.

AA: amino acid

AD: activation domain

ATP: adenosine 5`-triphosphate

BD: binding domain

BSA: bovine serum albumin

DAPI: 4',6-diamidino-2-phenylindole

DTT: dithiothreitol

ECL: enhanced chemiluminescence

EDTA: ethylenedinitrilotetraacetic acid

EGTA: ethylene-gycol-tetraacetic acid

E.coli: Escherichia coli

FCS: fetal calf serum

GFP: green fluorescent protein

GST: glutathione S-transferase

HCl: hydrochloric acid

IF: Immunofluorescence

IgG: Immunglobulin G

IP: immunoprecipitation

IPTG: isopropyl-beta-D-thiogalactopyranoside

kDa: kilo Dalton

KD: kinase dead

KT: KT

MBP: maltose binding protein

MS: mass spectrometry

MW: molecular weight

MT: microtubule

OD: optical density

PBD: Polo-box domain

PBS: phosphate-buffered saline

PCR: polymerase chain reaction

PIPES: 1,4-Piperazinediethanesulfonic acid

PTEMF: Pipes, Triton X-100, EGTA, $MgCl_2$, Formaldehyde

RNA: ribonucleic acid

RT: room temperature

SAC: spindle assembly checkpoint

SDS-PAGE: sodium dodecylsulfate polyacrylamid gelelectrophoresis

siRNA: small interference ribonucleic acid

T111: threonine at position 111

WT: wild-type

ACKNOWLEDGMENT

My grateful thanks go to Prof. Erich Nigg for giving me the opportunity of working in his excellently organized lab and for all his advice and support.

I am thankful to PD Dr. Angelika Böttger for her expert evaluation of this manuscript.

My special thanks go to my supervisor Dr. Ulrike Grüneberg for introducing me into the field of mitosis and for teaching me patiently the different techniques.

I like to thank Dr. Francis Barr, Dr. Herman Sillje, Dr. Roman Körner, Dr. Rüdiger Neef, Julia Kleylein-Sohn, Anja Hanisch, Evelyn Fuchs, Alexander Haas and Albert Ries for helpful discussions and technical support. I offer my thanks to all postdocs, PhD students and technicians in this department for their scientific support and helpfulness.

Of course, the friendship of all the people in the department and the institute, especially of Hans-Georg von Ribbeck, Mirjam Classen, Claudia Szmala, Anja Hanisch and Evelyn Fuchs is greatly appreciated.

I am indebted to Mirjam Classen for heading the graduate program with me and for adhering to our nobility of ideals.

Great thanks go to my beloved friends Anke Schmidt, Christina Mehling, Thomas Thein and Sr. M. Veronika for accompanying my hitherto path of live faithfully.

I am very grateful to my loved boyfriend Oliver Borgards.

My deepest gratitude goes to my parents, Hildegard Thein and Leo Thein for all their support and for providing me the opportunity of gaining excellent education.

REFERENCES

Abaza, A., J.M. Soleilhac, J. Westendorf, M. Piel, I. Crevel, A. Roux, and F. Pirollet. 2003. M phase phosphoprotein 1 is a human plus-end-directed kinesin-related protein required for cytokinesis. *J Biol Chem*. 278:27844-52.

Abrieu, A., L. Magnaghi-Jaulin, J.A. Kahana, M. Peter, A. Castro, S. Vigneron, T. Lorca, D.W. Cleveland, and J.C. Labbe. 2001. Mps1 is a kinetochore-associated kinase essential for the vertebrate mitotic checkpoint. *Cell*. 106:83-93.

Acquaviva, C., F. Herzog, C. Kraft, and J. Pines. 2004. The anaphase promoting complex/cyclosome is recruited to centromeres by the spindle assembly checkpoint. *Nat Cell Biol*. 6:892-8.

Ahonen, L.J., M.J. Kallio, J.R. Daum, M. Bolton, I.A. Manke, M.B. Yaffe, P.T. Stukenberg, and G.J. Gorbsky. 2005. Polo-like kinase 1 creates the tension-sensing 3F3/2 phosphoepitope and modulates the association of spindle-checkpoint proteins at kinetochores. *Curr Biol*. 15:1078-89.

Alberts, B., Johnson, A., Lewis J., Raff, M., Roberts, K., Walter, P. 2002. Molecular Biology of the Cell, Fourth Edition.

Amor, D.J., P. Kalitsis, H. Sumer, and K.H. Choo. 2004. Building the centromere: from foundation proteins to 3D organization. *Trends Cell Biol*. 14:359-68.

Andrews, P.D., Y. Ovechkina, N. Morrice, M. Wagenbach, K. Duncan, L. Wordeman, and J.R. Swedlow. 2004. Aurora B regulates MCAK at the mitotic centromere. *Dev Cell*. 6:253-68.

Balczon, R., L. Bao, W.E. Zimmer, K. Brown, R.P. Zinkowski, and B.R. Brinkley. 1995. Dissociation of centrosome replication events from cycles of DNA synthesis and mitotic division in hydroxyurea-arrested Chinese hamster ovary cells. *J Cell Biol*. 130:105-15.

Bardin, A.J., and A. Amon. 2001. Men and sin: what's the difference? *Nat Rev Mol Cell Biol*. 2:815-26.

Barr, F.A., H.H. Sillje, and E.A. Nigg. 2004. Polo-like kinases and the orchestration of cell division. *Nat Rev Mol Cell Biol*. 5:429-40.

Bastiaens, P., M. Caudron, P. Niethammer, and E. Karsenti. 2006. Gradients in the self-organization of the mitotic spindle. *Trends Cell Biol*. 16:125-34.

Berdnik, D., and J.A. Knoblich. 2002. Drosophila Aurora-A is required for centrosome maturation and actin-dependent asymmetric protein localization during mitosis. *Curr Biol*. 12:640-7.

Blangy, A., H.A. Lane, P. d'Herin, M. Harper, M. Kress, and E.A. Nigg. 1995. Phosphorylation by p34cdc2 regulates spindle association of human Eg5, a kinesin-related motor essential for bipolar spindle formation in vivo. *Cell*. 83:1159-69.

Bornens, M. 2002. Centrosome composition and microtubule anchoring mechanisms. *Curr Opin Cell Biol*. 14:25-34.

Brennan, I.M., U. Peters, T.M. Kapoor, and A.F. Straight. 2007. Polo-like kinase controls vertebrate spindle elongation and cytokinesis. *PLoS ONE*. 2:e409.

Brinkley, B.R. 2001. Managing the centrosome numbers game: from chaos to stability in cancer cell division. *Trends Cell Biol*. 11:18-21.

Brinkley, B.R., and E. Stubblefield. 1966. The fine structure of the kinetochore of a mammalian cell in vitro. *Chromosoma*. 19:28-43.

Brouhard, G.J., and A.J. Hunt. 2005. Microtubule movements on the arms of mitotic chromosomes: polar ejection forces quantified in vitro. *Proc Natl Acad Sci U S A*. 102:13903-8.

Burkard, M.E., C.L. Randall, S. Larochelle, C. Zhang, K.M. Shokat, R.P. Fisher, and P.V. Jallepalli. 2007. Chemical genetics reveals the requirement for Polo-like kinase 1 activity in positioning RhoA and triggering cytokinesis in human cells. *Proc Natl Acad Sci U S A*. 104:4383-8.

Carazo-Salas, R.E., G. Guarguaglini, O.J. Gruss, A. Segref, E. Karsenti, and I.W. Mattaj. 1999. Generation of GTP-bound Ran by RCC1 is required for chromatin-induced mitotic spindle formation. *Nature*. 400:178-81.

Carroll, P.E., M. Okuda, H.F. Horn, P. Biddinger, P.J. Stambrook, L.L. Gleich, Y.Q. Li, P. Tarapore, and K. Fukasawa. 1999. Centrosome hyperamplification in human cancer: chromosome instability induced by p53 mutation and/or Mdm2 overexpression. *Oncogene*. 18:1935-44.

Casenghi, M., P. Meraldi, U. Weinhart, P.I. Duncan, R. Korner, and E.A. Nigg. 2003. Polo-like kinase 1 regulates Nlp, a centrosome protein involved in microtubule nucleation. *Dev Cell*. 5:113-25.

Cassimeris, L., and J. Morabito. 2004. TOGp, the human homolog of XMAP215/Dis1, is required for centrosome integrity, spindle pole organization, and bipolar spindle assembly. *Mol Biol Cell*. 15:1580-90.

Chalamalasetty, R.B., S. Hummer, E.A. Nigg, and H.H. Sillje. 2006. Influence of human Ect2 depletion and overexpression on cleavage furrow formation and abscission. *J Cell Sci*. 119:3008-19.

Chan, G.K., S.A. Jablonski, V. Sudakin, J.C. Hittle, and T.J. Yen. 1999. Human BUBR1 is a mitotic checkpoint kinase that monitors CENP-E functions at kinetochores and binds the cyclosome/APC. *J Cell Biol*. 146:941-54.

Chan, G.K., S.T. Liu, and T.J. Yen. 2005. Kinetochore structure and function. *Trends Cell Biol*. 15:589-98.

Chan, G.K., B.T. Schaar, and T.J. Yen. 1998. Characterization of the kinetochore binding domain of CENP-E reveals interactions with the kinetochore proteins CENP-F and hBUBR1. *J Cell Biol*. 143:49-63.

Chang, D.C., N. Xu, and K.Q. Luo. 2003. Degradation of cyclin B is required for the onset of anaphase in Mammalian cells. *J Biol Chem*. 278:37865-73.

Chang, M.S., C.J. Huang, M.L. Chen, S.T. Chen, C.C. Fan, J.M. Chu, W.C. Lin, and Y.C. Yang. 2001. Cloning and characterization of hMAP126, a new member of mitotic spindle-associated proteins. *Biochem Biophys Res Commun*. 287:116-21.

Chen, R.H., A. Shevchenko, M. Mann, and A.W. Murray. 1998. Spindle checkpoint protein Xmad1 recruits Xmad2 to unattached kinetochores. *J Cell Biol*. 143:283-95.

Chen, R.H., J.C. Waters, E.D. Salmon, and A.W. Murray. 1996. Association of spindle assembly checkpoint component XMAD2 with unattached kinetochores. *Science*. 274:242-6.

Ciferri, C., J. De Luca, S. Monzani, K.J. Ferrari, D. Ristic, C. Wyman, H. Stark, J. Kilmartin, E.D. Salmon, and A. Musacchio. 2005. Architecture of the human ndc80-hec1 complex, a critical constituent of the outer kinetochore. *J Biol Chem*. 280:29088-95.

Ciosk, R., W. Zachariae, C. Michaelis, A. Shevchenko, M. Mann, and K. Nasmyth. 1998. An ESP1/PDS1 complex regulates loss of sister chromatid cohesion at the metaphase to anaphase transition in yeast. *Cell*. 93:1067-76.

Cleveland, D.W., Y. Mao, and K.F. Sullivan. 2003. Centromeres and kinetochores: from epigenetics to mitotic checkpoint signaling. *Cell*. 112:407-21.

De Antoni, A., C.G. Pearson, D. Cimini, J.C. Canman, V. Sala, L. Nezi, M. Mapelli, L. Sironi, M. Faretta, E.D. Salmon, and A. Musacchio. 2005. The Mad1/Mad2 complex as a template for Mad2 activation in the spindle assembly checkpoint. *Curr Biol*. 15:214-25.

DeLuca, J.G., Y. Dong, P. Hergert, J. Strauss, J.M. Hickey, E.D. Salmon, and B.F. McEwen. 2005. Hec1 and nuf2 are core components of the kinetochore outer plate essential for organizing microtubule attachment sites. *Mol Biol Cell*. 16:519-31.

DeLuca, J.G., B.J. Howell, J.C. Canman, J.M. Hickey, G. Fang, and E.D. Salmon. 2003. Nuf2 and Hec1 are required for retention of the checkpoint proteins Mad1 and Mad2 to kinetochores. *Curr Biol*. 13:2103-9.

DeLuca, J.G., B. Moree, J.M. Hickey, J.V. Kilmartin, and E.D. Salmon. 2002. hNuf2 inhibition blocks stable kinetochore-microtubule attachment and induces mitotic cell death in HeLa cells. *J Cell Biol*. 159:549-55.

den Elzen, N., and J. Pines. 2001. Cyclin A is destroyed in prometaphase and can delay chromosome alignment and anaphase. *J Cell Biol*. 153:121-36.

Desai, A., and T.J. Mitchison. 1997. Microtubule polymerization dynamics. *Annu Rev Cell Dev Biol*. 13:83-117.

Desai, A., S. Verma, T.J. Mitchison, and C.E. Walczak. 1999. Kin I kinesins are microtubule-destabilizing enzymes. *Cell*. 96:69-78.

Doree, M., and T. Hunt. 2002. From Cdc2 to Cdk1: when did the cell cycle kinase join its cyclin partner? *J Cell Sci*. 115:2461-4.

Doxsey, S. 2001. Re-evaluating centrosome function. *Nat Rev Mol Cell Biol*. 2:688-98.

Dujardin, D., U.I. Wacker, A. Moreau, T.A. Schroer, J.E. Rickard, and J.R. De Mey. 1998. Evidence for a role of CLIP-170 in the establishment of metaphase chromosome alignment. *J Cell Biol*. 141:849-62.

Elbashir, S.M., J. Harborth, W. Lendeckel, A. Yalcin, K. Weber, and T. Tuschl. 2001. Duplexes of 21-nucleotide RNAs mediate RNA interference in cultured mammalian cells. *Nature*. 411:494-8.

Elia, A.E., L.C. Cantley, and M.B. Yaffe. 2003a. Proteomic screen finds pSer/pThr-binding domain localizing Plk1 to mitotic substrates. *Science*. 299:1228-31.

Elia, A.E., P. Rellos, L.F. Haire, J.W. Chao, F.J. Ivins, K. Hoepker, D. Mohammad, L.C. Cantley, S.J. Smerdon, and M.B. Yaffe. 2003b. The molecular basis for phosphodependent substrate targeting and regulation of Plks by the Polo-box domain. *Cell*. 115:83-95.

Elowe, S., S. Hummer, A. Uldschmid, X. Li, and E.A. Nigg. 2007. Tension-sensitive Plk1 phosphorylation on BubR1 regulates the stability of kinetochore microtubule interactions. *Genes Dev*. 21:2205-19.

Euteneuer, U., and J.R. McIntosh. 1981. Structural polarity of kinetochore microtubules in PtK1 cells. *J Cell Biol*. 89:338-45.

Eyers, P.A., and J.L. Maller. 2004. Regulation of Xenopus Aurora A activation by TPX2. *J Biol Chem*. 279:9008-15.

Fang, G., H. Yu, and M.W. Kirschner. 1998. The checkpoint protein MAD2 and the mitotic regulator CDC20 form a ternary complex with the anaphase-promoting complex to control anaphase initiation. *Genes Dev*. 12:1871-83.

Ferrari, S. 2006. Protein kinases controlling the onset of mitosis. *Cell Mol Life Sci*. 63:781-95.

Flemming, W. 1882. Zellsubstanz, Kern und Zellteilung. *F. W. C. Vogel, Leipzig*.

Foltz, D.R., L.E. Jansen, B.E. Black, A.O. Bailey, J.R. Yates, 3rd, and D.W. Cleveland. 2006. The human CENP-A centromeric nucleosome-associated complex. *Nat Cell Biol*. 8:458-69.

Fry, A.M., P. Meraldi, and E.A. Nigg. 1998. A centrosomal function for the human Nek2 protein kinase, a member of the NIMA family of cell cycle regulators. *Embo J*. 17:470-81.

Fujiwara, T., M. Bandi, M. Nitta, E.V. Ivanova, R.T. Bronson, and D. Pellman. 2005. Cytokinesis failure generating tetraploids promotes tumorigenesis in p53-null cells. *Nature*. 437:1043-7.

Gaglio, T., A. Saredi, and D.A. Compton. 1995. NuMA is required for the organization of microtubules into aster-like mitotic arrays. *J Cell Biol*. 131:693-708.

Gandhi, R., P.J. Gillespie, and T. Hirano. 2006. Human Wapl is a cohesin-binding protein that promotes sister-chromatid resolution in mitotic prophase. *Curr Biol*. 16:2406-17.

Geley, S., E. Kramer, C. Gieffers, J. Gannon, J.M. Peters, and T. Hunt. 2001. Anaphase-promoting complex/cyclosome-dependent proteolysis of human cyclin A starts at the beginning of mitosis and is not subject to the spindle assembly checkpoint. *J Cell Biol*. 153:137-48.

Gergely, F., V.M. Draviam, and J.W. Raff. 2003. The ch-TOG/XMAP215 protein is essential for spindle pole organization in human somatic cells. *Genes Dev*. 17:336-41.

Gil-Bernabe, A.M., F. Romero, M.C. Limon-Mortes, and M. Tortolero. 2006. Protein phosphatase 2A stabilizes human securin, whose phosphorylated forms are degraded via the SCF ubiquitin ligase. *Mol Cell Biol*. 26:4017-27.

Gimenez-Abian, J.F., I. Sumara, T. Hirota, S. Hauf, D. Gerlich, C. de la Torre, J. Ellenberg, and J.M. Peters. 2004. Regulation of sister chromatid cohesion between chromosome arms. *Curr Biol*. 14:1187-93.

Glover, D.M., I.M. Hagan, and A.A. Tavares. 1998. Polo-like kinases: a team that plays throughout mitosis. *Genes Dev*. 12:3777-87.

Glover, D.M., M.H. Leibowitz, D.A. McLean, and H. Parry. 1995. Mutations in aurora prevent centrosome separation leading to the formation of monopolar spindles. *Cell*. 81:95-105.

Goepfert, T.M. 2004. Centrosome Anomalies in Cancer: From Early Observations to Animal Models. In Centrosomes in Developments and Disease, Erich A. Nigg, ed.:323-333.

Golan, A., Y. Yudkovsky, and A. Hershko. 2002. The cyclin-ubiquitin ligase activity of cyclosome/APC is jointly activated by protein kinases Cdk1-cyclin B and Plk. *J Biol Chem*. 277:15552-7.

Golsteyn, R.M., K.E. Mundt, A.M. Fry, and E.A. Nigg. 1995. Cell cycle regulation of the activity and subcellular localization of Plk1, a human protein kinase implicated in mitotic spindle function. *J Cell Biol*. 129:1617-28.

Gorr, I.H., D. Boos, and O. Stemmann. 2005. Mutual inhibition of separase and Cdk1 by two-step complex formation. *Mol Cell*. 19:135-41.

Gromley, A., A. Jurczyk, J. Sillibourne, E. Halilovic, M. Mogensen, I. Groisman, M. Blomberg, and S. Doxsey. 2003. A novel human protein of the maternal centriole is required for the final stages of cytokinesis and entry into S phase. *J Cell Biol*. 161:535-45.

Gruber, J., J. Harborth, J. Schnabel, K. Weber, and M. Hatzfeld. 2002. The mitotic-spindle-associated protein astrin is essential for progression through mitosis. *J Cell Sci*. 115:4053-9.

Gruneberg, U., R. Neef, R. Honda, E.A. Nigg, and F.A. Barr. 2004. Relocation of Aurora B from centromeres to the central spindle at the metaphase to anaphase transition requires MKlp2. *J Cell Biol*. 166:167-72.

Guacci, V., E. Hogan, and D. Koshland. 1994. Chromosome condensation and sister chromatid pairing in budding yeast. *J Cell Biol*. 125:517-30.

Habedanck, R., Y.D. Stierhof, C.J. Wilkinson, and E.A. Nigg. 2005. The Polo kinase Plk4 functions in centriole duplication. *Nat Cell Biol*. 7:1140-6.

Hagting, A., N. Den Elzen, H.C. Vodermaier, I.C. Waizenegger, J.M. Peters, and J. Pines. 2002. Human securin proteolysis is controlled by the spindle checkpoint and reveals when the APC/C switches from activation by Cdc20 to Cdh1. *J Cell Biol*. 157:1125-37.

Hames, R.S., S.L. Wattam, H. Yamano, R. Bacchieri, and A.M. Fry. 2001. APC/C-mediated destruction of the centrosomal kinase Nek2A occurs in early mitosis and depends upon a cyclin A-type D-box. *Embo J*. 20:7117-27.

Hanisch, A., A. Wehner, E.A. Nigg, and H.H. Sillje. 2006. Different Plk1 functions show distinct dependencies on Polo-Box domain-mediated targeting. *Mol Biol Cell*. 17:448-59.

Hannak, E., M. Kirkham, A.A. Hyman, and K. Oegema. 2001. Aurora-A kinase is required for centrosome maturation in Caenorhabditis elegans. *J Cell Biol*. 155:1109-16.

Hardwick, K.G., R.C. Johnston, D.L. Smith, and A.W. Murray. 2000. MAD3 encodes a novel component of the spindle checkpoint which interacts with Bub3p, Cdc20p, and Mad2p. *J Cell Biol*. 148:871-82.

Hartwell, L.H., and D. Smith. 1985. Altered fidelity of mitotic chromosome transmission in cell cycle mutants of S. cerevisiae. *Genetics*. 110:381-95.

Hauf, S., R.W. Cole, S. LaTerra, C. Zimmer, G. Schnapp, R. Walter, A. Heckel, J. van Meel, C.L. Rieder, and J.M. Peters. 2003. The small molecule Hesperadin reveals a role for Aurora B in correcting kinetochore-microtubule attachment and in maintaining the spindle assembly checkpoint. *J Cell Biol*. 161:281-94.

Hauf, S., E. Roitinger, B. Koch, C.M. Dittrich, K. Mechtler, and J.M. Peters. 2005. Dissociation of cohesin from chromosome arms and loss of arm cohesion during early mitosis depends on phosphorylation of SA2. *PLoS Biol*. 3:e69.

Hauf, S., I.C. Waizenegger, and J.M. Peters. 2001. Cohesin cleavage by separase required for anaphase and cytokinesis in human cells. *Science*. 293:1320-3.

Hayden, J.H., S.S. Bowser, and C.L. Rieder. 1990. Kinetochores capture astral microtubules during chromosome attachment to the mitotic spindle: direct visualization in live newt lung cells. *J Cell Biol*. 111:1039-45.

Heald, R., R. Tournebize, T. Blank, R. Sandaltzopoulos, P. Becker, A. Hyman, and E. Karsenti. 1996. Self-organization of microtubules into bipolar spindles around artificial chromosomes in Xenopus egg extracts. *Nature*. 382:420-5.

Hinchcliffe, E.H., F.J. Miller, M. Cham, A. Khodjakov, and G. Sluder. 2001. Requirement of a centrosomal activity for cell cycle progression through G1 into S phase. *Science*. 291:1547-50.

Hinchcliffe, E.H., and G. Sluder. 2001. "It takes two to tango": understanding how centrosome duplication is regulated throughout the cell cycle. *Genes Dev*. 15:1167-81.

Hirano, T. 2005. Cell biology: holding sisters for repair. *Nature*. 433:467-8.

Hirokawa, N., Y. Noda, and Y. Okada. 1998. Kinesin and dynein superfamily proteins in organelle transport and cell division. *Curr Opin Cell Biol*. 10:60-73.

Hoffmann, I., P.R. Clarke, M.J. Marcote, E. Karsenti, and G. Draetta. 1993. Phosphorylation and activation of human cdc25-C by cdc2--cyclin B and its involvement in the self-amplification of MPF at mitosis. *Embo J*. 12:53-63.

Hofmann, K., P. Bucher, and A.V. Kajava. 1998. A model of Cdc25 phosphatase catalytic domain and Cdk-interaction surface based on the presence of a rhodanese homology domain. *J Mol Biol*. 282:195-208.

Holland, A.J., F. Bottger, O. Stemmann, and S.S. Taylor. 2007. Protein phosphatase 2A and separase form a complex regulated by separase autocleavage. *J Biol Chem*. 282:24623-32.

Holland, A.J., and S.S. Taylor. 2006. Cyclin-B1-mediated inhibition of excess separase is required for timely chromosome disjunction. *J Cell Sci*. 119:3325-36.

Holmfeldt, P., S. Stenmark, and M. Gullberg. 2004. Differential functional interplay of TOGp/XMAP215 and the KinI kinesin MCAK during interphase and mitosis. *Embo J*. 23:627-37.

Holt, S.V., M.A. Vergnolle, D. Hussein, M.J. Wozniak, V.J. Allan, and S.S. Taylor. 2005. Silencing Cenp-F weakens centromeric cohesion, prevents chromosome alignment and activates the spindle checkpoint. *J Cell Sci*. 118:4889-900.

Honda, R., R. Korner, and E.A. Nigg. 2003. Exploring the functional interactions between Aurora B, INCENP, and survivin in mitosis. *Mol Biol Cell*. 14:3325-41.

Howell, B.J., D.B. Hoffman, G. Fang, A.W. Murray, and E.D. Salmon. 2000. Visualization of Mad2 dynamics at kinetochores, along spindle fibers, and at spindle poles in living cells. *J Cell Biol*. 150:1233-50.

Howell, B.J., B.F. McEwen, J.C. Canman, D.B. Hoffman, E.M. Farrar, C.L. Rieder, and E.D. Salmon. 2001. Cytoplasmic dynein/dynactin drives kinetochore protein transport to the spindle poles and has a role in mitotic spindle checkpoint inactivation. *J Cell Biol*. 155:1159-72.

Howell, B.J., B. Moree, E.M. Farrar, S. Stewart, G. Fang, and E.D. Salmon. 2004. Spindle checkpoint protein dynamics at kinetochores in living cells. *Curr Biol*. 14:953-64.

Howman, E.V., K.J. Fowler, A.J. Newson, S. Redward, A.C. MacDonald, P. Kalitsis, and K.H. Choo. 2000. Early disruption of centromeric chromatin organization in centromere protein A (Cenpa) null mice. *Proc Natl Acad Sci U S A*. 97:1148-53.

Hoyt, M.A., L. Totis, and B.T. Roberts. 1991. S. cerevisiae genes required for cell cycle arrest in response to loss of microtubule function. *Cell*. 66:507-17.

Hunter, A.W., M. Caplow, D.L. Coy, W.O. Hancock, S. Diez, L. Wordeman, and J. Howard. 2003. The kinesin-related protein MCAK is a microtubule depolymerase

that forms an ATP-hydrolyzing complex at microtubule ends. *Mol Cell*. 11:445-57.

Hut, H.M., W. Lemstra, E.H. Blaauw, G.W. Van Cappellen, H.H. Kampinga, and O.C. Sibon. 2003. Centrosomes split in the presence of impaired DNA integrity during mitosis. *Mol Biol Cell*. 14:1993-2004.

Hwang, L.H., L.F. Lau, D.L. Smith, C.A. Mistrot, K.G. Hardwick, E.S. Hwang, A. Amon, and A.W. Murray. 1998. Budding yeast Cdc20: a target of the spindle checkpoint. *Science*. 279:1041-4.

Izumi, T., and J.L. Maller. 1993. Elimination of cdc2 phosphorylation sites in the cdc25 phosphatase blocks initiation of M-phase. *Mol Biol Cell*. 4:1337-50.

Jablonski, S.A., G.K. Chan, C.A. Cooke, W.C. Earnshaw, and T.J. Yen. 1998. The hBUB1 and hBUBR1 kinases sequentially assemble onto kinetochores during prophase with hBUBR1 concentrating at the kinetochore plates in mitosis. *Chromosoma*. 107:386-96.

Jang, Y.J., S. Ma, Y. Terada, and R.L. Erikson. 2002. Phosphorylation of threonine 210 and the role of serine 137 in the regulation of mammalian polo-like kinase. *J Biol Chem*. 277:44115-20.

Jaspersen, S.L., J.F. Charles, R.L. Tinker-Kulberg, and D.O. Morgan. 1998. A late mitotic regulatory network controlling cyclin destruction in Saccharomyces cerevisiae. *Mol Biol Cell*. 9:2803-17.

Jokelainen, P.T. 1967. The ultrastructure and spatial organization of the metaphase kinetochore in mitotic rat cells. *J Ultrastruct Res*. 19:19-44.

Joshi, H.C. 1998. Microtubule dynamics in living cells. *Curr Opin Cell Biol*. 10:35-44.

Kaiser, B.K., Z.A. Zimmerman, H. Charbonneau, and P.K. Jackson. 2002. Disruption of centrosome structure, chromosome segregation, and cytokinesis by misexpression of human Cdc14A phosphatase. *Mol Biol Cell*. 13:2289-300.

Kallio, M.J., V.A. Beardmore, J. Weinstein, and G.J. Gorbsky. 2002a. Rapid microtubule-independent dynamics of Cdc20 at kinetochores and centrosomes in mammalian cells. *J Cell Biol*. 158:841-7.

Kallio, M.J., M.L. McCleland, P.T. Stukenberg, and G.J. Gorbsky. 2002b. Inhibition of aurora B kinase blocks chromosome segregation, overrides the spindle checkpoint, and perturbs microtubule dynamics in mitosis. *Curr Biol*. 12:900-5.

Kang, Y.H., J.E. Park, L.R. Yu, N.K. Soung, S.M. Yun, J.K. Bang, Y.S. Seong, H. Yu, S. Garfield, T.D. Veenstra, and K.S. Lee. 2006. Self-regulated Plk1 recruitment to kinetochores by the Plk1-PBIP1 interaction is critical for proper chromosome segregation. *Mol Cell*. 24:409-22.

Kapoor, T.M., M.A. Lampson, P. Hergert, L. Cameron, D. Cimini, E.D. Salmon, B.F. McEwen, and A. Khodjakov. 2006. Chromosomes can congress to the metaphase plate before biorientation. *Science*. 311:388-91.

Karsenti, E., and I. Vernos. 2001. The mitotic spindle: a self-made machine. *Science*. 294:543-7.

Keryer, G., H. Ris, and G.G. Borisy. 1984. Centriole distribution during tripolar mitosis in Chinese hamster ovary cells. *J Cell Biol*. 98:2222-9.

Khodjakov, A., R.W. Cole, B.R. Oakley, and C.L. Rieder. 2000. Centrosome-independent mitotic spindle formation in vertebrates. *Curr Biol*. 10:59-67.

Kim, A.J., and S.A. Endow. 2000. A kinesin family tree. *J Cell Sci*. 113 Pt 21:3681-2.

Kim, S.H., D.P. Lin, S. Matsumoto, A. Kitazono, and T. Matsumoto. 1998. Fission yeast Slp1: an effector of the Mad2-dependent spindle checkpoint. *Science*. 279:1045-7.

Kimura, K., M. Hirano, R. Kobayashi, and T. Hirano. 1998. Phosphorylation and activation of 13S condensin by Cdc2 in vitro. *Science*. 282:487-90.

Kitajima, T.S., T. Sakuno, K. Ishiguro, S. Iemura, T. Natsume, S.A. Kawashima, and Y. Watanabe. 2006. Shugoshin collaborates with protein phosphatase 2A to protect cohesin. *Nature*. 441:46-52.

Kline-Smith, S.L., A. Khodjakov, P. Hergert, and C.E. Walczak. 2004. Depletion of centromeric MCAK leads to chromosome congression and segregation defects due to improper kinetochore attachments. *Mol Biol Cell*. 15:1146-59.

Kraft, C., F. Herzog, C. Gieffers, K. Mechtler, A. Hagting, J. Pines, and J.M. Peters. 2003. Mitotic regulation of the human anaphase-promoting complex by phosphorylation. *Embo J*. 22:6598-609.

Kramer, E.R., N. Scheuringer, A.V. Podtelejnikov, M. Mann, and J.M. Peters. 2000. Mitotic regulation of the APC activator proteins CDC20 and CDH1. *Mol Biol Cell*. 11:1555-69.

Krek, W., and E.A. Nigg. 1991. Mutations of p34cdc2 phosphorylation sites induce premature mitotic events in HeLa cells: evidence for a double block to p34cdc2 kinase activation in vertebrates. *Embo J*. 10:3331-41.

Kueng, S., B. Hegemann, B.H. Peters, J.J. Lipp, A. Schleiffer, K. Mechtler, and J.M. Peters. 2006. Wapl controls the dynamic association of cohesin with chromatin. *Cell*. 127:955-67.

Kufer, T.A., H.H. Sillje, R. Korner, O.J. Gruss, P. Meraldi, and E.A. Nigg. 2002. Human TPX2 is required for targeting Aurora-A kinase to the spindle. *J Cell Biol*. 158:617-23.

Kumagai, A., and W.G. Dunphy. 1996. Purification and molecular cloning of Plx1, a Cdc25-regulatory kinase from Xenopus egg extracts. *Science*. 273:1377-80.

Lane, H.A., and E.A. Nigg. 1996. Antibody microinjection reveals an essential role for human polo-like kinase 1 (Plk1) in the functional maturation of mitotic centrosomes. *J Cell Biol*. 135:1701-13.

Lange, B.M. 2002. Integration of the centrosome in cell cycle control, stress response and signal transduction pathways. *Curr Opin Cell Biol*. 14:35-43.

Lee, K.S., T.Z. Grenfell, F.R. Yarm, and R.L. Erikson. 1998. Mutation of the polo-box disrupts localization and mitotic functions of the mammalian polo kinase Plk. *Proc Natl Acad Sci U S A*. 95:9301-6.

Leidel, S., M. Delattre, L. Cerutti, K. Baumer, and P. Gonczy. 2005. SAS-6 defines a protein family required for centrosome duplication in C. elegans and in human cells. *Nat Cell Biol*. 7:115-25.

Lenart, P., M. Petronczki, M. Steegmaier, B. Di Fiore, J.J. Lipp, M. Hoffmann, W.J. Rettig, N. Kraut, and J.M. Peters. 2007. The small-molecule inhibitor BI 2536 reveals novel insights into mitotic roles of polo-like kinase 1. *Curr Biol*. 17:304-15.

Leung, G.C., J.W. Hudson, A. Kozarova, A. Davidson, J.W. Dennis, and F. Sicheri. 2002. The Sak polo-box comprises a structural domain sufficient for mitotic subcellular localization. *Nat Struct Biol*. 9:719-24.

Li, R., and A.W. Murray. 1991. Feedback control of mitosis in budding yeast. *Cell*. 66:519-31.

Lindon, C., and J. Pines. 2004. Ordered proteolysis in anaphase inactivates Plk1 to contribute to proper mitotic exit in human cells. *J Cell Biol*. 164:233-41.

Lingle, W.L., W.H. Lutz, J.N. Ingle, N.J. Maihle, and J.L. Salisbury. 1998. Centrosome hypertrophy in human breast tumors: implications for genomic stability and cell polarity. *Proc Natl Acad Sci U S A*. 95:2950-5.

Lingle, W.L., and J.L. Salisbury. 2001. Methods for the analysis of centrosome reproduction in cancer cells. *Methods Cell Biol*. 67:325-36.

Liu, D., X. Ding, J. Du, X. Cai, Y. Huang, T. Ward, A. Shaw, Y. Yang, R. Hu, C. Jin, and X. Yao. 2007. Human NUF2 Interacts with Centromere-associated Protein E and Is Essential for a Stable Spindle Microtubule-Kinetochore Attachment. *J Biol Chem*. 282:21415-21424.

Lowery, D.M., D. Lim, and M.B. Yaffe. 2005. Structure and function of Polo-like kinases. *Oncogene*. 24:248-59.

Luo, X., Z. Tang, G. Xia, K. Wassmann, T. Matsumoto, J. Rizo, and H. Yu. 2004. The Mad2 spindle checkpoint protein has two distinct natively folded states. *Nat Struct Mol Biol*. 11:338-45.

Mack, G.J., and D.A. Compton. 2001. Analysis of mitotic microtubule-associated proteins using mass spectrometry identifies astrin, a spindle-associated protein. *Proc Natl Acad Sci U S A*. 98:14434-9.

Maiato, H., J. DeLuca, E.D. Salmon, and W.C. Earnshaw. 2004. The dynamic kinetochore-microtubule interface. *J Cell Sci*. 117:5461-77.

Maiato, H., E.A. Fairley, C.L. Rieder, J.R. Swedlow, C.E. Sunkel, and W.C. Earnshaw. 2003. Human CLASP1 is an outer kinetochore component that regulates spindle microtubule dynamics. *Cell*. 113:891-904.

Mailand, N., C. Lukas, B.K. Kaiser, P.K. Jackson, J. Bartek, and J. Lukas. 2002. Deregulated human Cdc14A phosphatase disrupts centrosome separation and chromosome segregation. *Nat Cell Biol*. 4:317-22.

Mao, Y., A. Desai, and D.W. Cleveland. 2005. Microtubule capture by CENP-E silences BubR1-dependent mitotic checkpoint signaling. *J Cell Biol*. 170:873-80.

Martin-Lluesma, S., V.M. Stucke, and E.A. Nigg. 2002. Role of Hec1 in spindle checkpoint signaling and kinetochore recruitment of Mad1/Mad2. *Science*. 297:2267-70.

Matsumura, S., F. Toyoshima, and E. Nishida. 2007. Polo-like kinase 1 facilitates chromosome alignment during prometaphase through BubR1. *J Biol Chem*. 282:15217-27.

Mayer, T.U., T.M. Kapoor, S.J. Haggarty, R.W. King, S.L. Schreiber, and T.J. Mitchison. 1999. Small molecule inhibitor of mitotic spindle bipolarity identified in a phenotype-based screen. *Science*. 286:971-4.

Mayr, M.I., S. Hummer, J. Bormann, T. Gruner, S. Adio, G. Woehlke, and T.U. Mayer. 2007. The human kinesin Kif18A is a motile microtubule depolymerase essential for chromosome congression. *Curr Biol*. 17:488-98.

Mazumdar, M., and T. Misteli. 2005. Chromokinesins: multitalented players in mitosis. *Trends Cell Biol*. 15:349-55.

Mazumdar, M., S. Sundareshan, and T. Misteli. 2004. Human chromokinesin KIF4A functions in chromosome condensation and segregation. *J Cell Biol*. 166:613-20.

McEwen, B.F., G.K. Chan, B. Zubrowski, M.S. Savoian, M.T. Sauer, and T.J. Yen. 2001. CENP-E is essential for reliable bioriented spindle attachment, but chromosome alignment can be achieved via redundant mechanisms in mammalian cells. *Mol Biol Cell*. 12:2776-89.

McEwen, B.F., C.E. Hsieh, A.L. Mattheyses, and C.L. Rieder. 1998. A new look at kinetochore structure in vertebrate somatic cells using high-pressure freezing and freeze substitution. *Chromosoma*. 107:366-75.

McGuinness, B.E., T. Hirota, N.R. Kudo, J.M. Peters, and K. Nasmyth. 2005. Shugoshin prevents dissociation of cohesin from centromeres during mitosis in vertebrate cells. *PLoS Biol*. 3:e86.

Mei, J., X. Huang, and P. Zhang. 2001. Securin is not required for cellular viability, but is required for normal growth of mouse embryonic fibroblasts. *Curr Biol*. 11:1197-201.

Meraldi, P., and E.A. Nigg. 2001. Centrosome cohesion is regulated by a balance of kinase and phosphatase activities. *J Cell Sci*. 114:3749-57.

Meraldi, P., and E.A. Nigg. 2002. The centrosome cycle. *FEBS Lett*. 521:9-13.

Merdes, A., R. Heald, K. Samejima, W.C. Earnshaw, and D.W. Cleveland. 2000. Formation of spindle poles by dynein/dynactin-dependent transport of NuMA. *J Cell Biol*. 149:851-62.

Mishima, M., S. Kaitna, and M. Glotzer. 2002. Central spindle assembly and cytokinesis require a kinesin-like protein/RhoGAP complex with microtubule bundling activity. *Dev Cell*. 2:41-54.

Mitchison, J.M. 1971. The Biology of the Cell Cycle. *Cambridge: Cambridge University Press*.

Mitchison, T., and M. Kirschner. 1984. Dynamic instability of microtubule growth. *Nature*. 312:237-42.

Mollinari, C., J.P. Kleman, W. Jiang, G. Schoehn, T. Hunter, and R.L. Margolis. 2002. PRC1 is a microtubule binding and bundling protein essential to maintain the mitotic spindle midzone. *J Cell Biol*. 157:1175-86.

Moritz, M., M.B. Braunfeld, J.W. Sedat, B. Alberts, and D.A. Agard. 1995. Microtubule nucleation by gamma-tubulin-containing rings in the centrosome. *Nature*. 378:638-40.

Morrow, C.J., A. Tighe, V.L. Johnson, M.I. Scott, C. Ditchfield, and S.S. Taylor. 2005. Bub1 and aurora B cooperate to maintain BubR1-mediated inhibition of APC/CCdc20. *J Cell Sci*. 118:3639-52.

Mundt, K.E., R.M. Golsteyn, H.A. Lane, and E.A. Nigg. 1997. On the regulation and function of human polo-like kinase 1 (PLK1): effects of overexpression on cell cycle progression. *Biochem Biophys Res Commun*. 239:377-85.

Murray, A.W. 2004. Recycling the cell cycle: cyclins revisited. *Cell*. 116:221-34.

Musacchio, A., and K.G. Hardwick. 2002. The spindle checkpoint: structural insights into dynamic signalling. *Nat Rev Mol Cell Biol*. 3:731-41.

Musacchio, A., and E.D. Salmon. 2007. The spindle-assembly checkpoint in space and time. *Nat Rev Mol Cell Biol*. 8:379-93.

Nasmyth, K., and C.H. Haering. 2005. The structure and function of SMC and kleisin complexes. *Annu Rev Biochem*. 74:595-648.

Neef, R., U. Gruneberg, R. Kopajtich, X. Li, E.A. Nigg, H. Sillje, and F.A. Barr. 2007. Choice of Plk1 docking partners during mitosis and cytokinesis is controlled by the activation state of Cdk1. *Nat Cell Biol*. 9:436-44.

Neef, R., C. Preisinger, J. Sutcliffe, R. Kopajtich, E.A. Nigg, T.U. Mayer, and F.A. Barr. 2003. Phosphorylation of mitotic kinesin-like protein 2 by polo-like kinase 1 is required for cytokinesis. *J Cell Biol*. 162:863-75.

Nigg, E.A. 2001. Mitotic kinases as regulators of cell division and its checkpoints. *Nat Rev Mol Cell Biol*. 2:21-32.

Nigg, E.A. 2002. Centrosome aberrations: cause or consequence of cancer progression? *Nat Rev Cancer*. 2:815-25.

Nurse, P. 1990. Universal control mechanisms regulating onset of M-phase. *Nature*:503-508.

O'Connell, C.B., and A.L. Khodjakov. 2007. Cooperative mechanisms of mitotic spindle formation. *J Cell Sci*. 120:1717-22.

Palmer, D.K., K. O'Day, H.L. Trong, H. Charbonneau, and R.L. Margolis. 1991. Purification of the centromere-specific protein CENP-A and demonstration that it is a distinctive histone. *Proc Natl Acad Sci U S A*. 88:3734-8.

Paoletti, A., M. Moudjou, M. Paintrand, J.L. Salisbury, and M. Bornens. 1996. Most of centrin in animal cells is not centrosome-associated and centrosomal centrin is confined to the distal lumen of centrioles. *J Cell Sci*. 109 (Pt 13):3089-102.

Papi, M., E. Berdougo, C.L. Randall, S. Ganguly, and P.V. Jallepalli. 2005. Multiple roles for separase auto-cleavage during the G2/M transition. *Nat Cell Biol*. 7:1029-35.

Paweletz, N. 2001. Walther Flemming: pioneer of mitosis research. *Nat Rev Mol Cell Biol*. 2:72-5.

Pereira, A.L., A.J. Pereira, A.R. Maia, K. Drabek, C.L. Sayas, P.J. Hergert, M. Lince-Faria, I. Matos, C. Duque, T. Stepanova, C.L. Rieder, W.C. Earnshaw, N. Galjart, and H. Maiato. 2006. Mammalian CLASP1 and CLASP2 cooperate to ensure

mitotic fidelity by regulating spindle and kinetochore function. *Mol Biol Cell*. 17:4526-42.

Pereira, G., and E. Schiebel. 2003. Separase regulates INCENP-Aurora B anaphase spindle function through Cdc14. *Science*. 302:2120-4.

Peter, M., E. Heitlinger, M. Haner, U. Aebi, and E.A. Nigg. 1991. Disassembly of in vitro formed lamin head-to-tail polymers by CDC2 kinase. *Embo J*. 10:1535-44.

Peters, J.M. 2002. The anaphase-promoting complex: proteolysis in mitosis and beyond. *Mol Cell*. 9:931-43.

Peters, J.M. 2006. The anaphase promoting complex/cyclosome: a machine designed to destroy. *Nat Rev Mol Cell Biol*. 7:644-56.

Petronczki, M., M. Glotzer, N. Kraut, and J.M. Peters. 2007. Polo-like kinase 1 triggers the initiation of cytokinesis in human cells by promoting recruitment of the RhoGEF Ect2 to the central spindle. *Dev Cell*. 12:713-25.

Piel, M., J. Nordberg, U. Euteneuer, and M. Bornens. 2001. Centrosome-dependent exit of cytokinesis in animal cells. *Science*. 291:1550-3.

Pihan, G.A., A. Purohit, J. Wallace, H. Knecht, B. Woda, P. Quesenberry, and S.J. Doxsey. 1998. Centrosome defects and genetic instability in malignant tumors. *Cancer Res*. 58:3974-85.

Pines, J. 2006. Mitosis: a matter of getting rid of the right protein at the right time. *Trends Cell Biol*. 16:55-63.

Pinsky, B.A., C.V. Kotwaliwale, S.Y. Tatsutani, C.A. Breed, and S. Biggins. 2006. Glc7/protein phosphatase 1 regulatory subunits can oppose the Ipl1/aurora protein kinase by redistributing Glc7. *Mol Cell Biol*. 26:2648-60.

Reynolds, N., and H. Ohkura. 2003. Polo boxes form a single functional domain that mediates interactions with multiple proteins in fission yeast polo kinase. *J Cell Sci*. 116:1377-87.

Riedel, C.G., V.L. Katis, Y. Katou, S. Mori, T. Itoh, W. Helmhart, M. Galova, M. Petronczki, J. Gregan, B. Cetin, I. Mudrak, E. Ogris, K. Mechtler, L. Pelletier, F. Buchholz, K. Shirahige, and K. Nasmyth. 2006. Protein phosphatase 2A protects centromeric sister chromatid cohesion during meiosis I. *Nature*. 441:53-61.

Rieder, C.L. 1981. The structure of the cold-stable kinetochore fiber in metaphase PtK1 cells. *Chromosoma*. 84:145-58.

Rieder, C.L., and S.P. Alexander. 1990. Kinetochores are transported poleward along a single astral microtubule during chromosome attachment to the spindle in newt lung cells. *J Cell Biol*. 110:81-95.

Rieder, C.L., R.W. Cole, A. Khodjakov, and G. Sluder. 1995. The checkpoint delaying anaphase in response to chromosome monoorientation is mediated by an inhibitory signal produced by unattached kinetochores. *J Cell Biol*. 130:941-8.

Rieder, C.L., and H. Maiato. 2004. Stuck in division or passing through: what happens when cells cannot satisfy the spindle assembly checkpoint. *Dev Cell*. 7:637-51.

Rieder, C.L., and E.D. Salmon. 1998. The vertebrate cell kinetochore and its roles during mitosis. *Trends Cell Biol*. 8:310-8.

Santamaria, A., R. Neef, U. Eberspacher, K. Eis, M. Husemann, D. Mumberg, S. Prechtl, V. Schulze, G. Siemeister, L. Wortmann, F.A. Barr, and E.A. Nigg. 2007. Use of the Novel Plk1 Inhibitor ZK-Thiazolidinone to Elucidate Functions of Plk1 in Early and Late Stages of Mitosis. *Mol Biol Cell*.

Sawin, K.E., K. LeGuellec, M. Philippe, and T.J. Mitchison. 1992. Mitotic spindle organization by a plus-end-directed microtubule motor. *Nature*. 359:540-3.

Sawin, K.E., and T.J. Mitchison. 1995. Mutations in the kinesin-like protein Eg5 disrupting localization to the mitotic spindle. *Proc Natl Acad Sci U S A*. 92:4289-93.

Saxton, W.M., D.L. Stemple, R.J. Leslie, E.D. Salmon, M. Zavortink, and J.R. McIntosh. 1984. Tubulin dynamics in cultured mammalian cells. *J Cell Biol*. 99:2175-86.

Schaar, B.T., G.K. Chan, P. Maddox, E.D. Salmon, and T.J. Yen. 1997. CENP-E function at kinetochores is essential for chromosome alignment. *J Cell Biol*. 139:1373-82.

Seong, Y.S., K. Kamijo, J.S. Lee, E. Fernandez, R. Kuriyama, T. Miki, and K.S. Lee. 2002. A spindle checkpoint arrest and a cytokinesis failure by the dominant-negative polo-box domain of Plk1 in U-2 OS cells. *J Biol Chem*. 277:32282-93.

Shah, J.V., E. Botvinick, Z. Bonday, F. Furnari, M. Berns, and D.W. Cleveland. 2004. Dynamics of centromere and kinetochore proteins; implications for checkpoint signaling and silencing. *Curr Biol*. 14:942-52.

Sharp, D.J., G.C. Rogers, and J.M. Scholey. 2000. Microtubule motors in mitosis. *Nature*. 407:41-7.

Sluder, G., and C.L. Rieder. 1985. Centriole number and the reproductive capacity of spindle poles. *J Cell Biol*. 100:887-96.

Stegmeier, F., M. Rape, V.M. Draviam, G. Nalepa, M.E. Sowa, X.L. Ang, E.R. McDonald, 3rd, M.Z. Li, G.J. Hannon, P.K. Sorger, M.W. Kirschner, J.W. Harper, and S.J. Elledge. 2007. Anaphase initiation is regulated by antagonistic ubiquitination and deubiquitination activities. *Nature*. 446:876-81.

Stegmeier, F., R. Visintin, and A. Amon. 2002. Separase, polo kinase, the kinetochore protein Slk19, and Spo12 function in a network that controls Cdc14 localization during early anaphase. *Cell*. 108:207-20.

Stemmann, O., H. Zou, S.A. Gerber, S.P. Gygi, and M.W. Kirschner. 2001. Dual inhibition of sister chromatid separation at metaphase. *Cell*. 107:715-26.

Steuer, E.R., L. Wordeman, T.A. Schroer, and M.P. Sheetz. 1990. Localization of cytoplasmic dynein to mitotic spindles and kinetochores. *Nature*. 345:266-8.

Strausfeld, U., A. Fernandez, J.P. Capony, F. Girard, N. Lautredou, J. Derancourt, J.C. Labbe, and N.J. Lamb. 1994. Activation of p34cdc2 protein kinase by microinjection of human cdc25C into mammalian cells. Requirement for prior phosphorylation of cdc25C by p34cdc2 on sites phosphorylated at mitosis. *J Biol Chem*. 269:5989-6000.

Stucke, V.M., C. Baumann, and E.A. Nigg. 2004. Kinetochore localization and microtubule interaction of the human spindle checkpoint kinase Mps1. *Chromosoma*. 113:1-15.

Sudakin, V., G.K. Chan, and T.J. Yen. 2001. Checkpoint inhibition of the APC/C in HeLa cells is mediated by a complex of BUBR1, BUB3, CDC20, and MAD2. *J Cell Biol*. 154:925-36.

Sudakin, V., D. Ganoth, A. Dahan, H. Heller, J. Hershko, F.C. Luca, J.V. Ruderman, and A. Hershko. 1995. The cyclosome, a large complex containing cyclin-selective ubiquitin ligase activity, targets cyclins for destruction at the end of mitosis. *Mol Biol Cell*. 6:185-97.

Sullivan, K.F., M. Hechenberger, and K. Masri. 1994. Human CENP-A contains a histone H3 related histone fold domain that is required for targeting to the centromere. *J Cell Biol*. 127:581-92.

Sumara, I., J.F. Gimenez-Abian, D. Gerlich, T. Hirota, C. Kraft, C. de la Torre, J. Ellenberg, and J.M. Peters. 2004. Roles of polo-like kinase 1 in the assembly of functional mitotic spindles. *Curr Biol*. 14:1712-22.

Sumara, I., E. Vorlaufer, P.T. Stukenberg, O. Kelm, N. Redemann, E.A. Nigg, and J.M. Peters. 2002. The dissociation of cohesin from chromosomes in prophase is regulated by Polo-like kinase. *Mol Cell*. 9:515-25.

Sunkel, C.E., and D.M. Glover. 1988. polo, a mitotic mutant of Drosophila displaying abnormal spindle poles. *J Cell Sci*. 89 (Pt 1):25-38.

Tanaka, T.U., N. Rachidi, C. Janke, G. Pereira, M. Galova, E. Schiebel, M.J. Stark, and K. Nasmyth. 2002. Evidence that the Ipl1-Sli15 (Aurora kinase-INCENP) complex promotes chromosome bi-orientation by altering kinetochore-spindle pole connections. *Cell*. 108:317-29.

Tang, Z., H. Shu, D. Oncel, S. Chen, and H. Yu. 2004. Phosphorylation of Cdc20 by Bub1 provides a catalytic mechanism for APC/C inhibition by the spindle checkpoint. *Mol Cell*. 16:387-97.

Tang, Z., H. Shu, W. Qi, N.A. Mahmood, M.C. Mumby, and H. Yu. 2006. PP2A is required for centromeric localization of Sgo1 and proper chromosome segregation. *Dev Cell*. 10:575-85.

Tanudji, M., J. Shoemaker, L. L'Italien, L. Russell, G. Chin, and X.M. Schebye. 2004. Gene silencing of CENP-E by small interfering RNA in HeLa cells leads to missegregation of chromosomes after a mitotic delay. *Mol Biol Cell*. 15:3771-81.

Taylor, S.S., E. Ha, and F. McKeon. 1998. The human homologue of Bub3 is required for kinetochore localization of Bub1 and a Mad3/Bub1-related protein kinase. *J Cell Biol*. 142:1-11.

Taylor, S.S., and F. McKeon. 1997. Kinetochore localization of murine Bub1 is required for normal mitotic timing and checkpoint response to spindle damage. *Cell*. 89:727-35.

Tirnauer, J.S., J.C. Canman, E.D. Salmon, and T.J. Mitchison. 2002. EB1 targets to kinetochores with attached, polymerizing microtubules. *Mol Biol Cell*. 13:4308-16.

Toyoshima-Morimoto, F., E. Taniguchi, and E. Nishida. 2002. Plk1 promotes nuclear translocation of human Cdc25C during prophase. *EMBO Rep*. 3:341-8.

Toyoshima-Morimoto, F., E. Taniguchi, N. Shinya, A. Iwamatsu, and E. Nishida. 2001. Polo-like kinase 1 phosphorylates cyclin B1 and targets it to the nucleus during prophase. *Nature*. 410:215-20.

Trinkle-Mulcahy, L., and A.I. Lamond. 2006. Mitotic phosphatases: no longer silent partners. *Curr Opin Cell Biol*. 18:623-31.

Tsou, M.F., and T. Stearns. 2006a. Controlling centrosome number: licenses and blocks. *Curr Opin Cell Biol*. 18:74-8.

Tsou, M.F., and T. Stearns. 2006b. Mechanism limiting centrosome duplication to once per cell cycle. *Nature*.

Tsou, M.F., and T. Stearns. 2006c. Mechanism limiting centrosome duplication to once per cell cycle. *Nature*. 442:947-51.

Uhlmann, F., and K. Nasmyth. 1998. Cohesion between sister chromatids must be established during DNA replication. *Curr Biol*. 8:1095-101.

Uhlmann, F., D. Wernic, M.A. Poupart, E.V. Koonin, and K. Nasmyth. 2000. Cleavage of cohesin by the CD clan protease separin triggers anaphase in yeast. *Cell*. 103:375-86.

Vagnarelli, P., and W.C. Earnshaw. 2004. Chromosomal passengers: the four-dimensional regulation of mitotic events. *Chromosoma*. 113:211-22.

van Vugt, M.A., and R.H. Medema. 2004. Checkpoint adaptation and recovery: back with Polo after the break. *Cell Cycle*. 3:1383-6.

Vazquez-Novelle, M.D., V. Esteban, A. Bueno, and M.P. Sacristan. 2005. Functional homology among human and fission yeast Cdc14 phosphatases. *J Biol Chem*. 280:29144-50.

Visintin, R., K. Craig, E.S. Hwang, S. Prinz, M. Tyers, and A. Amon. 1998. The phosphatase Cdc14 triggers mitotic exit by reversal of Cdk-dependent phosphorylation. *Mol Cell*. 2:709-18.

Waizenegger, I., J.F. Gimenez-Abian, D. Wernic, and J.M. Peters. 2002. Regulation of human separase by securin binding and autocleavage. *Curr Biol*. 12:1368-78.

Waizenegger, I.C., S. Hauf, A. Meinke, and J.M. Peters. 2000. Two distinct pathways remove mammalian cohesin from chromosome arms in prophase and from centromeres in anaphase. *Cell*. 103:399-410.

Wakefield, J.G., J.Y. Huang, and J.W. Raff. 2000. Centrosomes have a role in regulating the destruction of cyclin B in early Drosophila embryos. *Curr Biol*. 10:1367-70.

Wang, Y., and T.Y. Ng. 2006. Phosphatase 2A negatively regulates mitotic exit in Saccharomyces cerevisiae. *Mol Biol Cell*. 17:80-9.

Watanabe, N., H. Arai, Y. Nishihara, M. Taniguchi, N. Watanabe, T. Hunter, and H. Osada. 2004. M-phase kinases induce phospho-dependent ubiquitination of somatic Wee1 by SCFbeta-TrCP. *Proc Natl Acad Sci U S A*. 101:4419-24.

Watanabe, Y., and T.S. Kitajima. 2005. Shugoshin protects cohesin complexes at centromeres. *Philos Trans R Soc Lond B Biol Sci*. 360:515-21, discussion 521.

Wilde, A., S.B. Lizarraga, L. Zhang, C. Wiese, N.R. Gliksman, C.E. Walczak, and Y. Zheng. 2001. Ran stimulates spindle assembly by altering microtubule dynamics and the balance of motor activities. *Nat Cell Biol*. 3:221-7.

Wojcik, E., R. Basto, M. Serr, F. Scaerou, R. Karess, and T. Hays. 2001. Kinetochore dynein: its dynamics and role in the transport of the Rough deal checkpoint protein. *Nat Cell Biol*. 3:1001-7.

Wolf, F., C. Wandke, N. Isenberg, and S. Geley. 2006. Dose-dependent effects of stable cyclin B1 on progression through mitosis in human cells. *Embo J*. 25:2802-13.

Wong, C., and T. Stearns. 2003. Centrosome number is controlled by a centrosome-intrinsic block to reduplication. *Nat Cell Biol*. 5:539-44.

Wong, O.K., and G. Fang. 2006. Loading of the 3F3/2 antigen onto kinetochores is dependent on the ordered assembly of the spindle checkpoint proteins. *Mol Biol Cell*. 17:4390-9.

Wood, K.W., R. Sakowicz, L.S. Goldstein, and D.W. Cleveland. 1997. CENP-E is a plus end-directed kinetochore motor required for metaphase chromosome alignment. *Cell*. 91:357-66.

Xia, G., X. Luo, T. Habu, J. Rizo, T. Matsumoto, and H. Yu. 2004. Conformation-specific binding of p31(comet) antagonizes the function of Mad2 in the spindle checkpoint. *Embo J*. 23:3133-43.

Yamaguchi, S., H. Okayama, and P. Nurse. 2000. Fission yeast Fizzy-related protein srw1p is a G(1)-specific promoter of mitotic cyclin B degradation. *Embo J*. 19:3968-77.

Yao, X., A. Abrieu, Y. Zheng, K.F. Sullivan, and D.W. Cleveland. 2000. CENP-E forms a link between attachment of spindle microtubules to kinetochores and the mitotic checkpoint. *Nat Cell Biol*. 2:484-91.

Yao, X., K.L. Anderson, and D.W. Cleveland. 1997. The microtubule-dependent motor centromere-associated protein E (CENP-E) is an integral component of kinetochore corona fibers that link centromeres to spindle microtubules. *J Cell Biol*. 139:435-47.

Ye, K., Y. Ke, N. Keshava, J. Shanks, J.A. Kapp, R.R. Tekmal, J. Petros, and H.C. Joshi. 1998. Opium alkaloid noscapine is an antitumor agent that arrests metaphase and induces apoptosis in dividing cells. *Proc Natl Acad Sci U S A*. 95:1601-6.

Yen, T.J., D.A. Compton, D. Wise, R.P. Zinkowski, B.R. Brinkley, W.C. Earnshaw, and D.W. Cleveland. 1991. CENP-E, a novel human centromere-associated protein required for progression from metaphase to anaphase. *Embo J*. 10:1245-54.

Yen, T.J., G. Li, B.T. Schaar, I. Szilak, and D.W. Cleveland. 1992. CENP-E is a putative kinetochore motor that accumulates just before mitosis. *Nature*. 359:536-9.

Yu, H. 2006. Structural activation of Mad2 in the mitotic spindle checkpoint: the two-state Mad2 model versus the Mad2 template model. *J Cell Biol*. 173:153-7.

Yuce, O., A. Piekny, and M. Glotzer. 2005. An ECT2-centralspindlin complex regulates the localization and function of RhoA. *J Cell Biol*. 170:571-82.

Zachariae, W., M. Schwab, K. Nasmyth, and W. Seufert. 1998. Control of cyclin ubiquitination by CDK-regulated binding of Hct1 to the anaphase promoting complex. *Science*. 282:1721-4.

Zheng, Y., M.L. Wong, B. Alberts, and T. Mitchison. 1995. Nucleation of microtubule assembly by a gamma-tubulin-containing ring complex. *Nature*. 378:578-83.

Zhou, J., D. Panda, J.W. Landen, L. Wilson, and H.C. Joshi. 2002. Minor alteration of microtubule dynamics causes loss of tension across kinetochore pairs and activates the spindle checkpoint. *J Biol Chem*. 277:17200-8.

Zhou, T., J.P. Aumais, X. Liu, L.Y. Yu-Lee, and R.L. Erikson. 2003. A role for Plk1 phosphorylation of NudC in cytokinesis. *Dev Cell*. 5:127-38.

LEBENSLAUF

PERSÖNLICHE DATEN

Geburtsdatum	22. März 1979
Geburtsort	Haßfurt
Familienstand	ledig
Nationalität	deutsch

STUDIUM UND AUSBILDUNG

Seit September 2004	**Max-Planck Instiut für Biochemie.**, Martinsried Promotion „Functional characterization of the mitotic-spindle and kinetochore associated protein astrin“
Oktober 1998 - Juni 2004	**Technische Universität Braunschweig** Studium der Biotechnologie Studiumsschwerpunkte: Bioverfahrenstechnik, Technische Chemie, Molekularbiologie, Mikrobiologie und Zellbiologie
September 2003 - April 2004	**Infineon Technologies AG**, München Diplomarbeit „3D-Weillenleiterstruktur als Substrat für DNA-Microarrays“
November 2002 - Februar 2002	**Institut für Genetik der TU Braunschweig** Studienarbeit „Molekularbiologische und phylogenetische Charakterisierung Calvin Zyklus spezifischer cDNA Sequenzen der Rotalge *Chondrus crispus“*
August 1989 - Juni 1998	**Gymnasium der Englischen Fräulein**, Bamberg **Internat der Englischen Fräulein**
Februar 1996	Schüleraustausch: Charlston, USA
Juni 1995	Schüleraustausch: Marseille, Frankreich

PRAKTIKA

Mai 2002 - August 2002	**F. Hoffmann La Roche Ltd.**, Basel Bioprozesstechnik, Optimierung der transienten Transfektion in Säugetierzellen für die Herstellung humaner Antikörper
Juli 2001 - August 2001	**Gesellschaft für Biotechnologische Forschung**, Braunschweig Laborpraktikum in der Abteilung Organ- und Gewebekultur

STIPENDIEN UND AUSZEICHNUNGEN

September 2006	Reisestipendium und „Spetsai International Young Investigator Award“ der **FEBS** (Federation of European Biochemical Societies), Summer School 2006 (Spetsai, Griechenland)
seit Dezember 2002	Online-Stipendium bei **e-fellows.net**
Mai 2000 - März 2004	Stipendium der **Stiftung der Deutschen Wirtschaft** (sdw)
Juli 1998	Schülerehrenpreis 1998 der Stadt Bamberg (für das beste Abitur)

ZUSATZQUALIFIKATIONEN

September 2006	Kurs für den Umgang mit radioaktiven Stoffen
Dezember 2004	Fortbildung Biologische Sicherheit §15 GenTSV

KENNTNISSE

Sprachkenntnisse	Englisch: fließend Französisch: Grundkenntnisse
IT-Kenntnisse	Microsoft Office: Anwenderkenntnisse Adobe Photoshop, Adobe Illustrator: Anwenderkenntnisse

ENGAGEMENT UND INTERESSEN

seit September 2007	Leiterin der Fachgruppe Naturwissenschaften der sdw-Alumni
Januar 2006 - Dezember 2006	Doktorandensprecherin des Max-Planck Instituts für Biochemie
Oktober 2002 - Juli 2003	Leiterin der sdw-Stipendiatengruppe Braunschweig
Februar 2000 - Februar 2003	stellvertretende Obfrau des Fechtvereins der TU Braunschweig
April 2000 - März 2002	Mitglied des Konzils der TU Braunschweig
Interessen	Schwimmen, Joggen, Wandern, Literatur, Kunst und Malen

PUBLIKATIONEN

ARTIKEL

Kerstin H. Thein, Julia Kleylein-Sohn, Erich A. Nigg and Ulrike Gruneberg, Astrin is required for the maintenance of sister chromatid cohesion and centrosome integrity, Journal of Cell Biology, 2007

M. H. Klühr, A. Sauermann, C. A. Elsner, **K. H. Thein**, and S. K. Dertinger, Partially Oxidized Macroporous Silicon: AThree-Dimensional Photonic Matrix for Microarray Applications, Advanced Materials, 2006

Stephan K. Dertinger, Marco Kluehr, Christian A. Elsner, Alexander Sauermann, Kristin Rüffer, Petra M. Nicklaus and **Kerstin Thein**, A three-dimensional waveguide substrate for DNA-microarrays based on macroporous silicon, Physica Status Solidi(A), Applied Research, Volume 202, Issue 8, 2005

Stephan K. Dertinger, Marco Kluehr, Christian A. Elsner, Alexander Sauermann, Kristin Rüffer, Petra M. Nicklaus and **Kerstin Thein**, A three-dimensional waveguide structure as a support for genomic and proteomic microarrays, Lap-on-a-Chip: Platforms, Devices and Applications, Linda A. Smith, Daniel Sobek,, Editors, Proceedings of SPIE Vol. 5591, 2004

SEMINARVORTRÄGE UND POSTER

Kerstin H. Thein, Erich A. Nigg and Ulrike Grueneberg, Analysis of the mitotic-spindle-associated protein astrin, FEBS (Federation of European Biochemical Societies) Summer School on Molecular and Cell Biology at Spetsai 2006, (Poster und Vortrag)

Kerstin H. Thein, Erich A. Nigg and Ulrike Grueneberg, Analyzing the microtubule binding properties of astrin, ELSO (European Life Scientist Organization) 2005, Dresden (Poster)